THE PHYSICAL PROPERTIES OF DEEP OCEAN SEDIMENTS FROM THE NORTHERN ATLANTIC: A COMPARISON OF IN SITU AND LABORATORY METHODS

by

DAVID SAMUEL GOLDBERG

B.S., Massachusetts Institute of Technology
(1981)

SUBMITTED TO THE DEPARTMENT OF
EARTH AND PLANETARY SCIENCE IN PARTIAL
FULFILLMENT OF THE
REQUIREMENTS FOR THE
DEGREE OF

MASTER OF SCIENCE

at the

MASSACHUSETTS INSTITUTE OF TECHNOLOGY

August 1981

© Massachusetts Institute of Technology 1981

Signature of Author _____
Dept. of Earth and Planetary Sciences
August 7, 1981

Certified by _____
John G. Sclater
Thesis Supervisor

Accepted by _____
Chairman, Department Committee

Lindgren
MASSACHUSETTS INSTITUTE OF TECHNOLOGY
JAN 6 1982
LIBRARIES

THE PHYSICAL PROPERTIES OF DEEP OCEAN SEDIMENTS FROM THE NORTHERN ATLANTIC: A COMPARISON OF IN SITU AND LABORATORY METHODS

by

David Samuel Goldberg

Submitted in partial fulfillment of
the requirements for the degree of
Master of Science at the
Massachusetts Institute of Technology

ABSTRACT

Dense thermal conductivity measurements were obtained during the Atlantis II cruise number 108 leg 5 using the needle probe technique at 15 cm sampling intervals on fourteen recovered cores. These core stations are located at four heat flow sites on the Blake-Bahama Ridge in 110 to 165 ma well-sedimented crust between 25° and 27°N latitude and 68° and 74°W longitude. The mean and standard deviation of the thermal conductivities in mcal/(cm s °C) are 2.248 and 0.113, 2.526 and 0.231, 2.331 and 0.108, and 2.310 and 0.126 at sites HF 1 to HF 4, 110 ma to 165 ma crust, respectively. These needle probe measurements are within about 5% of the arithmetic mean, except for measurements at site HF 2 where large variations in water content are observed. The standard deviation of thermal conductivity measurement using the needle probe on fused silica glass is defined as the reproducibility of this technique, about 4.7%.

Thermal conductivity measurements using the in situ "violin" probe were made during the Knorr 77 cruise at locations within .5 km of the AII108-5 heat flow sites. The mean and standard deviation of the in situ values in mcal/(cm s °C) are 2.53 and 0.12, 2.17 and 0.02, and 2.20 and 0.03 at sites HF 2, HF 3, and HF 4 respectively. In situ conductivity measurements are shown to be generally within the standard deviations of the needle probe measurements, about 5%. In situ conductivities have been previously found to lie within about 5% of conductivities measured using the needle probe on sediments from the northeastern Pacific. The in situ measurements from the KR77 cruise lie within about 4% of their arithmetic mean, but are the result of single penetrations with ideal temperature decay histories.

ACKNOWLEDGEMENTS

I wish to acknowledge John Sclater and Dick Von Herzen for their continued advice and help throughout my graduate program. I also acknowledge MIT Sea Grant and John Sclater for their undergraduate and graduate support.

Dick Von Herzen was extremely helpful in aquiring the needle probe conductivity data. Earl Davis aquired and reduced the *in situ* conducitivity data. I am grateful to John Roberts for his help in data reduction and Lawrence Hobbie for help in preparation of this manuscript.

Finally, I thank my family and friends for their confidence through all, particularly when progress was slow.

Dedicated to all lost in the Bermuda Triangle.

TABLE OF CONTENTS

LIST OF FIGURES

Appendicies

LIST OF TABLES

INTRODUCTION

Observation of marine heat flow requires the measurement of thermal conductivity and temperature gradient in seafloor sediments. The instrument designed for these measurements by Ewing and Gerard (1962) consists of fragile thermistors strapped in outrigger fashion to a single penetration core barrel. These thermistors measure the seafloor temperature gradient, and the core is recovered for laboratory measurement of thermal conductivity. The needle probe measurement of thermal conductivity (Von Herzen and Maxwell, 1959) is a method of transient heating and measuring the temperature of the sediment through sensors in a hypodermic needle. The technique has a 5% reproducibility and a 1% standard error determined by the standard deviation of thermal conductivity measurements on fused silica glass (Goldberg et al., 1980).

The most recent design of heat flow instrumentation by Lister (1979) involves a multi-penetration "violin-bow" probe consisting of a thin temperature sensor/heater stretched along a strong steel rod. A series of thermistors and a heater allow simultaneous temperature gradient and in situ thermal conductivity measurements to be telemetered from the underwater instrument, greatly increasing the efficiency of data aquisition. The resiliant "violin-bow" probe can make several sequential penetrations on one lowering, whereas the coring apparatus is full after one penetration and must

be recovered. In situ conductivity measurement has previously been shown to lie within 5% of needle probe measurements by Hyndeman et al., (1979) using 2 m cores of samples from the northeastern Pacific.

The R/V Atlantis II cruise number 108, leg 5 in May 1981 retrieved seven 30' (9.15 m) piston cores and six 6' to 18' gravity cores from four designated heat flow stations in the northern Atlantic. The location of the stations is shown in figure 1a. The stations, as shown on the map, are seaward of the Blake Magnetic Anomaly, on the Blake-Bahama outer Ridge between approximately 25° and 27°N latitude and 68° and 74°W longitude. On the AII108 cruise, the thermal conductivity of the recovered piston and gravity cores was measured every 15 cm along the core using the needle probe technique. The cores were sealed and stored for subsequent water content and chemical content measurements at the same sampling locations as the needle probe measurements.

The four heat flow sites chosen on the AII108-5 cruise coincide within .5 km, by acoustic and satellite navigation, with three heat flow sites from the R/V Knorr cruise number 77 in March 1980 and one heat flow site from the R/V Atlantis II cruise number 97 in February 1978. The three Knorr sites located on the Blake-Bahama Ridge include six multiple penetration, "pogo-probe", stations where in situ thermal conductivity was reliably measured using the Lister probe. The Atlantis II 97 site is on the eastern

Figure 1a. Map showing location of AII108 and KN77 heat flow stations, DSDP drill sites, and magnetic lineations. Four sites HF 1 to HF 4 are determined by each cluster of stations, east to west (from Semkin, 1980).

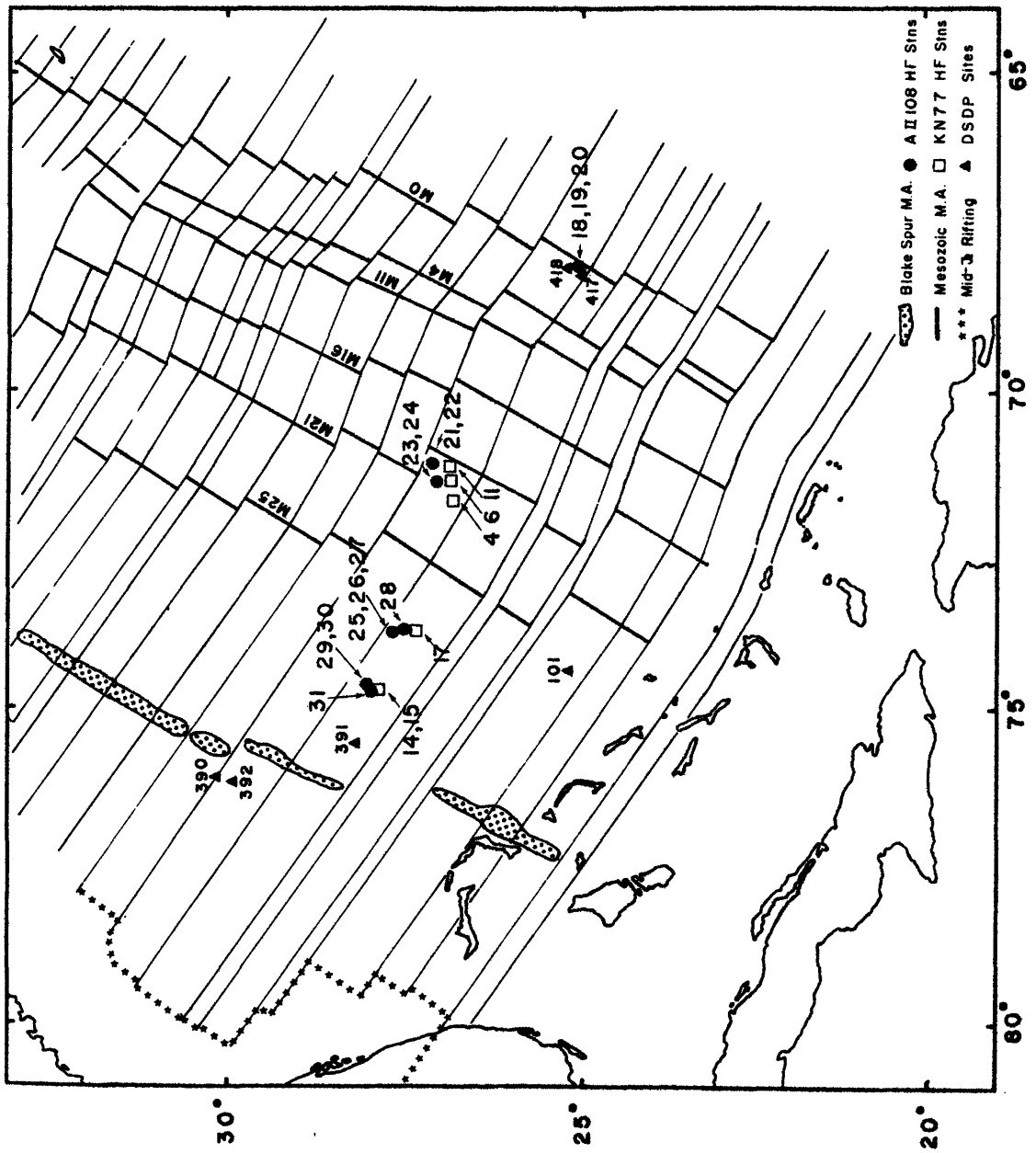
Blake Spur M.A. ● A II 108 HF Stns
Mesozoic M.A. □ KN77 HF Stns
Mid-3 Rifting ▲ DSDP Sites
M0
M4
M11
M16
M21
M25
18,19,20
23,24
21,22
4 6 11
25,26,27
28
29,30
31
14,15
101
390
391
392
30°
25°
20°
80°
75°
70°
65°

edge of the Hatteras abyssal plain and includes five piston cores on which thermal conductivity was measured using the needle probe technique.

In this report, an overview of the instrumentation and calibration of both in situ and needle probe techniques of measuring thermal conductivity is presented, and the conductivity and supporting water content analysis from the AII108, KR77, and AII97 cruises are presented and compared. Thermal conductivity from the deep penetrating cores (up to 9.15 m) and the correspnding in situ stations are compared at each site by statistical analysis. As a result of the high sampling density, a strong correlation is shown in the plots between thermal conductivity and water content versus depth. Finally, an interpretation of the errors from the variation in the data of both measurement techniques is given.

WHOI-80-34

THERMAL CONDUCTIVITY MEASUREMENT OF FUSED SILICA GLASS

by

D. Goldberg, R. P. Von Herzen
and J. Sclater

WOODS HOLE OCEANOGRAPHIC INSTITUTION
Woods Hole, Massachusetts 02543

August 1980

TECHNICAL REPORT

Supported by the National Science Foundation under Grant OCE 79-09448.

Reproduction in whole or in part is permitted for any purpose of the United States Government. This report should be cited as: Woods Hole Oceanographic Institution Technical Report WHOI-80-34.

Approved for Distribution:

John I. Ewing, Chairman
Department of Geology & Geophysics

ABSTRACT

The reproducibility of thermal conductivity measurements on fused silica glass by various investigators using different techniques suggests its suitability as a standard for such measurements. Our laboratory measurements with the needle probe technique on chip samples of silica glass saturated with water gave a value of 3.287 ± 0.154 (S.D.) mcal/cm s °C (n = 21) at 25 °C, which is within about 1% of the previously determined values and the value given by the manufacturer for this material. The good agreement indicates that the flat-plate steady-state and needle probe transient methods give the same value for this material, and that the water-saturated chip technique is an accurate method to measure thermal conductivity of isotropic samples.

INTRODUCTION

The comparison and calibration of different needle probes by measurement of a consistent conductivity standard provided the motivation for this study. The needle probe method described by Von Herzen and Maxwell (1959) is a transient technique for measuring the thermal conductivity of sediments. The technique approximates an infinite line heat source which creates temperature change proportional to the logarithm of time in the surrounding sediment medium. The heat source is generated through a single resistance loop of known characteristics and is placed in a hollow needle with a thermistor to measure temperature at the middle of its length.

When a constant current through the wire applies heat to the sample, the monitored thermistor gives the change in temperature as a function of time theoretically expressed as (Jaeger, 1958):

$$T(t) = \frac{q}{4\pi K} \ln (4\alpha t/Ba^2) \qquad \text{(Eq. 1)}$$

where

$T(t)$ = temperature as a function of time

t = time

q = heat per unit length per unit time

K = thermal conductivity of the sample

α = thermal diffusivity of the sample

a = probe radius

B = 1.7811

Jaeger's equation solved for K over a distinct time interval (t_2-t_1) after the heat has been applied gives:

$$K = \frac{q}{4\pi(\Delta T)} \ln \frac{t_2}{t_1} \qquad \text{(Eq. 2)}$$

where

K = thermal conductivity

ΔT = change in temperature over the time interval (t_2-t_1)

q = heat input

$$= \frac{(\text{heater voltage})^2(0.2389)(2)}{(\text{heater resistance})(\text{heater length})}$$

note: the factor of 2 in the numerator results from the two lengths of resistance wire in the needle as a result of its loop construction.

After the heat has been applied for about 10 seconds, the temperature/time relation approaches a logarithmic asymptote which is valid for two (2) minutes, when the radial boundaries of the 2 cm diameter sample vials begin to affect the temperature. The mean slope of the plotted temperatures versus logarithm of time allows the thermal conductivity, K, to be calculated using the constants from equation 2.

Thermal conductivity of a hard-rock sample can be measured using the needle probe by taking measurements on fragments of that sample (Horai and Baldridge, 1972). The sample is pulverized and saturated with water, packed in a cylindrical container, and the needle probe is inserted into the mixture along the axis. The conductivity of the saturated mixture is modelled as packed spheres of rock in a water matrix, and is determined by the conductivity of its solid and fluid components and the porosity of the mixture (Woodside and Messmer, 1961):

$$K_m = K_r^{(1-\phi)} K_w^{\phi} \qquad \text{(Eq. 3)}$$

where,

K_m = thermal conductivity of the mixture of saturated rock chips and water

K_r = thermal conductivity of the solid rock

K_w = thermal conductivity of water

ϕ = porosity or volume fraction of water in the mixture

Woodside and Messmer's relation solved for K_r gives:

$$K_r = (K_m K_w^{-\phi})^{1/(1-\phi)} \qquad \text{(Eq. 4)}$$

This formula enables the conductivity of a solid rock to be calculated from the porosity, the known conductivity of water (Clark, 1966), and a measured value of the conductivity of its water saturated fragments.

PROCEDURE

The application of the needle probe technique on a fused silica glass standard, chosen for its consistent physical properties, requires a pulverized, saturated sample whose conductivity is reduced to zero porosity by Woodside and Messmer's relation.

The glass sample is crushed with a mortar and pestle into a powder having a 0.5 mm maximum grain diameter. The sample is divided into standard 2 cm diameter plastic vials which are weighed. The powder is saturated with water in a moderate vacuum (20 torr) and agitated to eliminate air bubbles, and any excess water is decanted off of the saturated sample. The sample is weighed again. The difference between the dry and saturated weights gives the volume of interstitial water.

The weight of the dry sample divided by its density gives its volume. If the density of the sample is not known, as is the usual case for sediment samples, the volume of the

saturated sample can be calculated by weighing a volume of water equal to the volume of the saturated sample and subtracting the volume of interstitial water. In appendix B, this method is used to check the given density of the standard and to estimate error.

The porosity, ϕ, of the saturated sample is determined by the volume fraction of water in the volume of the mixture:

$$\phi = \frac{V_w}{V_w + V_s} \qquad \text{(Eq. 5)}$$

where

V_w = calculated volume of water

V_s = calculated volume of the sample

In appendix A, the porosity is calculated from equation 5 and used to determine solid sample conductivity in equation 4.

To measure thermal conductivity using the WHOI-MIT needle probe apparatus (see figures 1 and 2), the saturated sample should first equilibrate to room temperature. A KWH-series needle is inserted into the sample and connected with the "K-box" on function switch 3. Two decade resistance boxes connect to cal 1 and cal 2, function switches 1 and 2, and the heater power is applied by function switch 4. A voltmeter and a chart recorder are also plugged into the K-box.

The temperature of the sample is measured by the thermistor on function 3 as a voltage on the voltmeter. Decade box 1, cal 1, is set to match this voltage reading, and the determined resistance is converted to an ambient

temperature by computed calibration sheets for each KWH-series needle. A temperature 2°C above the measured ambient is chosen, and decade box 1, cal 1, is set to the corresponding resistance. A temperature 7°C above the measured ambient is chosen, and decade box 2, cal 2, is set to the corresponding resistance. The chart recorder is calibrated to the upper and lower temperatures as its zero and full scale bounds, respectively, by the offset and gain controls on the apparatus. The linear recorder scale is maintained by a linearizing bridge circuit in the K-box.

The chart recorder, set at a rate of 4 inches per minute, and the heater power are turned on. The trace on the chart record between 10 seconds and 2.0 minutes will be a logarithmic function of temperature versus time. The temperature values at 0.25 minute intervals on the chart record are plotted on 2 cycle, 70 division semi-log paper, and a linear, best-fit extrapolation to the edges gives the 0.1 minute (t_1) and 10.0 minute (t_2) temperatures. A value for ΔT can be calculated and used in equation 2 to find conductivity, K (see figures 3 and 4).

FUSED SILICA GLASS STANDARD

The thermal conductivity of fused silica glass has been documented by numerous experiments using steady-state methods. A compilation of these values is shown in figure 5. An extrapolation of each data group to 25°C by least

squares regression gives a mean value of 3.093 mcal/cm s ^{o}C with a standard deviation of 0.232 mcal/cm s ^{o}C. The significant scatter may be due to different samples or apparatus used, but each shows a similar linear increase with temperature, indicating similar temperature coefficients.

Other measurements of the conductivity of fused silica at room temperature have been in close agreement. Sass et al (1971) measured 17 fused silica samples using a chip steady-state technique at 3.29 ± .02 mcal/cm s °C, and a solid disc steady-state measurement at 3.26 ± .02 mcal/cm s °C. Ratcliffe (1959), using hot plate and cold bath steady-state methods, determined a value of 3.28 ± .02 mcal/cm s °C. Birch and Clark (1940) measured conductivity of fused silica at 3.26 ± .03 mcal/cm s °C with the steady-state method. The conductivity of fused silica glass is well-constrained by these measurements and is a good standard for needle probe calibration. The standard error intervals determined for these values are purely statistical, not systematic, and are not necessarily representative of the total error for each study.

A fused silica sample of known thermal conductivity was chosen as the standard for needle probe calibration. Corning (Corning Glass Co., Corning, N.Y.) fused silica no. 7940 was obtained for its specified physical properties and high purity. The thermal conductivity of this glass was given by the manufacturer as 3.29 mcal/cm s °C, and the density as 2.202 g/cm^3.

DATA AND DISCUSSION

Thermal conductivity of fused silica standard was measured using four KWH-series needles, nos. 4, 5, 9, and 12, by the technique described above. The calculated conductivities are corrected using a porosity value $\phi = 0.3419$, as determined in appendix A, from equation 4. The conductivity measurements are shown in appendix C and are plotted in figure 6.

The mean conductivity of all measurements (n = 21) on three silica samples is 3.287 ± 0.154 (S.D.) mcal/cm s ^{o}C. The mean of the values determined by each needle, the right-hand column in appendix C, varies from 3.248 ± 0.192 to 3.338 ± 0.159 mcal/cm s ^{o}C. The mean of these four values is 3.294 ± 0.152 ($\pm 4.6\%$). The conductivity values measured by each needle gives a mean and deviation close to those determined by all measurements. This implies that the variation between needles is within the experimental error for any measurement and is probably not a significant source of error. Similarly, the mean conductivity value for each sample of silica glass is within the mean $\pm$ standard deviation of the other two samples, so that there is no significant difference between samples.

The standard deviation of all measurements, about 4.7% of the mean, is only a statistical result and ignores the systematic errors. This is the reproducibility of the technique using any needle, and is approximately the same as that determined by Von Herzen and Maxwell (1959). Since the error between the needles is negligible, the standard error of all 21 measurements, 0.03 mcal/cm s ^{o}C, gives a 1% interval of confidence in the relative mean determined.

Errors that may cause systematic variations include curve fit variations, porosity variation and measurement accuracy, and thermistor calibration. The linear curve used in the analog plotting can be reproduced within a 2% error interval. The porosity may change with time due to the settling of sediment spheres in a water matrix. In addition, air saturation and measurement losses may affect the porosity, creating a small error noticeable by a difference in the weight of the sample before and after saturation. Lastly, a recent recalibration of the thermistors gave a change of 2% for a 5° drift in the measured temperature. These possible systematic errors do not affect the interval of reproducibility of 4.7%, nor the confidence of the relative mean determined, but could bias absolute value obtained.

The statistical mean has only a -0.091% difference from the given conductivity by Corning of 3.29 mcal/cm s °C, and the mean of the values determined separately by each needle a +0.12% difference. These values are also close to the conductivity of fused silica determined by earlier experimentors, as summarized above. The excellent agreement of these average values with previous values suggests that our data and the needle probe technique do not have any systematic biases greater than about 1%.

Appendix A: Porosity

V_S = Volume of silica
W_S = Weight of silica
V_W = Volume of interstitial water = W_W
W_W = Weight of interstitial water
$W_{W'}$ = Weight of equivalent volume of water
W_C = Weight of container
$W_t = W_S + W_W + W_C$
ρ_W = Density of water (Clark, 1966)
ρ_S = Density of silica (Corning)

$$\rho = \frac{V_W}{V_W + V_S}$$

$V_W = W_W/\rho_W$
$V_S = W_S/\rho_S$
$V_W + V_S = W_W/\rho_W + W_S/\rho_S$

	sample 1	sample 2
W_C	20.45	98.61
$W_C + W_S$	64.81	185.60
$W_C + W_S + W_W$	75.26	206.04
W_W	10.45	20.44
W_S	44.36	87.00
ρ_W	0.997	0.997
ρ_S	2.202	2.202
V_W	10.481	20.502
V_S	20.415	39.510
$V_W + V_S$	36.626	60.012
$V_W/V_W + V_S$	0.3422	0.3416
ϕ(%)	34.22	34.16

ϕ_{mean} = 34.19%

Appendix B: Density of Fused Silica

V_s = Volume of silica
W_s = Weight of silica
V_w = Volume of interstitial water = W_w
W_w = Weight of interstitial water from appendix A
$W_{w'}$ = Weight of equivalent volume of water
W_c = Weight of container
$W_t = W_s + W_w + W_c$

$V_s = W_{w'} - W_w - W_c$
$V_s = (39.58\ g) - (10.45\ g) - (9.32\ g)$
$V_s = 19.81\ cm^3$

$W_s = W_t - W_w - W_c$
$W_s = (63.20\ g) - (10.45\ g) - (9.32\ g)$
$W_s = 43.43\ g$

$\rho = W_s/V_s$
$\rho = (43.43\ g)/(19.81\ cm^3)$
$\rho = 2.192\ g/cm^3$
$\rho_{Corning} = 2.202\ g/cm^3$

Error = -0.45%

Appendix C: Thermal Conductivity of Fused Silica

KWH needle	Sample	K_m	$K_r(\rho = .3419)$*	K_{mean}	σ
4	1	2.460	3.236		
4	2	2.531	3.379		
4	2	2.467	3.250	3.328	0.102
4	2	2.564	3.446		
5	2	2.370	3.058		
5	3	2.541	3.399		
5	3	2.533	3.383	3.264	0.153
5	2	2.508	3.333		
5	2	2.415	3.147		
9	1	2.527	3.371		
9	1	2.417	3.151		
9	2	2.365	3.048		
9	3	2.471	3.258	3.248	0.192
9	2	2.621	3.563		
9	2	2.503	3.322		
9	1	2.351	3.021		
12	1	2.552	3.442		
12	2	2.412	3.141		
12	2	2.449	3.214	3.338	0.159
12	1	2.602	3.524		
12	2	2.527	3.371		
	K_{mean}	2.485	3.287	3.294	
	σ	0.0767	0.154	0.152	
	$K_{Corning}$		3.29		
	Error		-0.091%	+0.12%	

* Thermal conductivity of water assumed 1.45 TCU (Clark, 1966, Table 21-14)

Also see bibliography p. 99-100.

References

Akens, J.J., WHOI-MIT thermal conductivity apparatus, unpublished, 1978.

Ballard, S., McCarthy, K., and Davis, W., Method for measuring the thermal conductivity of small samples of poorly conducting materials such as optical crystals. Rev. Sci. Instr., v. 21, p. 905, 1950.

Birch, F., and H. Clark, The thermal conductivity of rocks and its dependence on temperature and composition. Amer. Journ. Sci., v. 238, 1940.

Clark, S.P., Thermal conductivity. Handbook of Physical Constants, Geol. Soc. of Amer., publ., p. 472, 1966.

Eucken, A., Ann. Phys. Leipzig, v. 34, p. 185, 1911.

Horai, K., and S. Baldridge, Thermal conductivity of nineteen igneous rocks 1. Application to the method of thermal conductivity of rocks. Phys. Earth and Planet. Inter., v. 5, p. 151, 1972.

Ito, S., Mazda Res. Rep., v. 4, p. 188, 1928.

Kayes, G.W., and W.F. Higgins, Proc. Roy. Soc. A., v.133, p. 335, 1926.

King, W., and G. Simmons, Heat flow near Orlando, Fla. and Uvalde, Tx. determined from well cuttings. Geothermics, v. 1, p. 133, 1972.

Langseth, M.G., Techniques of measuring heat flow through the ocean floor. Journ. Geophys. Res., v. 70, p. 58, 1966.

Moritz, G., Heat flow in the Cost B-2 well, unpublished, 1979.

Ratcliffe, E.H., Thermal conductivity of fused and crystalline quartz. Brit. Journ. of Appl. Phys., v. 10, p. 22, 1959.

Sass, J.A., A.H. Lachenbruch, and R.J. Munroe, Thermal conductivity of rocks from measurements on fragments, and its application to heat flow determinations. Journ. Geophys. Res., v. 76, p. 3391, 1971.

Seeman, H.G., Phys, Rev., v. 31, p. 119, 1928.

VonHerzen, R., and A. Maxwell, Thermal conductivity of deep-sea sediments by the needle-probe method. Journ Geophys. Res., v. 64, p. 1557, 1959.

Weaks, J., and Seifert, H., Journ. Am. Ceram. Soc., v. 35, p. 15, 1952.

Woodside, W., and J.H. Messmer, Thermal conductivity of porous media. Journ. Appl. Phys., v. 32, p. 1688, 1961.

Figure 1. Analog conductivity apparatus. A. K-box. B. Conductivity needle probe. C. Chart recorder. D. Decade resistance boxes. E. Multimeter.

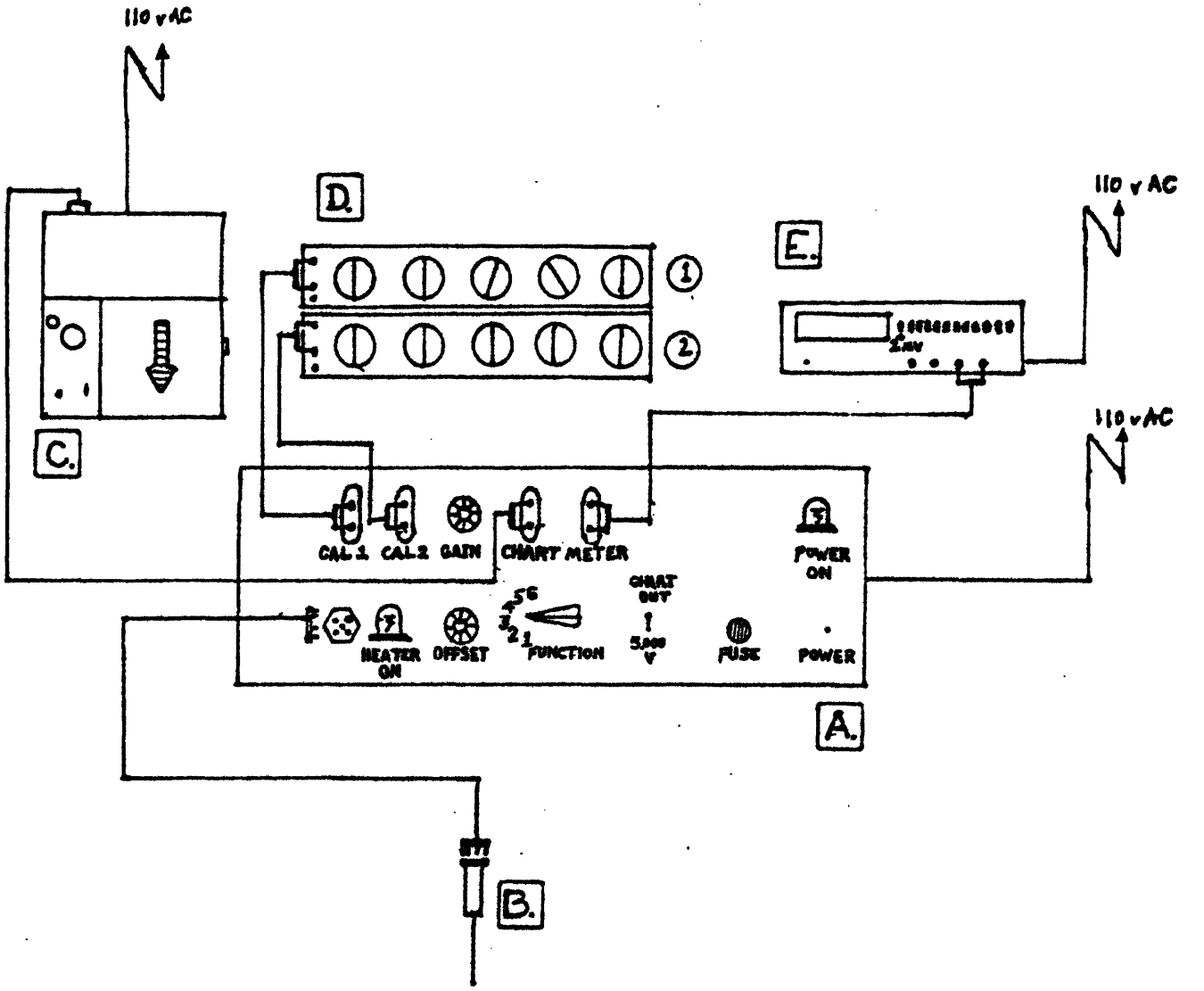

Fig. 1. Conductivity Apparatus. A. K-box. B. Conductivity needle probe. C. Chart recorder. D. Decade resistance boxes. E. Multimeter.

Figure 2. Schematic circuit diagram of the analog K-box. The six function switch positions are: 1. CAL 1, Htr off. 2. CAL 2, Htr off. 3. KNEEDLE, Htr off. 4. KNEEDLE, Htr on. 5. CAL 1, Htr on. 6. CAL 2, Htr on.

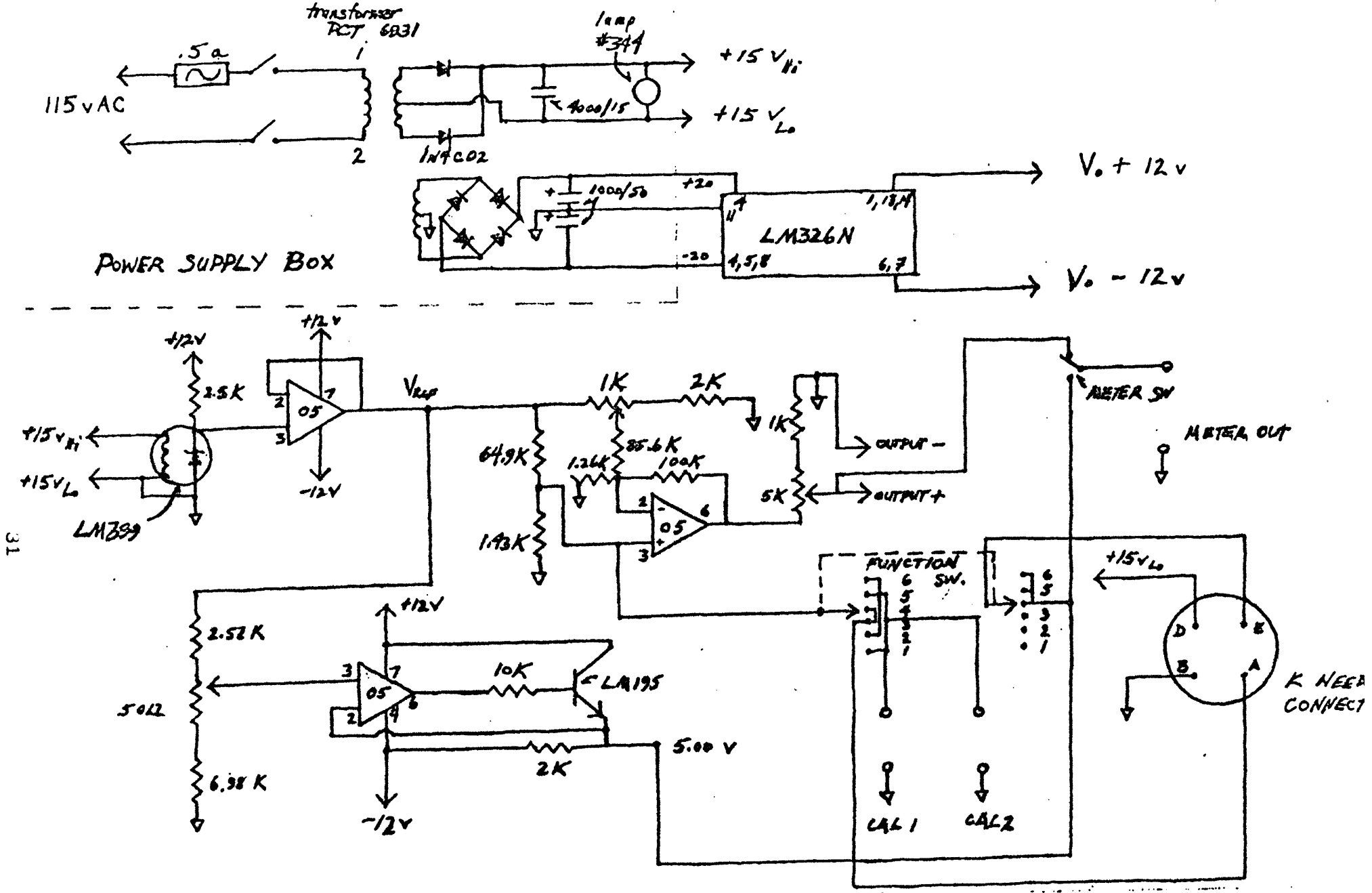
transformer
PCT 6831
lamp
#344
.5a
115 v AC
1
2
1N4002
+15 V Hi
+15 V Lo
4000/15
1000/50
+20
-20
LM326N
1, 18, N
11
4, 5, 8
6, 7
V₀ + 12 v
V₀ - 12 v
POWER SUPPLY BOX
+12V
-12V
2.5K
LM399
+15 V Hi
+15 V Lo
05
VREF
1K
2K
64.9K
1.26K
35.6K
100K
1.43K
1K
5K
OUTPUT -
OUTPUT +
METER SW
METER OUT
FUNCTION SW.
2.52 K
5.00 K
6.98 K
10K
LM195
5.00 V
2K
CAL 1
CAL 2
D
E
B
A

Figure 3. Typical chart record of conductivity measurement of fused silica. Temperatures are chosen at 0.25 minute intervals and plotted in figure 4.

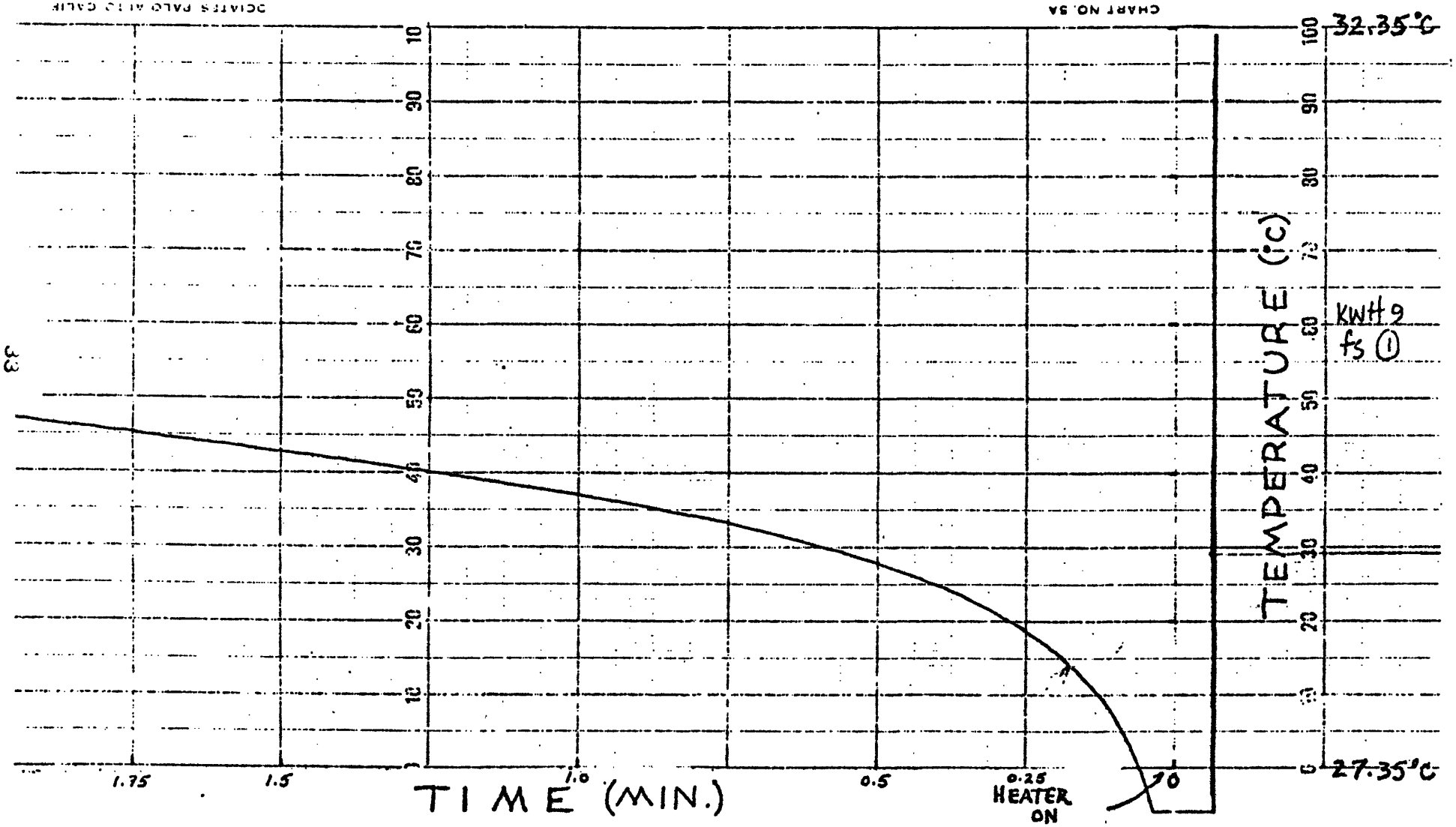
32.35°C
KWH 9
fs (1)
TEMPERATURE (°C)
27.35°C
TIME (MIN.)
1.75
1.5
1.0
0.5
0.25
HEATER ON
0
100
90
80
70
60
50
40
30
20
10
0

Figure 4. Typical logarithmic plot of temperature versus the logarithm of time. The value of K determined is of the silica and water mixture. The divergence of the line near two minutes is due to the boundary effect of the container.

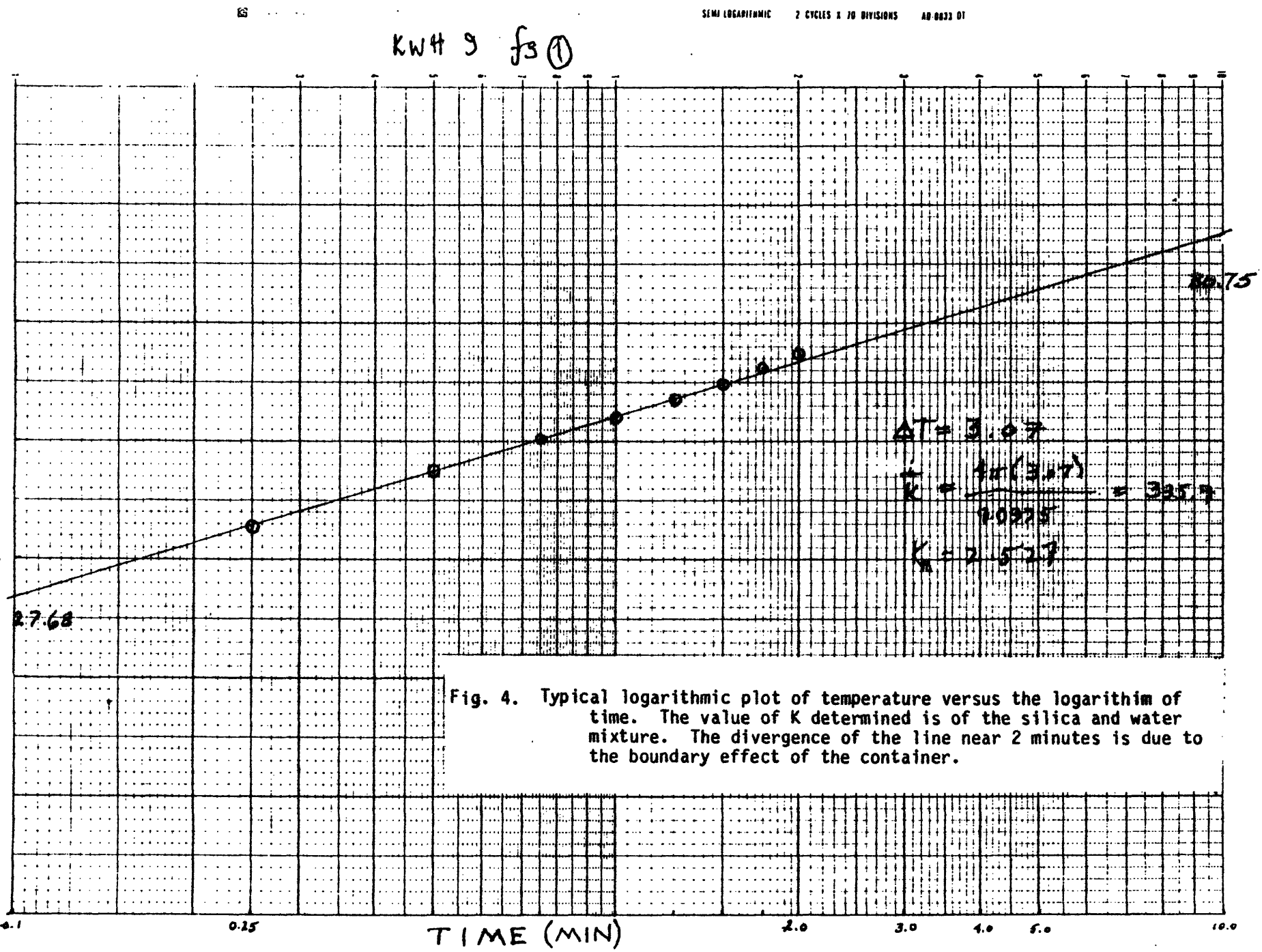

Fig. 4. Typical logarithmic plot of temperature versus the logarithim of time. The value of K determined is of the silica and water mixture. The divergence of the line near 2 minutes is due to the boundary effect of the container.

Figure 5. Compilation of previous measurements of thermal conductivity of fused silica glass. The mean value is 3.093 mcal/(cm s °C) at 25°C.

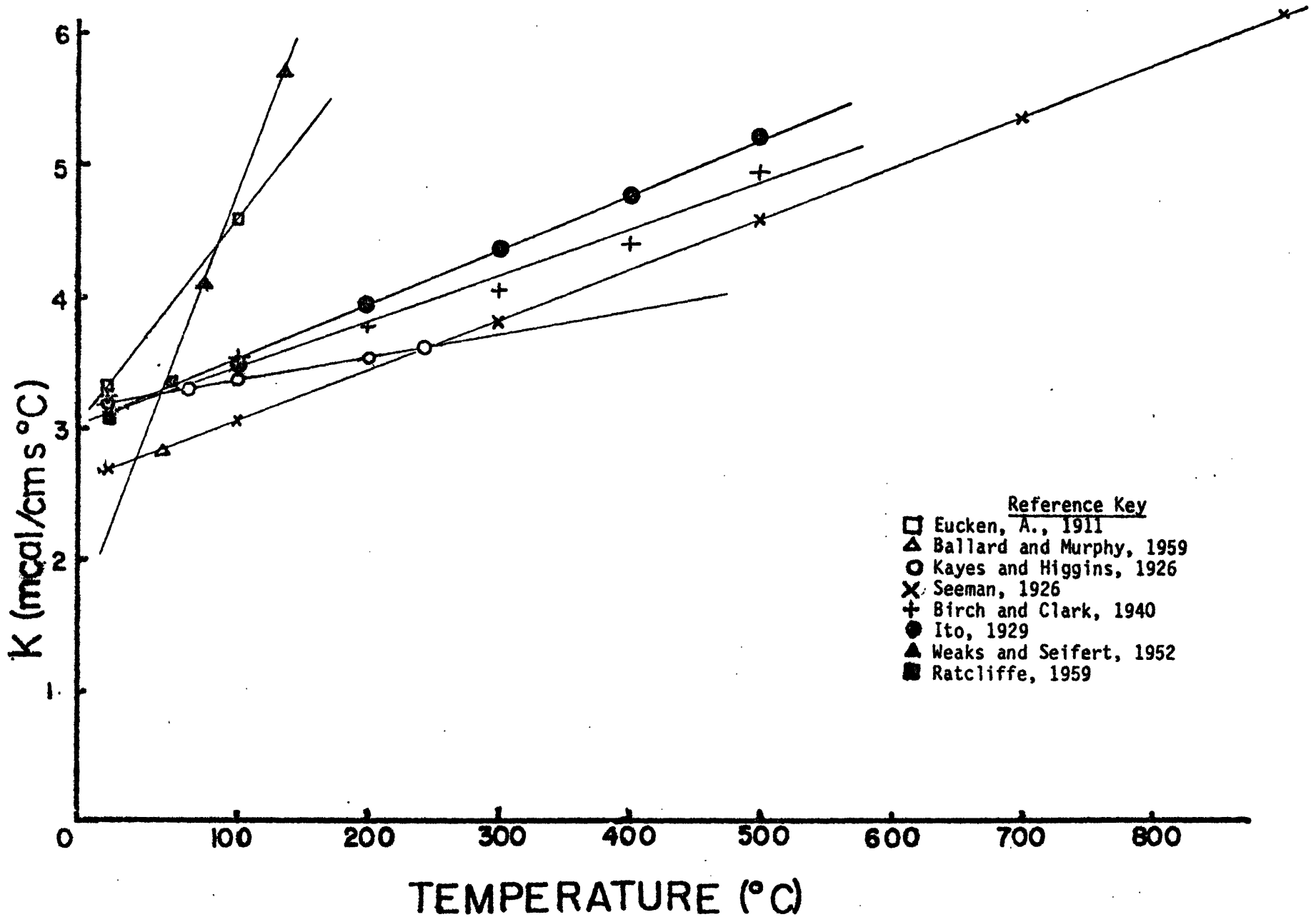
K (mcal/cm s °C)
TEMPERATURE (°C)
0
100
200
300
400
500
600
700
800
1
2
3
4
5
6
Reference Key
Eucken, A., 1911
Ballard and Murphy, 1959
Kayes and Higgins, 1926
Seeman, 1926
Birch and Clark, 1940
Ito, 1929
Weaks and Seifert, 1952
Ratcliffe, 1959

Figure 6. Needle probe measurement of thermal conductivity on fused silica glass. The mean value (n=21) is 3.287 ± 0.154 (S.D.) mcal/(cm s °C).

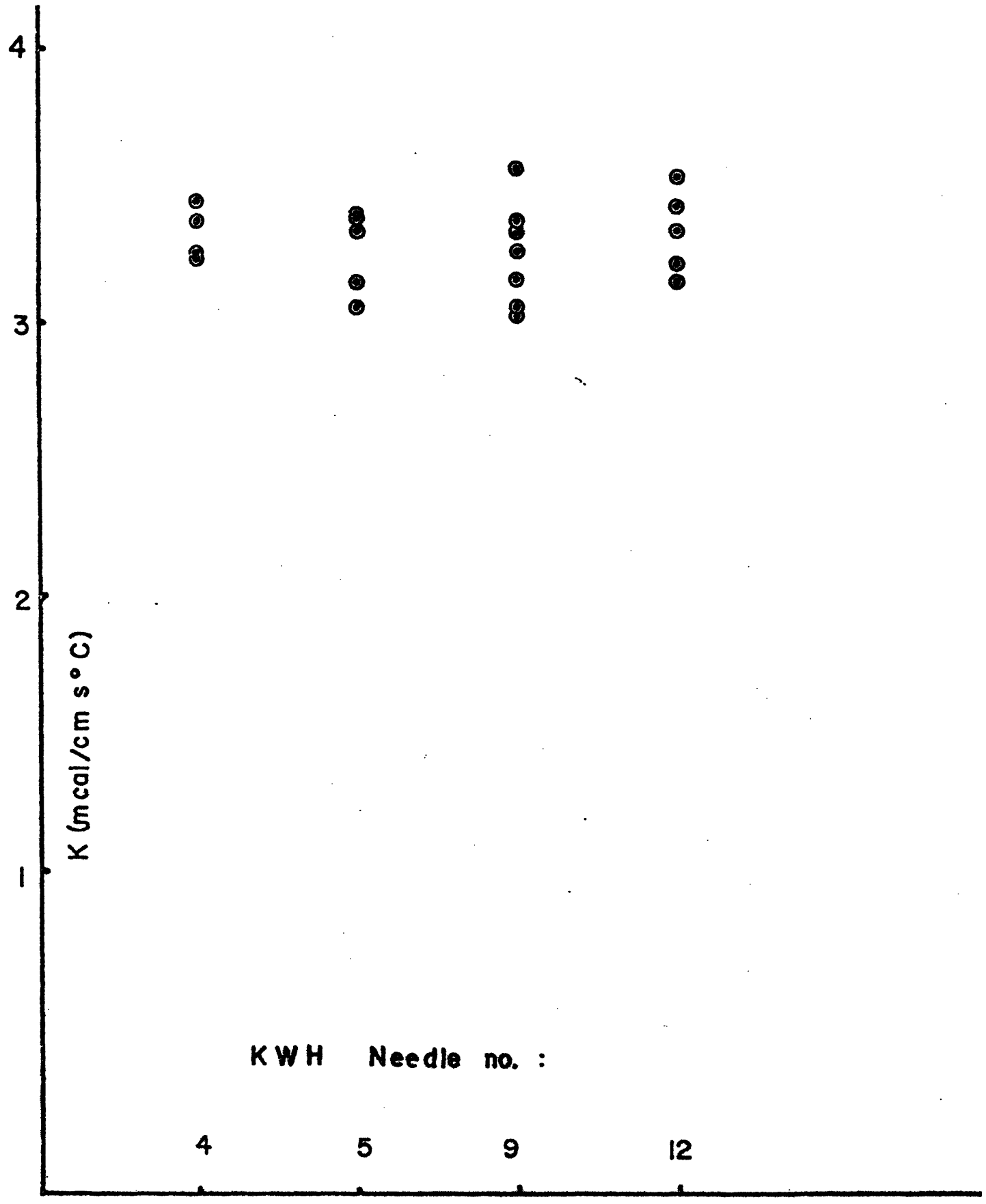
4
3
2
1
K (mcal/cm s °C)
KWH Needle no. :
4
5
9
12

II. DIGITAL CONDUCTIVITY MEASUREMENT

Introduction

The analog needle probe conductivity apparatus (Woods Hole Oceanographic Institution) described in the preceding chapter has been significantly automated by the JOIDES (Joint Oceanographic Institutions) digital conductivity system. Continuously heated needle probes can simultaneously measure up to five positions in a sample over a six minute interval. The data is digitized and punched onto paper tape in ASCII format. Five times the amount of data aquired in one analog run is encoded in each paper tape run. The punched data tape is subsequently processed to attain a numerical value of thermal conducitivty.

Instrumentation

The digital conductivity apparatus consists of a K-box, a digital voltmeter (DVM), a data punch, and five needle probes. A block diagram of the digital K system is shown in figure 7. The probes, K-box, DVM, and data punch are interconnected by wire. When the system operates normally, each conductivity run of about six minutes duration is punched onto about ten feet of paper tape. The software, paper tape, and conductivity program, as shown in the lower portion of figure 7, are loaded into a shipboard computer for immediate processing.

The K-needles operate identically in the analog and

Figure 7. Block diagram of digital conductivity system (from WHOI manual).

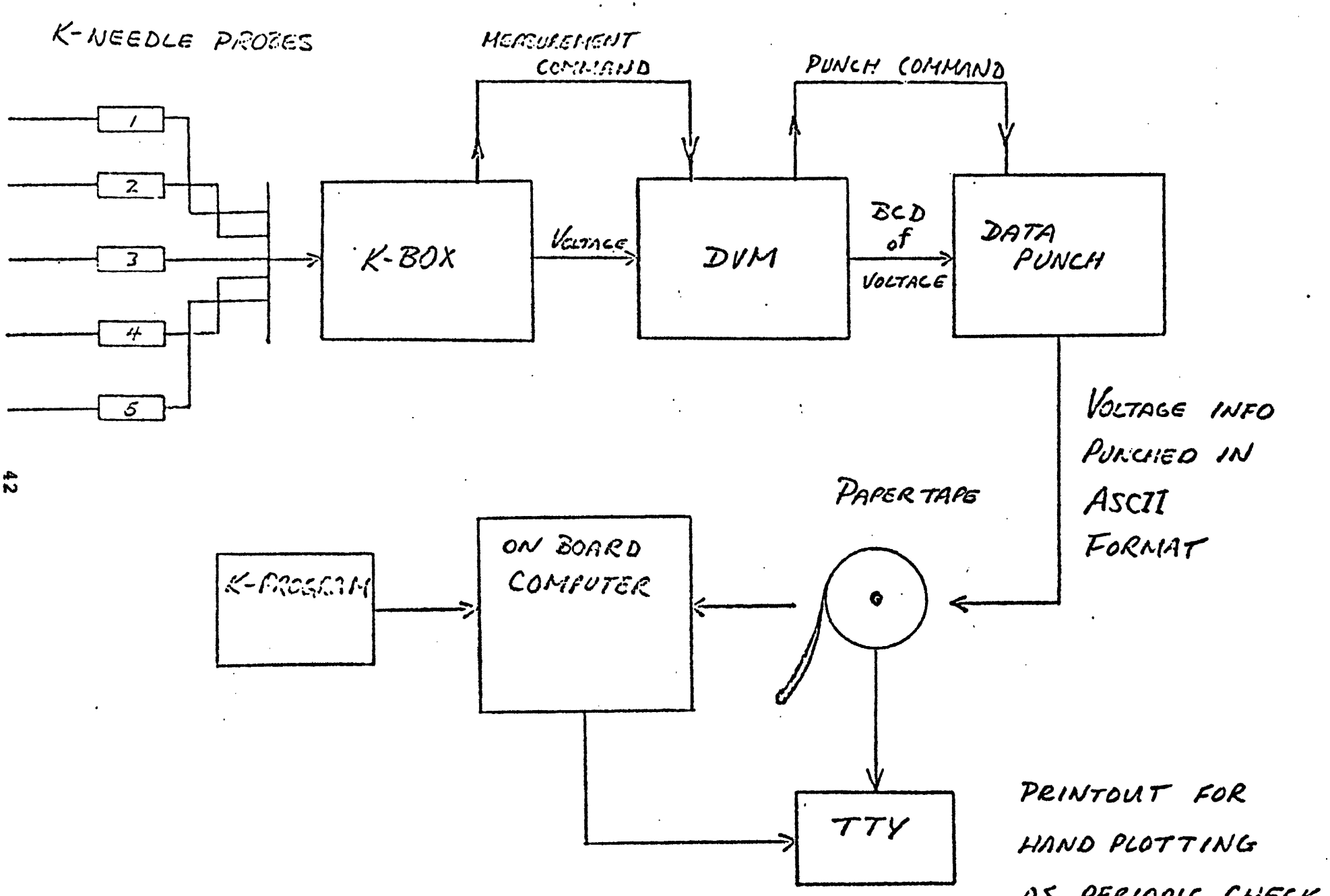
K-NEEDLE PROBES
1
2
3
4
5
MEASUREMENT COMMAND
PUNCH COMMAND
K-BOX
VOLTAGE
DVM
BCD of VOLTAGE
DATA PUNCH
VOLTAGE INFO PUNCHED IN ASCII FORMAT
PAPER TAPE
K-PROGRAM
ON BOARD COMPUTER
TTY
PRINTOUT FOR HAND PLOTTING AS PERIODIC CHECK

digital systems. Both connect by 4-pin plugs on leads to the K-box and measure temperature increase due to an internally heated wire using a high resistance thermistor. Up to five needles can be connected to the digital K-box.

The K-box is a shoe-box sized instrument containing the cycling, measuring, triggering, and timing mechanisms of the digital K system. The front panel of the K-box has controls and indicators for the internal functions. The heater, DVM, automatic counter, calibration, power, and probe-on switches are all controlled on the K-box panel. Also, a series of lights monitors the stepping cycle of measurement through the five needle series. A crystal clock in the K-box oscillates at three second intervals. Six positions--for the five needles and a reference position--are sequentially energized in a stepper switch at three second steps. The triggering mechanism ideally turns the heaters on and starts the stepping cycle immediately, sampling the first temperature at a one step (three second) delay.

A 5.0 volt base power supply in the K-box is connected to each needle and to a reference resistor when the cycling is initiated. The output voltage is measured at the reference position through a 4 kΩ and 10 kΩ precision (±.01%) resistor parallel circuit. The voltage measured at the reference position as the cycle steps through this internal circuit should be 2/7 of the base voltage or 1.430 volts, but this is not always the case. The power supply shows at least

a ±0.1% variation from constant output, as monitored on the DVM or read off of the paper tape. The resistance of each of the five wires connecting the needles to the K-box is approximately .5 Ω. This reduces the power supply voltage available to each heater wire by about .05 volts for each needle connected. Thus, the 5.0 v. base voltage is reduced to about 4.75 v. when five needles are in use. The reference voltage is monitored at about 1.41 ± .01 volts for the reduced base voltage, but an external DVM can be directly connected to monitor the reduced heater voltage.

The high resistance thermistors, 1500 Ω, are connected through the the stepper switch to a 10 kΩ precision resistor, which limits the current from the power supply to 0.435 ma. The stepping cycle measures the voltage at each thermistor. Voltage varies inversely with temperature of the sediment. This measurement can be made with or without the heaters on, which is controlled on the K-box panel. The "heater-off" setting is used to measure temperature drift in the equilibrated sediment prior to a heated conductivity run.

The output voltage data from the thermistors and the reference resistor are displayed on the DVM. The DVM is connected to the data punch which encodes the voltage data in ASCII format, adds a data statement and line number, and punches the paper tape.

There are two electrical problems observed with the K-box stepping cycle. First, the stepping cycle occasionally

skips a position (usually n=6) during a six minute run. This is probably caused by an overload of the 25 W capacitor (recently replaced by a larger one) which regulates the circuit. This problem results in a missed data line in the punched data.

Second, the "heater-on" time is not uniform with respect to the first data point sampled in the cycle, due to an electrical malfunction. The design of the K-box and the original data reduction program assumes (i) the heater is turned on at the moment the cycling is triggered, and that the first sampling point occurs one position, three seconds, later. This occurs at the beginning of about 50% of the runs. Other observed cases of the timing of the first data point with repect to the "heater-on" are: (ii) the first sampling point and the heater turn on instantaneously, or (iii) the heater does not turn on until the first position is sampled, three seconds after the cycling is triggered. These three cases each occur randomly and regularly during use of the K-box.

Both skipping and triggering inconsistencies in the stepping cycle are compensated for in data reduction.

Data Reduction

The data reduction program for the digital conductivity paper tape, THERMCON, is printed in appendix D. This is the latest version of THERMCON and streamlines data reduction

for data from the AII108 cruise. The program calculates the temperature from the output voltage data and prints it versus the time after triggering. From this information, a least squares fit is calculated of the temperature versus the logarithm of time profile and gives the thermal conductivity as its slope. In addition, THERMCON calculates the temperature drift rate and the curve fit parameter of the data that it uses in the least squares regression. Sample numerical output from THERMCON is printed in appendix D.

THERMCON calculates the resistances on the measured output voltages by Ohm's Law assuming a constant current through each needle probe thermistor of .435 ma. Temperature (T) is calculated from the resistance (R) by

$$T = (\alpha + \beta \ln R + \gamma(\ln R)^3)^{-1},$$

where α, β, and γ are the curve fit coefficients of a linear increase of temperature with resistance, precision calibrated in the laboratory to within .01°C for each needle probe thermistor. THERMCON then correlates these temperatures with the sampling time of each measurement after triggering. The slope of temperature versus the logarithm of time is calculated directly from needle constants and output voltage by

$$K = \frac{(\text{heater volt})^2 \times (\text{heater res/length}) \times (0.03802)}{C \times (\text{heater res})^2},$$

where C is the ratio of the determinants calculated from the output voltage and the timing cycle giving voltage as a

function of the logarithm of time.

The voltage data is input into the computer by a tape reader and an interface unit. The input data string numbers and lists four-decimal output voltage. The AppleII Microsoft (Basic) version of THERMCON is also loaded into the computer. The encoding programs CPMTR and APDOS are used to transfer the data string from DOS to Microsoft format. The compatible voltage data and THERMCON are then merged.

The keyed input called for by THERMCON are the initial, reference, and heater voltages, the voltage tolerance, the K-run identification, serial numbers of the needles used, and the date. The serial number is called in a program loop and reads the values of α, β, and γ for that particular needle. THERMCON can then be run with the data string.

THERMCON is designed to ignore the first two cycles of data, 36 seconds or 12 steps times 3 seconds/step, but to continue the count of cycles. It uses the asymptotic value of the next 16 cycles of data in the six minute run to reduce the scatter and to fit a closer least square regression to the data. Basically, the first data points are irrelevant values, but counted steps. Also, the CPMTR and APDOS programs wipe out the first data point in the string when transferring to Microsoft. It must be replaced by a fictitious value (i.e. .5000) to fill the stepping position lost, but is ignored for calculation.

The cycling problems described earlier must be

compensated for in processing by altering the data string. THERMCON has been modified to count the first data point and the "heater-on" time simultaneously, rather than separated by a delay after triggering. Since this timing alignment, (ii), occurs in close to 50% of the runs, it facilitates processing corrections. After the lost data point is replaced, the data string is correctly timed when the "heater-on" and the first data point occur simultaneously.

The first timing alignment described earlier, (i), a one step delay between the "heater-on" and the first sampling point, as originally designed, will give a one step offset in the temperature/time profile processed with the modified version of THERMCON. This is compensated for by an additional fictitious data point (i.e. .5000) added to the beginning of the data string. The third observed timing alignment, (iii), a one step delay of the "heater-on" time concurrent with the first sampling point, has a correctly aligned temperature/time profile for the modified program. These three observed timing situations are monitored by the external voltmeter connected to the heaters so that the timing of the "heater-on" and the first data point measurement can be recorded and corrected.

The other cycling problem, skipping, is corrected in data reduction by the insertion of an interpolated voltage at the skipped position in the data string. The skipped position is easily recognised by the presence of only four

voltage lines between any two reference voltages. The temperature/time profile is then realigned by this interpolated point to within about one second, since the skipped position lasts not the full three second step, but somewhere between one and three seconds. This one second offset creates a negligible error in the conductivity values. When skips occur more that once in any run, the interpolated values may or may not compensate for the misalignment in timing. Such runs are rare, but are usually rejected.

To ensure small external thermal perturbations, and to thereby maintain the accuracy of measuring at true ambient temperature, the drift should be less than .01°C/min. The calculated temperature drift rate by THERMCON occasionally gives invalid or erratic numbers, suggesting that a manual check would insure more satisfactory results. A check is performed after the needle have equilibrated for three to five minutes in the sediment by an external measurement of temperature drift. The digital apparatus is operated normally with the heaters turned off. The punched data is processed similarly to conductivity data, correcting for timing errors, and the temperature/time profile is then examined for large variations indicating large temperature drifts.

Another systematic check is the measurement of conductivity on isotropic standards of known conductivity. Two red rubber and two fused silica glass standards discussed

in chapter I are used regularly for field calibration of the needle probes. The use of standard calibrations supports consistency and accuracy of the method to within the 4.7% reproducibility determined in chapter I. The results and statistical analysis of the conductivity standard measurements made during the AII108 cruise using the JOIDES digital apparatus are discussed in chapter IV.

III. IN SITU CONDUCTIVITY MEASUREMENT

Introduction

The continuous heating method of thermal conductivity measurement (Von Herzen and Maxwell, 1959) applied to a cylindrical probe measures increasing temperature as it slowly approaches an asymtotic slope with time. The continuous heating in situ conductivity probe (Hubbert and Sclater, 1968) requires long in-bottom measurement times to approach asymtotic slope and can suffer large temperature drifts and mechanical disturbances. By introducing a pulse heat source (Lister, 1979) to the in situ thermal conductivity probe described by Hubbert and Sclater, the accuracy, energy conservation, and efficiency of measurement are enhanced. When using a short, calibrated heat pulse, the decay of temperature away from a cylindrical probe is theoretically a function of the diffusivity of the intruded sediment. The short heat pulse reduces the sensitivity to thermal contact between the probe and sediment, since the heat exchanged is only that needed to cool the probe.

The heat pulse is modelled as a delta function input in a known perfect conductor. The true temperature of the probe at any time, T_c, is related to the initial temperature of the probe, T_o, after the heat pulse by

$$Tc/To = F(\alpha, \tau) \qquad \text{(eq. 1)}$$

where $F(\alpha,\tau)$ is a decay function of time, t, and probe radius, a.

$$F(\alpha,\tau) = \int_0^\infty \frac{\exp(-\tau u^2)du}{u(\Delta u)} \qquad \text{(eq. 2)}$$

where

$$\Delta(u) = [u\, J_0(u) - \alpha J_1(u)]^2 + [u\, Y_0(u) - \alpha Y_1(u)]^2$$

$J_n(u)$ and $Y_n(u)$ are Bessel functions of the first and second kinds.

The time constant, τ, and probe constant, α, are given by

$$\tau = \kappa t/a^2 \quad \text{and} \quad \alpha = 2\pi a^2 \rho c/S \qquad \text{(eq. 3a,b)}$$

where

κ = thermal diffusivity
a = probe radius
t = time after heat pulse
ρ = density of the sediment
c = specific heat of the sediment
S = heat capacity of probe material

The solution for large values of τ (Blackwell, 1959) gives

$$F(\alpha,\tau) = \frac{1}{2\alpha\tau} - \frac{1}{4\alpha\tau^2} - \frac{(\alpha-2)}{4\alpha^2\tau^2}\ln\frac{4\tau-1}{1.7811} + O\left(\frac{\ln\tau}{\tau^3}\right) \text{ (eq. 4).}$$

The decay of the heat pulse in a cylindrical probe is analyzed by Lister (1979) to evaluate the effects of variations in material construction of the probe and sediment diffusivity. Lister's analysis of this variation of $F(\alpha,\tau)$ finds that a constant $\alpha = 2$ is a confident approximation giving less than 1% variation in conductivity calculations (Lister, 1979). This substitution in the third term and the resubstitution of large τ's in equation 4 reduce Blackwell's

formula to the asymtotic relation

$$T_a = T_o/2\alpha\tau \ . \qquad \text{(eq. 5a)}$$

Replacing α and τ in equation 5a with their equivalents in equation 3a,b gives

$$T_a/T_o = S/4\kappa\pi t \ . \qquad \text{(eq. 5b)}$$

The heat input q divided by the initial temperature rise T_o is the heat capacity of the probe ,S,

$$S = q/T_o \ . \qquad \text{(eq. 6)}$$

Substituting equation 6 into equation 5b, the temperature of the probe T_a at any time t can be given as

$$T_a = q/4\kappa\pi t \ . \qquad \text{(eq. 7)}$$

For large τ, the slope of the temperature decay versus the reciprocal of the time, 1/t, gives κ, the reciprocal conductivity, 1/K. The later-time slope of the temperature decay gives conductivity simply by its inverse, where time disturbances are easily noticeable "glitches" in the smooth curve.

A correction factor $C(\alpha,\tau)$ (Hyndeman et al., 1979) is defined to include the temperature decay for short-time temperatures. The correction factor, $C(\alpha,\tau) = T_a/T_c$, over the interval τ=1 to τ=5 gives only a 2% change in thermal conductivity. The poorly known thermal properties of the probe and sediment for τ<1 make evaluation of $C(\alpha,\tau)$ infeasible for this interval. The corrected temperature of the probe at any time, T_c, is therefore calculable to within

2% after one iteration of $C(\alpha, \tau)$ (Hyndeman et al., 1979).

Instrumentation

The Lister violin-bow probe consists of a steel strength member and a sensor. The steel strength tube is 5.7 cm in diameter and seven meters long, and the "violin-string" sensor is mounted under tension on three fins at a distance of one diameter away from the strength member. Seven thermistors and one reference resistor are housed within the steel rod equally separated along the seven meter length. The insulated heater wire runs through the length of the probe equidistant from the tube walls at each thermistor location. The center of the probe is filled with mineral oil to improve thermal contact between the thermistors and the sediment.

The thermal conductivity heat pulse is delivered to the instument's 3.0Ω heater wire by an electric cell regulated to 36 volts and a maximum 12 amp current. The heat pulse lasts about $.2\tau$ or approximately 14 seconds for the seven meter probe. The induced temperature increase above the ambient due to the heat pulse is about 1°C after one minute has elapsed. This is significantly larger than the frictional heating from penetration and short enough to approximate the delta function heat source.

The electronic and telemetric circuitry is housed in a pressure casing at the top of the steel tube. Weights are added on top of the casing to increase the penetration.

A crystal clock regulates temperature sampling at one second intervals at successive thermistors through eight separate wheatstone bridges (one for each thermistor and the reference resistor). The digital data is encoded in acoustic pulses and transmitted to the ship. The acoustic signal is received by hydrophone, demodulated, and recorded. The temperature versus time history represents the successful capture of the digital in situ conductivity data. Numerical analysis of the data can then be processed by computer for conductivity evaluation at each penetration.

The lowering of the instrument every .5 km at a ship speed of about 1 knot results in 20 to 25 penetrations of 15 minutes optimum duration. An acoustic pinger/transponder is attached several tens of meters up the wire to monitor the distance of the instrument from the bottom between penetrations.

Data Reduction

A typical trace history of the telemetered data is shown in figure 8. Five to ten minutes is allowed to attain equilibrium after each penetration and prior to the heat pulse. In this sample, the decay of the temperature is smooth after the heat pulse (no "glitches") so that thermal conductivity determination is a simple extrapolation of $F(\alpha, \tau)$ versus temperature.

Several systematic time delays are added to correct the

Figure 8. Typical temperature dacay history for *in situ* conductivity measurement (from Hyndeman *et al.*, 1979). (see text)

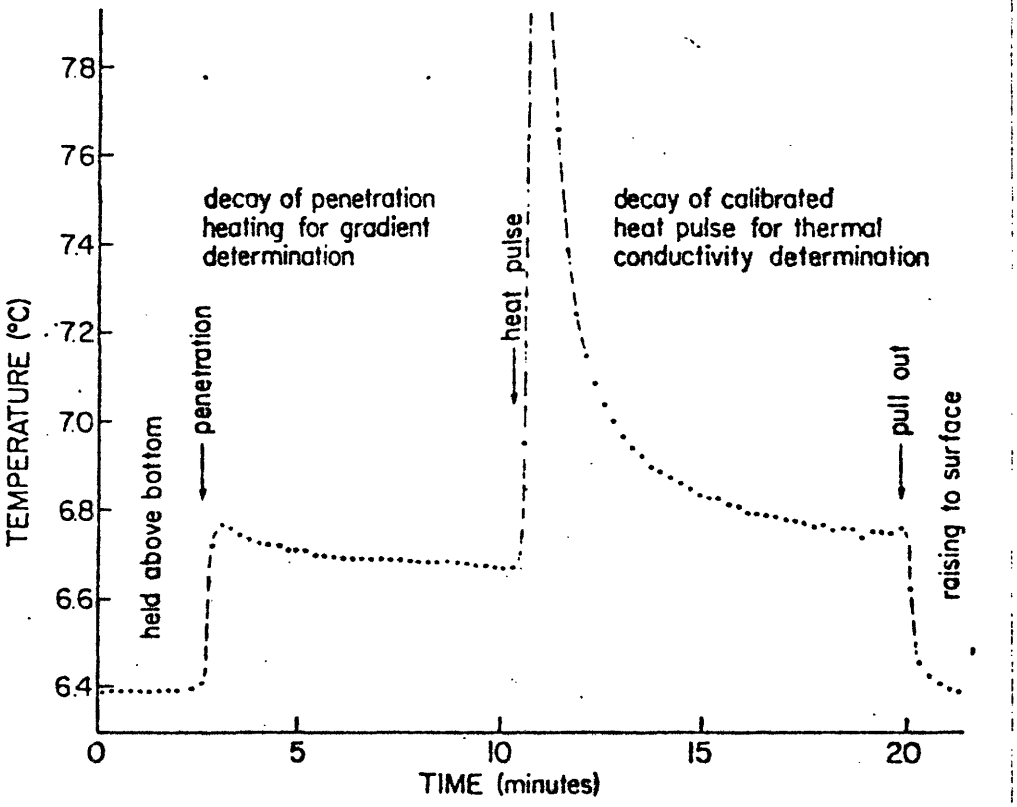
7.8
7.6
7.4
7.2
7.0
6.8
6.6
6.4
TEMPERATURE (°C)
held above bottom
penetration
decay of penetration heating for gradient determination
heat pulse
decay of calibrated heat pulse for thermal conductivity determination
pull out
raising to surface
0
5
10
15
20
TIME (minutes)

initial origin time in data reduction. First, the sampling of temperature at the seven thermistors is sequential after the initiated heat pulse. The sampling cycle is 1 second between thermistors, so that a standard delay constant, 1 second, is added to the origin time of the heat pulse, T_o, at each successive measurement.

Second, the thickness of the steel probe and the oil insulation between the thermistors and the sediment widens the heat pulse with time, so an effective origin time must be estimated. The effective origin time for each of the seven thermistors over several (n=5) penetrations averages to delay times of 17 seconds from T_o for the upper five thermistors and 35 seconds for the lower two. The unisotropic oil concentration in the probe causes variation in these values of about 2 seconds for some penetrations. The uncorrected effective origin time can create errors in excess of 5% in the calculated conductivity.

Third, the post-equilibrium mechanical slumping of the sediment creates an additional frictional heat input. These appear as "glitches" in the decay curve and are common in soft sediment. An additional delay time, T01, which estimates the ffset of the glitch, is added to the corrected origin time. The induced temperature rise then appears as an earlier time measurement and decays normally. These delays vary in duration up to several seconds.

Finally, the difference between the extrapolated

infinite time temperature from the decay of the heat pulse and the decay of the pre-pulse frictional heating, which ideally are equal, reveals a residual heat input after the heat pulse decays. The residual temperature, T_E, can be eliminated by the calculation of conductivity from the actual slope of temperature versus $F(\alpha,\tau)$, rather than from the difference of ambient and measured temperatures. This difference remains uncorrected, it may also result in a 5% error in conductivity.

The reduction of the complete temperature history of a penetration to $F(\alpha,\tau)$ versus temperature plots and conductivities involves a five subroutine program written by Linda Meinke at MIT. The program prints plots for each penetration of $F(\alpha,\tau)$ versus T_C and depth for all seven thermistors. The numerical output of the conductivities at each sampling at each thermistor and the delay time constants are listed for several penetrations in appendix G. The appearance of non-linearities or curvature in $F(\alpha,\tau)/T_C$ imply inaccurate data or delay constants or other perturbation to the decay history. The measurements and statistical analysis of the in situ conductivity data from the Knorr 77 cruise are listed in appendix G and detailed in chapter V.

IV. ATLANTIS II 108 LEG 5 HEAT FLOW DATA

Navigation

The navigation used during the Atlantis II 108 was primarily the Loran C acoustical transponder network (Hunt et al., 1974). Occasional satellite fixes were taken to determine the absolute location of the accoustic transponders. The Loran positions are an average of 0.5' south and 1.0' east of the satellite fixed positions. The accuracy of navigation with the Loran acoustic transponders and satellite fixes is estimated to be ±100 meters (Purdy et al., 1979).

Fourteen heat flow stations were cored at positions coincident within .5 km with heat flow stations from the KR77 and AII97 cruises. These are located at four heat flow sites in mesozoic well-sedimented, "A" environment (Sclater et al., 1976), basins. Site HF 1 is located in 110 ma crust, near anomaly M0, where piston cores PC 14, 15, and 16 were recovered. Four piston cores, PC 17, 18, 19, and 20, were recovered at HF 2 near anomaly M21, 145 ma crust. Both HF 3 and HF 4 are located between anomaly M25 and the Blake Magnetic Anomaly, where HF 4 is about 60 km west of HF 3, in 165 ma and 155 ma crust respectively. Three gravity cores were recovered at each site, GC 1 to GC 6 successively, and an additional pilot core, PG 21, at HF 3. Table 1 gives a summary of the piston and gravity core numbers, station

Table 1 -Summary AII108 leg 5 Stations

Sta#	Core	Site	Date	Depth (m)†	Latitude	Longitude
18	14 PC	1	23-5-81	5450	25°02.3"	68°03.0"
19	15 PC			5450	25°07.8"	68°04.5"
20	16 PC			5380	25°06.8"	68°01.4"
21	17 PC	2	24-5-81	5410	27°04.4"	71°06.8"
22	18 PC			5420	26°56.6"	71°09.7"
23	19 PC		25-5-81	5335	26°57.3"	71°24.6"
24	20 PC			5330	26°55.8"	71°25.2"
25	21 PC	3	26-5-81	4575	27°31.5"	73°45.0"
26	1 GC			4525	27°33.0"	73°48.1"
27	2 GC			4530	27°29.3"	73°50.2"
28	3 GC			4540	27°22.6"	73°48.4"
29*	4 GC	4	27-5-81	4795	27°58.0"	74°37.7"
30*	5 GC			4795	27°53.5"	74°42.1"
31*	6 GC			4820	27°55.5"	74°45.3"

* Position based on Loran C (see text)

† Depth in uncorrected meters (see text)

locations, and water depths during the AII108-5 cruise.

The water depths are calculated by echo sounding intervals assuming an average sound speed of 1.500 km/sec in salt water. The acoustic relay pinger emits 12 kHz sound vibrations which reflect from the seafloor and directly return to the hydrophone recorder aboard ship. The crossover time of the reflected and direct records gives the difference in times between the pinger to seafloor to ship and the pinger to ship arrivals, assuming the same velocity of travel. The crossovers occur when the difference between these arrivals equals an integral multiple of the speed of sound.

The depth is calculated geometrically for the pinger located directly beneath the ship by the speed of sound times one-half the difference in arrival times plus the pinger to ship arrival time. Calculation of these values are tabulated in Matthews (1939) for crossover times and mean vertical sounding velocity versus depth. The angle of the cable to the seafloor and variation in the speed of sound due to temperature, pressure, and salinity cause errors in the vertical mean evaluation of depth. They can be approximated using geometric relationships and correction tables in Matthews (1939). Since the study area has been often surveyed and accurate bathymetric maps are readily available, the estimates of depth were needed only to approximate the seafloor to core separation (±15 meters) to slow the cable

"pay out" at 30 meters before penetration. The angle of the cable varied about ±10° for most of the stations, and the echo sounding approximations and bathymetric map estimated the depth adequately (±15 meters) at all but one station. The depths are therfore shown as the uncorrected values estimated from simple echo sounding calculations.

The penetration of the piston and gravity cores is assumed to be nearly vertical, since the wire angle was usually less than 10° from vertical, no core barrels were damaged by skewed penetrations, and sediment recovery was nearly always maximum. Using a 30 foot, 9.15 meter, Ewing design piston core (Ewing and Gerrard, 1962), between 8.0 and 9.0 meters of sediment were usually recovered. On station 25, the cable to corehead link failed and the piston core apparatus was lost. On successive stations, the gravity coring apparatus usually recovered between 5.0 and 6.0 meters of sediment. The primary difference in result between the two coring techniques is penetration depth.

The piston core apparatus is tripped by a pilot gravity core, 1.53 meters in length, which pulls a piston and the intruded sediment up into the core barrel. The "pay out" is slower, easing the strain on the winch, and penetration depths are greatly increased over the gravity coring technique. The gravity core barrel and weight head are lowered at full speed "pay out" to generate the greatest possible impact force for penetration into the sediment.

Conductivity Measurement

Onboard laboratory measurements of thermal conductivity were made on each recovered core using the JOIDES digital conductivity system. The K-box and data punch were interconnected and plugged into the ship's generated 120 VAC power supply. An external voltmeter was also connected and used to monitor the "heater-on" origin time.

Core samples were equilibrated for 24 hours prior to measurement in the air conditioned laboratory to allow them to reach ambient room temperature. Thermal conductivity was usually measured during the evening to decrease the risk of large temperature drift caused by an outside to inside temperature difference. The temperature drift was checked by a separate run of the K-box with the heaters off at every other core section, each 1.53 meters in core length. Two conductivity runs were made on each core section.

Drift rates calculated by THERMCON and by separately monitored measurement do not generally correlate. This is probably due to erratic early-time temperature measurements which the reduction program smoothes over with a geometrical fit to the data. This is not troublesome since both values, calculated and computed, usually equal less than 0.01 °C/min drift rate. This is a negligible temperature error for the calculation of conductivity of this precision. Only a few measurements have exceptionally high drift rates of greater than .01°C/min and have to be rejected.

The core sections were moved infrequently and carefully, minimizing the internal water movement. No noticeable water migration, or disturbed air pockets were created during the measurement of thermal conductivity. All of the water content measurements are consistent, showing that the care taken aboard ship with the samples was effective.

Calibration

The needle probes were recalibrated at sea by thermal conductivity measurement of fused silica glass and rubber standards. The silica standards are identical to those described in chapter I. The red rubber standards are three inch diameter hard rubber cylinders which are easy to transport and use for rapid calibration. All of the standards had between 8 and 16 measurements made at sea. This assures the proper functioning of the needles, within the standard errors described in chapter I, and signals any gross mismeasurements.

The compilation of the fused silica thermal conductivity measured on the AII108 cruise is shown in Table 2. Two silica measurements were made at each of the six piston core stations 19 through 24, and two measurements each at gravity core stations 28 and 31. A total of 16 measurements were made using four different needle probes, serial numbers KWH 12, 9, 4, and 3. The arithmetic mean and

Table 2 - AII108 leg 5 Mean Silica Conductivity
[K in mcal/(cm sec °c)]

Meas.#	KWH serial #	K	Mean K (n=4)	Std. Deviation
1	3	2.979	2.959	0.119
2		3.719†		
3		3.094		
4		2.805		
5	4	2.948	2.900	0.078
6		4.013†		
7		2.790		
8		2.961		
9	9	2.600	2.897	0.387
10		1.090†		
11		3.520		
12		3.373		
13	12	2.607	2.700	0.119
14		3.700†		
15		2.625		
16		2.869		
Mean (n=12)		2.931	2.887	0.277

† Values rejected outside standard deviation

standard deviation of the 16 measurements are 2.981 and .645 mcal/(cm s °C), respectively, which includes four values outside of the standard deviation. The mean and standard deviation excluding those erratic values outside the standard deviation are 2.931 and .277 mcal/(cm s °C) (n=12), respectively. The averages for each separate needle, n=3, are near this latter mean and deviation.

The values excluded in determining the average conductivity of 2.931 ± .277 (n=12) are greater than 20% from the mean. A high temperature drift rate, mechanical disturbance, or program miscount are reasonable sources of the error. Unfortunately, the silica runs are short--a limit of two minutes is imposed by container reradiation of heat--and it is difficult effectively to monitor temperature drift or interpolate a skipped voltage.

The mean conductivity of these measurements is within about 10% of 2.485 mcal/(cm s °C), the mean value found in chapter I. The higher mean conductivity and deviation in the shipboard measurements are probably caused by poor temperature control, insufficient sampling positions from the shortened runs, or malfunctions of the digital K-box electronics which are not present using the analog technique. In our estimation, the silica standards provided an accurate systematic calibration of the needle probes for the precision available with the digital system.

The accuracy of rubber standard calibration is similar.

The values we measured and those measured by Von Herzen during leg 4 of the AII108 cruise are summarized in Table 3 at each of the rubber standard positions. Different needle probes, serial numbers KWH 12, 9, 6, 4, and 3 were inserted into holes drilled in the rubber and coated with thermal compound for an improved contact. Eight measurements were taken at positions 2A and 2B and sixteen at positions 1A, 1B, and 1C.

The arithmetic mean of the thermal conductivity at each position shown in Table 3 subjectively excludes a few measurements which deviate greatly. The standard deviation is then 10% or better at each position. The conductivity and standard deviation measured by Von Herzen on the same standards are systematically lower, but nearly all are within their deviations of our values. The deviation increases roughly as a factor of n; twice the scatter is observed for sixteen measurements as for eight. This may be indicative of the poor consistency of the rubber standards.

The reproduciblity of these standards is about 10%, but they provide an easy test of large biases is the system. The rubber standards logically have a reproducibility greater than the systematic error of the needle probe. The enlargement of the drilled holes with use, the conductivity of the thermal compound involved, and the entrappment of air bubbles during measurement all probably introduce erratic error into the conductivity. We feel that the results of

Table 3 - AII108 leg 5 Rubber Standard Conductivities
[K in mcal/(cm sec °C)]

Run	Standard Position:	1A	1B	1C	2A	2
1		2.466	2.571	2.309	5.585†	4.739†
2		2.535	2.333	2.548	2.427	2.390
3		2.740	2.537	2.925	2.503	2.440
4		3.314†	2.751	3.178		
5		3.242	2.874	3.368†	2.500	2.428
6		2.965	2.582	2.995	2.403	2.428
7		3.058	2.842	3.175	2.472	2.324
8		2.855	3.142	3.003	2.399	2.450
9		2.948	2.368	2.418	2.813	2.521
10		3.289	2.853	5.003†		
11		2.606	2.140	2.510		
12		3.127	3.532†	2.248		
13		2.718	2.121	2.489		
14		2.399	2.425	2.817		
15		2.275	2.870	2.749		
16		2.734	2.199	2.472		
Mean K		2.797	2.574	2.703	2.502	2.426
S.D.		0.289	0.299	0.304	0.133	0.055
n		15	15	14	7	7
Mean K'*		2.49	--	2.65	2.37	2.33
S.D.'		0.15	--	0.10	0.09	0.09
n'		7	--	5	9	9

* From AII108 leg 4 measured by R. Von Herzen
† Values rejected outside standard deviation

these standard measurements are adequate for the systematic errors involved and successful as a rough calibration. The use of fused silica as a laboratory standard gives an accurate reproducibility and standard error of measurement.

Statistical Analysis

Thermal conductivity measurements at 15 cm intervals in 14 recovered cores total about 600 measurements. This equals 120 runs, each involving 5 measurements, using the digital K apparatus. Needle probe serial numbers KWH 12, 9, 6, 4, and 3 were used in the same position order for all of the successful runs. One rubber standard (n=5), one silica (n=2), and two temperature drift (n=10) runs were made during the measurement of each six sections of sediment (about one piston core).

The digital punch data tape was processed at sea, but the reduction program used did not ignore the first two cycles of data and the reduced data had to be rejected. The reprocessing of the K data and the measurement of water content were done at Woods Hole Oceanographic Institution after the ship's return.

The number of sampling sites used in analysis of each core varies due to erratic measurements and different lengths of core recovered. Digital conductivity measurements are successful for all of the retrieved cores. Piston cores PC 14 and 15 had some preliminary measurement problems

including shorted thermistors and unmonitored heater origin times. The overloaded thermister measurements are excluded. The heater on time is assumed to be designated as a three second delay after triggering. This seems to give consistent conductivities for most runs in PC 14 and 15. The remaining twelve cores are monitored correctly for varying heater origin times and are corrected for in the processing of the data string as discussed in chapter II.

Pilot core conductivity and water content are not included in the analysis of each coring station. Pilot core values are often erratic due to superpenetration, repenetration, or skewed penetration of the smaller gravity core head. The conductivity and water content of the pilot core may or may not be representative of the upper meter and one-half of sediment. They therefore are recorded, but excluded in analysis.

The statistical analysis of the conductivity data is straightforward. Table 4 lists the labelling, physical, and mean conductivity data at each of the coring stations. The arithmetic mean, $\overline{K}$, and standard deviation, S.D., of all measurements at that station, n, are calculated in those respective columns in Table 4. These values are calculated by

$$\overline{K} = \sum_{n=1}^{N} K_n/N$$

Table 4 - AII108 leg 5 Mean Needle Probe Conductivity Measurements
[K in mcal/(cm sec °C)]

Sta#	Core	Length (cm)	#sec	n	Mean K	S.D.	FEK
18	14 PC	840	6	52	2.232	0.113	0.071
19	15 PC	845	6	55	2.277	0.120	0.073
20	16 PC	812	6	55	2.236	0.105	0.067
21	17 PC	750	5	45†	2.576	0.246	0.115
22	18 PC	848	6	47†	2.564	0.180	0.090
23	19 PC	603	4	30†	2.499	0.130	0.092
24	20 PC	857	6	45†	2.465	0.372	0.169
25	21 PG*	143	1	10	2.460	0.128	0.072
26	1 GC	210	2	15	2.400	0.098	0.061
27	2 GC	540	4	35	2.308	0.130	0.076
28	3 GC	566	4	35	2.276	0.097	0.063
29	4 GC	393	3	24	2.230	0.096	0.063
30	5 GC	343	3	29	2.376	0.192	0.101
31	6 GC	352	3	30	2.325	0.091	0.059

* Pilot core 21 PG is the only pilot data used for analysis
† Values rejected in calculation of mean conductivity (see text)

and

$$\sigma = \sqrt{\sum_{n=1}^{N}(K_n-\bar{K})/(N-1)} \ .$$

The range of mean conductivity at all the stations is 2.230 to 2.570 mcal/(cm s °C), about 10%, with standard deviations from 0.096 to 0.372.

If the standard deviation of all measurements in a core is over about 5% of the mean, the values outside of the interval first calculated are excluded, as previously mentioned. To sustain confidence in the reproducibility of needle probe measurement by calibration with fused silica, the erratic values due to either systematic or measurement errors are excluded. The only values excluded for this reason are from site HF 2, where a large variation in water content corresponds with standard deviations up to 20% in conductivity. Such great variation is not a result of a large standard error in a particular value, previously estimated at 1% by calibration (Goldberg et al., 1980), but real effects which distribute the scatter unevenly and skew the mean. A representative average, excluding values outside of the standard deviation, gives a more realistic average of the vast majority of measurements on that core. That number of measurements, n, shown in Table 4 is used for the arithmetic mean, and a standard deviation generally of less than 5% of this mean is observed for all stations.

The standard error, e, is a measure of the precision of

a particular measurement within the standard deviation of the other measurements of that core.

$$e = \frac{\sum_{n}^{N} \sigma_n}{\sqrt{n(n-1)}} \quad (0.8453)$$

For the number of measurements in each core, n = 20 to 55, the standard error is approximately .857σ or about 4% for the standard deviations of about 5% on these measurements.

Another measure of the accuracy is the fractional error of conductivity, FEK, as described by Galson (1979). This is simply the ratio of the standard deviation to the mean conductivity plus a buffer of .02 for the systematic biases of needle probe measurement.

$$FEK = \sigma/\overline{K} + .02$$

This value is calculated at each station in the last column of Table 4. It is generally .10 ± .05 for these measurements as listed and is an approximate measure of the scatter around the mean conductivity.

The average thermal conductivity at each site, HF 1 to HF 4, the average standard deviation, and the average FEK from the means at each coring station are listed in Table 5. The mean and deviation at each site are more representative of the scatter than an absolute value since the sediment properties and systematic errors give a wide range of values. The mean conductivities at sites HF 1, 3, and 4 have standard deviations of about 5%, .12 mcal/(cm s °C), and average total

Table 5 - AII108 leg 5 Average Needle Probe Conductivity:
Sites HF 1 to HF 4 [in mcal/(cm s °C)]

Site	#Stns	$\overline{K}$	$\overline{\sigma}$	$\overline{FEK}$
HF 1	3	2.248	0.113	0.070
HF 2	4	2.526	0.231	0.117
HF 3	3	2.331	0.108	0.067
HF 4	3	2.310	0.126	0.074

FEK of about .07, 7%. Site HF 2 has a standard deviation of .231 mcal/(cm s °C), 9%, and a total FEK of .117, 11.7%. This is representative of the wide variation in water content in the site HF 2 stations. The mean thermal conductivity at each site is precise, within a standard error of about 4%, and is a realistic representation of the physical scatter. The confidence in the needle probe technique and these results provide an stable basis for comparison.

Water Content

The water content is measured by water weight in a sediment sample. The fourteen cores, 66 sealed sections, were split, sampled, and resealed during the first week after the return of the AII to Woods Hole. The samples are taken by syringe of about 5 cc, at the same position in the core as were the needle probe measurements. The samples are weighed wet immediately after they are taken, oven dried, and weighed again. The water content of the sample is calculated by the difference in wet and dry sample weight divided by the dry sample weight:

$$W = \frac{\text{water weight}}{\text{solid weight}} .$$

The percent water by weight is simply the recalculation of the same measurements:

$$w = \frac{\text{water weight}}{\text{total weight}} .$$

The water content and thermal conductivity of each core at the AII108 leg 5 sites are plotted versus depth in the core from the sediment surface in figure 9 a, b, c, and d. Excellent inverse correlation between water content and conductivity is apparent in these figures. The magnitude of the variation in both K and W are comparable from the scale chosen, and the precise correlation between them is most obvious for large variations of K and W with Z, as at site HF 2.

A linear gradient of water content and conductivity with depth is apparent at some of the heat flow sites. At shallow depths in the cores, thermal conductivity theoretically decreases and water content increases due to underconsolidation of the sediments. At sites HF 2, HF 3, and HF 4 the inverse generally occurs, possibly caused by an overconsolidation of the sediment column resulting from the impact of the core barrel. The large variaition of conductivity and water content with depth is apparent at all the stations and limits the approximation of realistic linear gradients with depth to the upper two meters of the sediment column.

The relation between water content and conductivity has been empirically determined by Ratcliffe (1960), Lachenbruch and Marshall (1966), Crowe (1981), and others for different compositions of oceanic sediments. The water content and conductivity relation is suggested to be the result of a two-

Figure 9 (a,b,c,d). Needle probe thermal conductivity, K, and water content, W, versus depth, Z, for all Cores recovered during AII108 cruise. K is in mcal/(cm s °C), W is ratio of water to solid weight x 100, and Z is in meters. Cores are plotted in groups from each site, HF 1 to HF 4, in figure 10a through 10d, respectively.

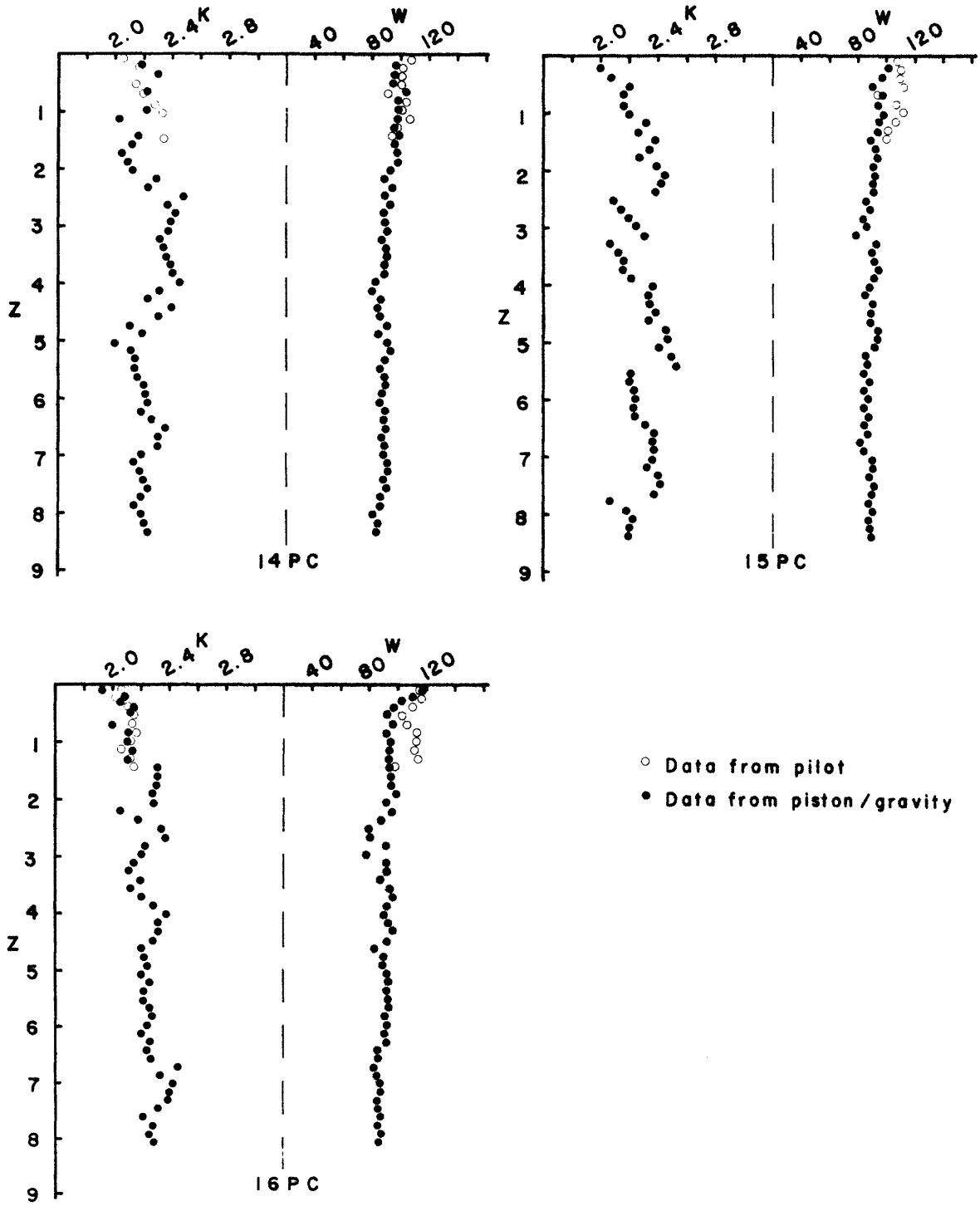
2.0
2.4 K
2.8
40
80 W
120
Z
1
2
3
4
5
6
7
8
9
14 PC
15 PC
16 PC
Data from pilot
Data from piston / gravity

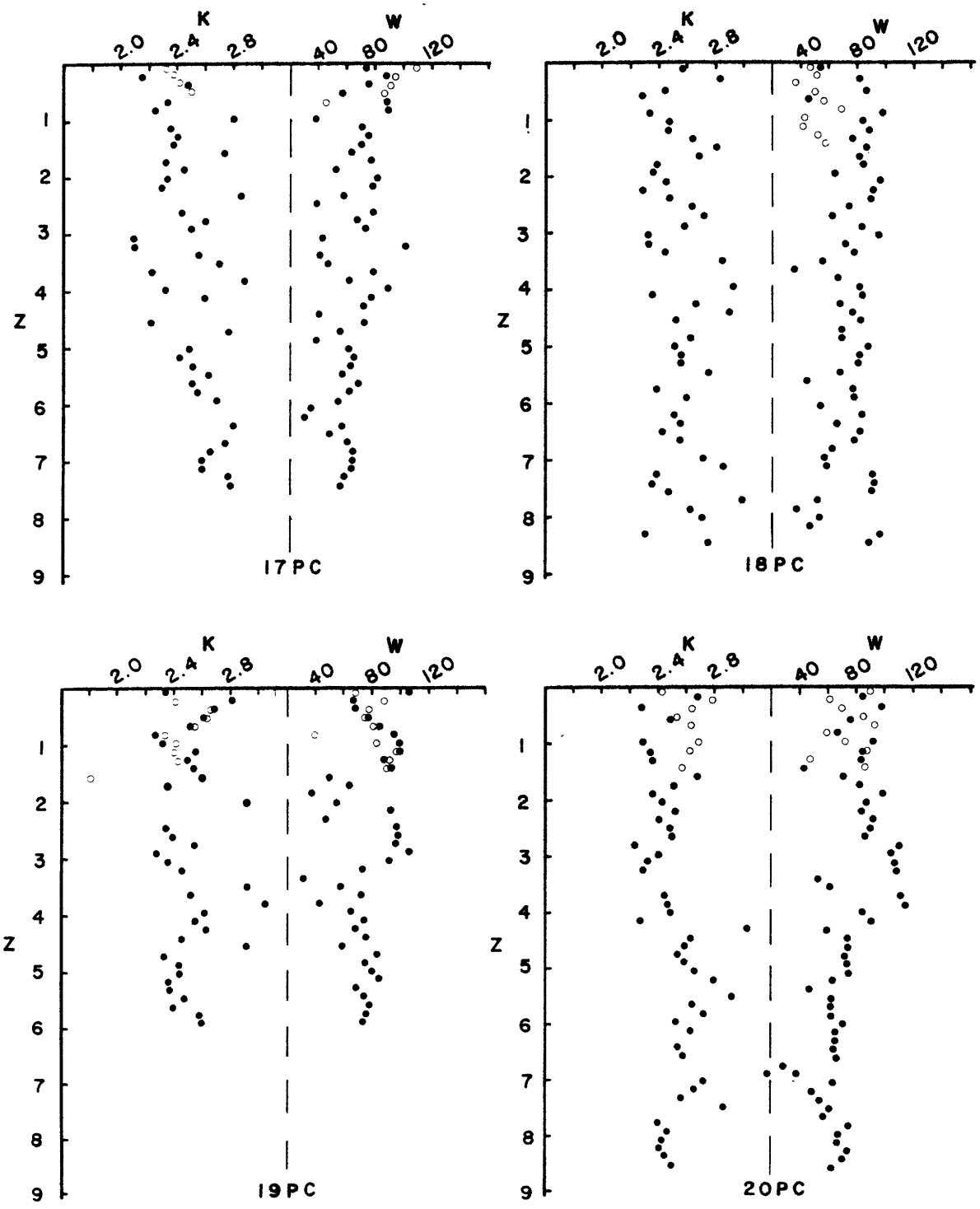
K
2.0
2.4
2.8
W
40
80
120
Z
1
2
3
4
5
6
7
8
9
17PC
18PC
19PC
20PC

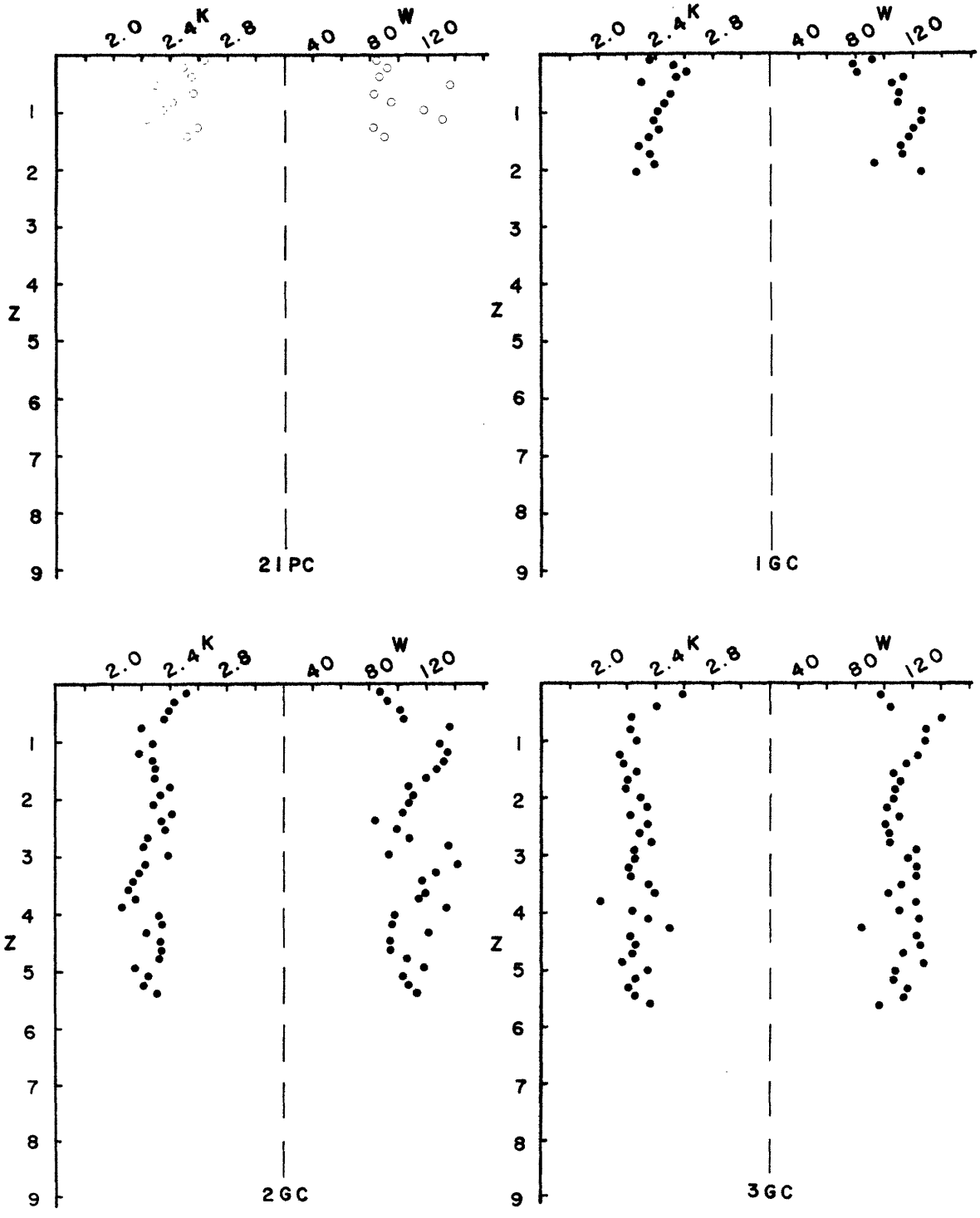
2.0
2.4
K
2.8
40
80
W
120
Z
1
2
3
4
5
6
7
8
9
21PC
1GC
2GC
3GC

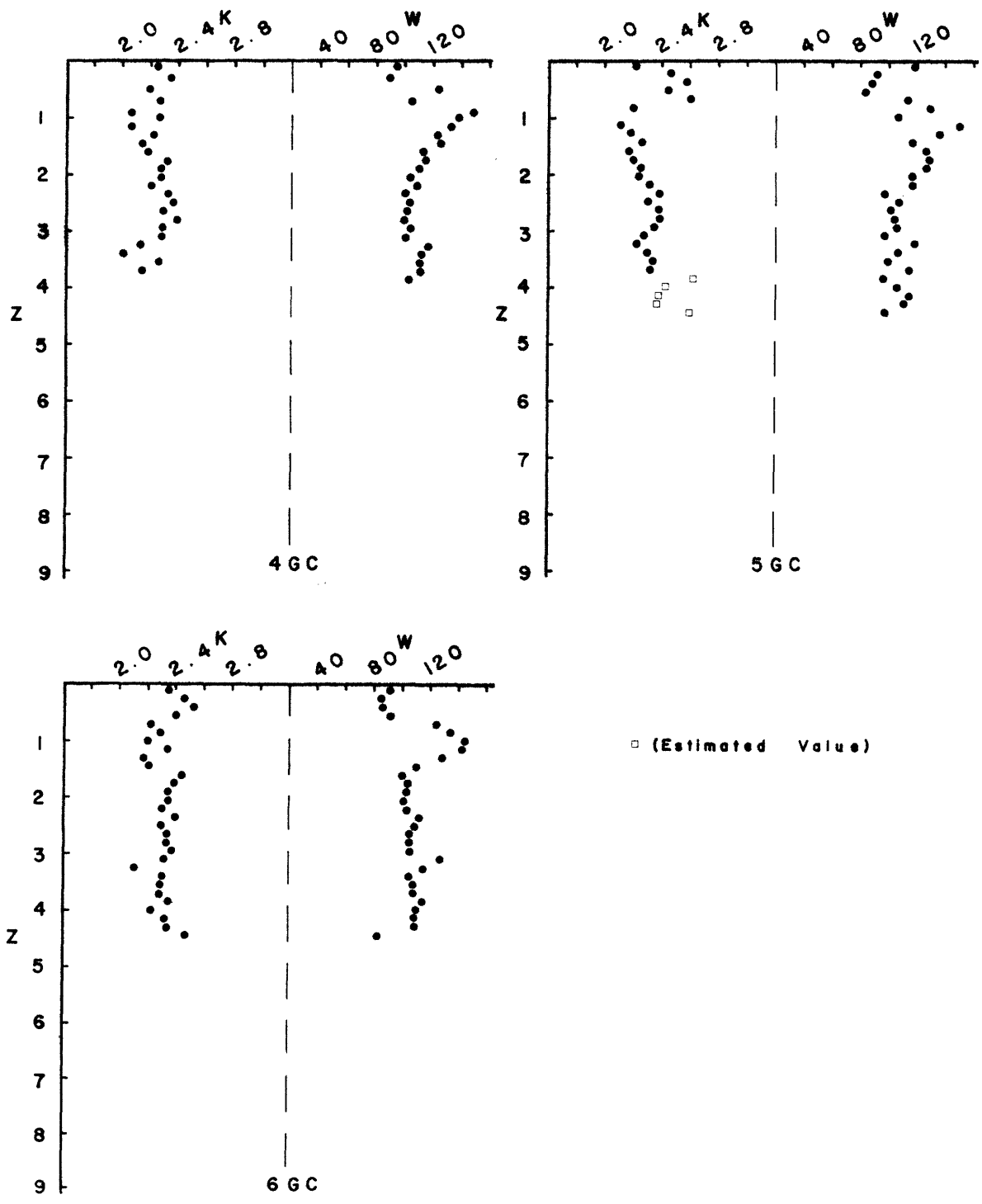
2.0
2.4
K
2.8
40
80
W
120
Z
1
2
3
4
5
6
7
8
9
4GC
5GC
6GC
□ (Estimated Value)

end member $CaCO_3/SiO_2$ system, in which the water content and carbonate content are inversely proportional (Crowe, 1981). This implies that the carbonate/silicate ratio of any particular sediment is essential to the relationship between water content and thermal conductivity.

Lachenbruch and Marshall (1966) studied Arctic Ocean sediments. Crowe studied Pacific clays and globingerina oozes. They are dissimilar sediments and have different relationships between K and W (Crowe, 1981). The cores sampled during the AII108 cruise are of several sediment types varying from site to site. Each has a slightly offset (either higher or lower) relationship with water content.

Representative data from the heat flow sites, one core from each, of conductivity and weight percent water are plotted in figure 10. The curves determined from Ratcliffe (1960) and Lachenbruch and Marshall (1966) are also drawn. The best fitting curve to the data is calculated in the form

$$K = (aw + b)^{-1} ,$$

to parallel Lachenbruch and Marshall. The equation of this best fit curve to our varied data is

$$K = [(1.475)w - (.14)]^{-1} .$$

The variety of sediment type at each site is apparent by the 10% scatter from the curve, similar to the four site range of mean conductivity. The curve shape is approximated with decreased scatter by the separate data from each site. An offset of the curve toward higher or lower conductivity

Figure 10. Needle probe thermal conductivity versus percent water by weight in representative cores from four heat flow sites. Thermal conductivity is in mcal/(cm s °C), and percent water is the ratio of water to total weight x 100%. The theoretical curves of Lachenbruch and Marshall (1966) and Ratcliffe (1960) and the best fit of the form $K = (aw + b)^{-1}$ are also plotted (see text).

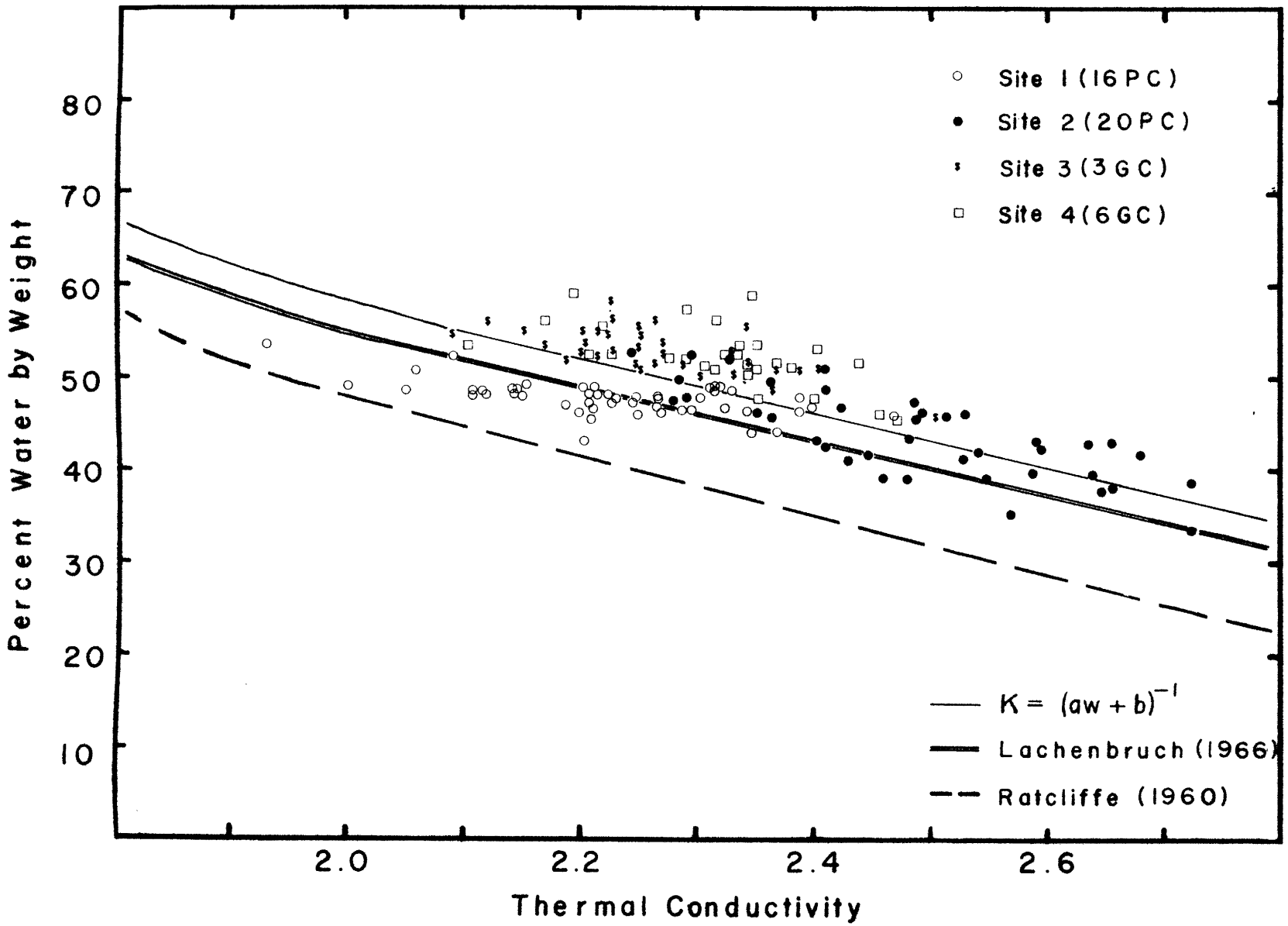
Site 1 (16 PC)
Site 2 (20 PC)
Site 3 (3 GC)
Site 4 (6 GC)
K = (aw + b)^-1
Lachenbruch (1966)
Ratcliffe (1960)
Percent Water by Weight
80
70
60
50
40
30
20
10
2.0
2.2
2.4
2.6
Thermal Conductivity

for each site would better represent the sediments sampled. The best fit curve shown is a compilation to relate K and w to within only 10%. To calculate conductivity from water content each site should be approximated by a more accurate relation than the compiled curve. In doing so, the scatter of the data from each site around an offset curve would be lowered to near 5%, so that the calculation of conductivity from the curve is as representative of an average as the mean of the needle probe measurements.

V. KNORR 77 AND ATLANTIS II 97 HEAT FLOW DATA

Location

The AII108 cruise sites HF 1 to 4 correspond with previosly sampled heat flow sites on the AII97 and KR77 cruises. Site HF 1 is coincident, within .5 km, with five piston cores recovered at five stations on the AII97 cruise. Sites HF 2, HF 3, and HF 4 are coincident with five representative penetrations of four violin probe stations taken on the KR77 cruise. Site 2 corresponds with station 11, penetration 1 (11-1); Site 3 corresponds with station 14, penetration 2 (14-2) and station 15, penetration 4 (15-4); Site 4 with station 17, penetrations 1 and 13 (17-1,13). These station locations are marked on figure 1 for reference. In addition, six two meter gravity cores were retrieved during the KR77 cruise, five at site 2 and one at site 3.

Statistical Analysis

The thermal conductivity measured on the piston cores from the AII97 used the digital conductivity apparatus. Needle probe sampling was made at 50 cm intervals along the five cores by L. Hobbie at Woods Hole Oceanographic Institution. Galson and Von Herzen used this data with pogo-probe temperature gradient information for heat flow approximations. The mean and standard deviation of the conductivities from all five cores at site HF 1 are 2.144 and

0.113 mcal/cm s °C, respectively (Galson, 1979). The calculated FEK for this mean conductivity is .072, 7.2%, and Galson describes these measurements as being within the 4% systematic error of the needle probe (Von Herzen and Maxwell, 1959).

The in situ thermal conductivity of the sediments represented by the five penetrations of the Lister probe at sites HF 2, HF 3, and HF 4. The original temperature decay histories of each penetration were reduced at MIT by E. Davis (Pacific Geoscience) to plots of $F(\alpha,\tau)$ and temperature. These plots are shown for penetrations 11-1, 14-2, 15-4, 17-1, and 17-13 in appendix F a, b, c, d, and e, respectively. The relation between $F(\alpha,\tau)$ and temperature is linear for all five of the penetration records at every sensor. The mean conductivity calculated from $F(\alpha,\tau)$ at the seven sensors therefore have small standard deviation, near 1% for penetrations at stations 14, 15, and 17. Other penetrations at pogo-probe stations not listed differ by the amount of curvature of $F(\alpha,\tau)$ at one or more sensor location. Few are rejected, but the curvature of $F(\alpha,\tau)$ with temperature decreases the accuracy of the conductivity as it deviates from a linear relation.

The numerical output of conductivity calculated at each sampling time at each sensor (n=7) is shown for the first five penetrations in appendix G, a through e. Through the decay history, eight to ten conductivity points are sampled

in cycle. The standard deviation of the ten or so points at each sensor is maintained as an interval of accuracy by excluding those outside, marked with asterisks. The mean of the conductivity values at each sensor is listed at the end of the printout as $\overline{K}$, along with interval temperature gradients, calculated heat flow, and temperature information. These average conductivities profile the variation with depth. A plot of $\overline{K}$ versus Z, sensors 7 to 1, is given for all five penetrations in appendix H, a through e. A linear gradient of conducitivity with depth is again a poor approximation for the majority of measurements.

The mean conductivities and standard deviations of all the values of each penetration at each site are given in Table 6. These values represent in situ conductivity calculated at the five ideal penetration locations at sites HF 2, HF 3, and HF 4 and the needle probe conductivity of the five piston cores at site HF 1. The mean of the in situ conductivities is representative of other penetrations, but has by comparison an extraordinarily low standard deviation, .02 to .03 mcal/(cm s °C). This is about a 1% scatter of the measurements at all sensor locations. It seems to be an unrealistic estimate of reproducibility of in situ conductivity for many measurements, but merely a scatter of these particularly linear results.

The fractional error of conductivity, FEK, is also calculated as $\sigma/\overline{K}$ + .02 as before, although the addition of

Table 6 - KR77 Average In Situ Conductivity:
Sites HF 1 to HF 4 [in mcal/(cm s °C)]

Site	pen#	$\overline{K}$	$\overline{\sigma}$	$\overline{FEK}$
HF 1	**	2.144	0.11	0.073
HF 2	11-1	2.53	0.12	0.067
HF 3	14-2 and 15-4	2.17	0.02	0.029
HF 4	17-1 and 17-13	2.20	0.03	0.034

** Data from needle probe measurments of cores from AII97

.02 absorbs some of the systematic biases in the in situ conductivity measurement, rather than in needle probe. This factor is not changed to standardize the comparison between in situ and needle probe errors and to estimate the reproducibility of in situ measurement. These FEK values are calculated in the last column of Table 6.

Water Content

Finally, the two meter gravity cores retrieved at sites HF 2 and HF 3 during th KR 77 cruise were measured for water content and correlated via Lachenbruch and Marshall (1966) to thermal conductivity. The arithmetic mean of the conductivity from water content at 10 cm sampling intervals is 2.34 mcal/(cm s °C) (n=81) at site HF 2 and 2.03 mcal/(cm s °C) (n=22) at site HF 3. These values are 10% lower than those measured in situ. The water content/conductivity relationship given by Lachenbruch and Marshall (1966) may not be representative of these sediments and should be shifted toward the 10% higher conductivities. Also, the shallow (two meter) cores penetrate into higher water content sediment than the deeper penetrations (seven meters) by the in situ probe, the high water content possibly causing the lower conductivity.

The in situ conductivities are accurate in our estimation to within 5% of the mean of all seven sensors, several times higher than the standard deviations of these

ideal penetrations. This estimation is arrived at by linear approximation of the curvature of $F(\alpha, \tau)$ and the systematic errors in approximation of the time delays for each sensor over all the penetrations on the KR77 cruise.

The additional buffer of .02 assumed in the in situ FEK calculation seems to be a reasonable bias for the systematic variation due to curvature and time delay approximations. Therefore, the in situ FEK is an estimate of the accuracy of an in situ conductivity measurement.

VI. COMPARISON OF NEEDLE PROBE AND IN SITU CONDUCTIVITY

The needle probes have been calibrated on fused silica to within 4.7% reproducibility and 1% standard error on each measurement (Goldberg et al., 1980). The needle probe conductivities from the AII108 cruise show scatter due to systematic error and water content variation of 5% of the mean at sites HF 1, HF 3, and HF 4 and 10% at site HF 2. The $\overline{FEK}$ values at these sites are about 7% and 12%, respectively.

In situ conductivity measurement has very low variation at these representative penetrations. About 5% scatter at site HF 2 and about 1% scatter at sites HF 3 and HF 4 are observed. The $\overline{FEK}$ values at these sites are about 7% and 3%, respectively. We feel that these are extraordinary results and should not be the base for reproducibility of the system.

The conductivity data from the AII108, AII97, and KR77 cruises can best be compared statistically at each heat flow site, HF 1 to HF 4. The needle probe and in situ means and errors at the sites, listed in Tables 5 and 6, are plotted on the axes of figure 11. The equivalue line drawn has a slope of 1. Three of the points are within the error bar (S.D.) of the needle probe to the equivalue line; site HF 3 is outside of its error by about 2%. The in situ error bars also cross the line except at sites HF 3 and HF 4, where the standard deviations are extemely low. A hypothetical variation of 5%

Figure 11. Average needle probe conductivity versus average *in situ* conductivity from measurements at the four heat flow sites HF 1 to HF 4. There are no *in situ* measurements at HF 1. The point shown is the comparison of needle probe measurements from the AII97 and AII108 cruises. Thermal conductivity in mcal/(cm s °C) is shown with error bars representing the average scatter of measurements about the mean.

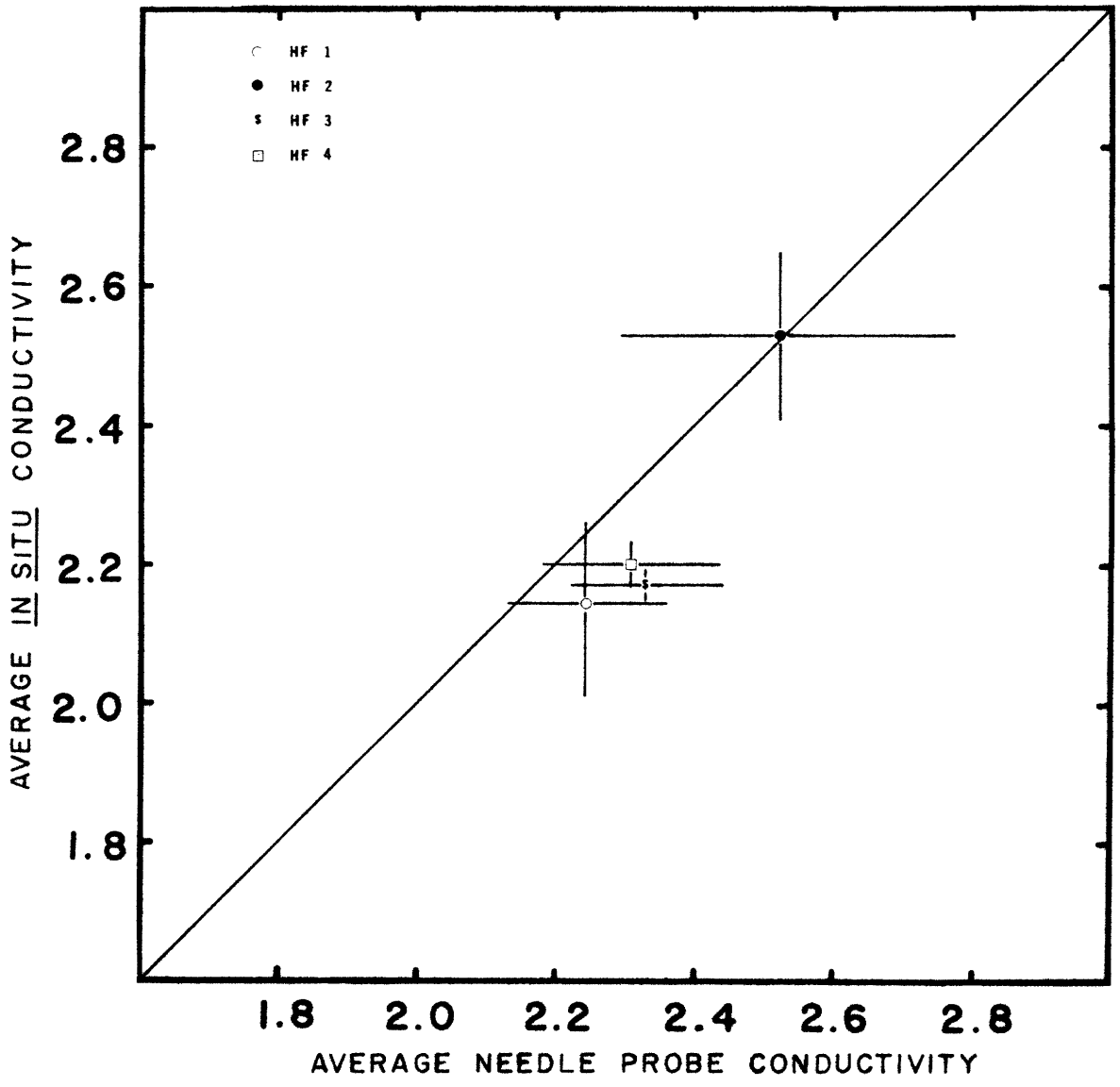
HF 1
HF 2
HF 3
HF 4
2.8
2.6
2.4
2.2
2.0
1.8
AVERAGE IN SITU CONDUCTIVITY
1.8
2.0
2.2
2.4
2.6
2.8
AVERAGE NEEDLE PROBE CONDUCTIVITY

of in situ conductivities would meet needle probe values. The bar diagram in figure 12 shows the comparison between needle probe and in situ conductivity and $\overline{FEK}$ values at each site. The $\overline{FEK}$ is over .10 only at site HF 2, needle probe, where the water content variation was also extreme. The correspondence between the mean conductivity is otherwise within the $\overline{FEK}$ at each site.

In situ conductivity measurement has been found to lie within 5% of needle probe measurement by Hyndeman et al., (1979) on several cores from the northeastern Pacific retrieved near pogo-probe stations.

The similar scatter in the data for most of the needle probe and in situ conducitivity data suggests that the two techniques measure to within the standard deviation of the needle probe measurements. The strong correlation of the mean and $\overline{FEK}$ values of both methods "calibrate" the in situ measurements to within about 5% of measurement using the needle probe. The large scatter at site HF 2, needle probe, and low scatter at site HF 3 and HF 4, in situ, seem to be reasonably described by physical or statistical causes. The reliable measurements considered from the northern Atlantic cruises AII108, AII97, and KR77 lie within the 5% accuracy of needle probe measurement. Thermal conductivity measured by either technique will have about a 5% reproducibility and usually give values within about 5% of the other.

Figure 12. Average needle probe (shaded dark grey) and in situ (shaded light grey) conductivity, K, and fractional error in conductivity, FEK, (see text) plotted at the four heat flow sites. Conductivities are in mcal/(cm s °C), and FEK is the ratio of standard deviation to average conductivity plus .02.

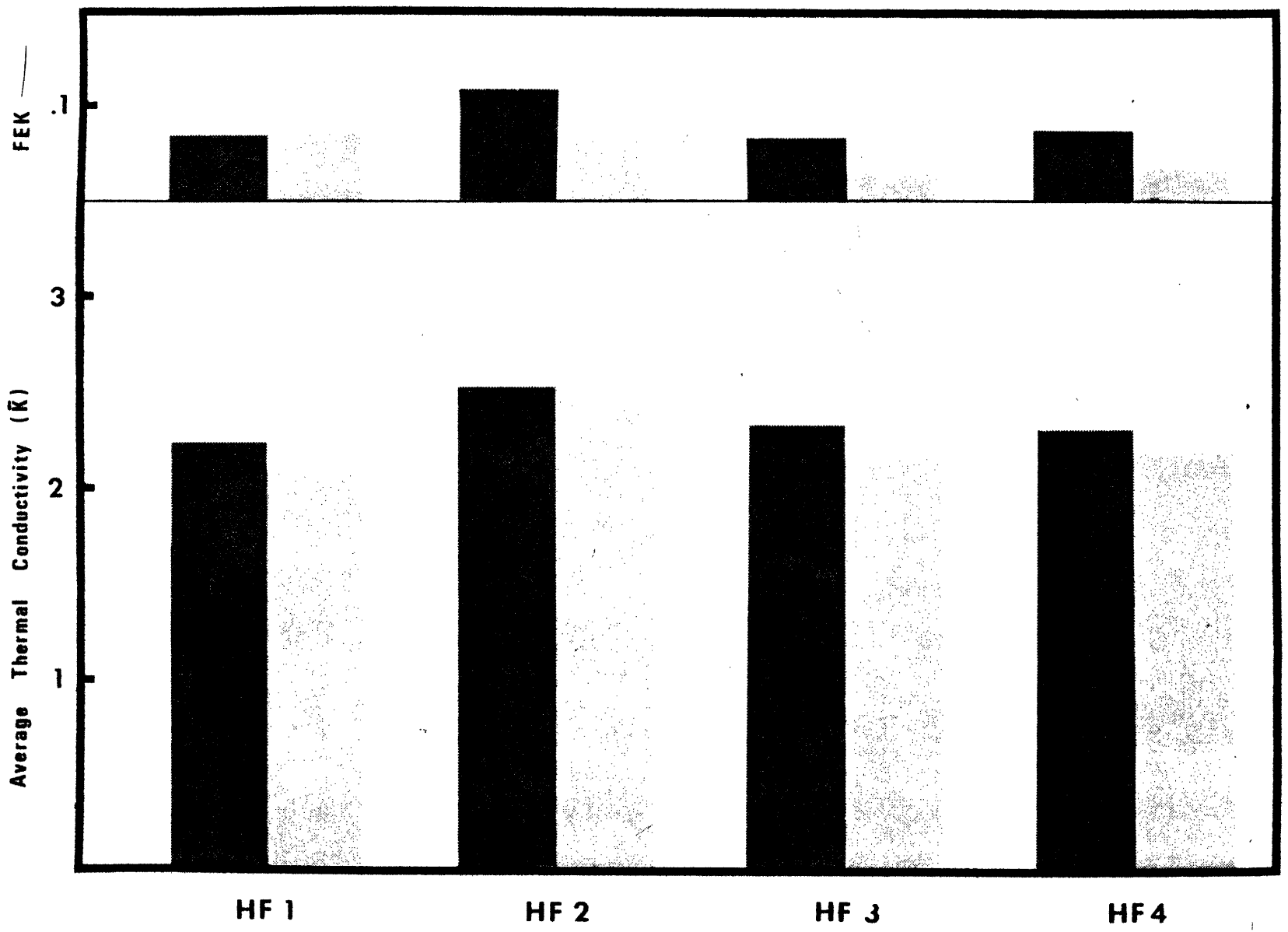
FEK
.1
3
2
1
Average Thermal Conductivity (K)
HF 1
HF 2
HF 3
HF 4

BIBLIOGRAPHY

Carslaw and Jaeger, Conductivity of heat in solids, 2nd ed., Clarendon press, Oxford, Eng., 1959.

Crowe, J., Mechanisms of heat transport through the floor of the equatorial Pacific ocean, MIT thesis, © MIT, 1981.

Galson, D.A., An investigation of the thermal structure in the vicinity of IPOD sites 417 and 418, MIT thesis, © MIT, 1979.

Galson, D.A. and R.P. Von Herzen, A heat flow survey on anomaly M0 south of the Bermuda Rise, Earth and Pl. Sci. Letters, in press, 1981.

Goldberg, D.S., R.P. Von Herzen, and J.G. Sclater, Thermal conductivity of fused silica glass, WHOI Technical Report, WHOI 80-34, 1980.

Hunt, M.M., W.M. Margret, D.A. Moller, K.R. Peal, W.K, Smith, and R.C. Spindel, An acoustic navigations system, WHOI Technical Report, WHOI 74-6, 1974.

Huppert, H.E. and J.G. Sclater, On the in situ measurement of the thermal conductivity fo deep sea sediments, Marine Geophysical Laboratory Memorandum 191, Scripps Inst. of Oceanography, 1968.

Hyndeman, R.D., E.E. Davis, and J.A. Wright, The measurement of marine geothermal heat flow by a multipenetration probe with digital acoustic telemetry and in situ conductivity, Marine Geophys. Res. 84, 24 pg., 1979.

Lachenbruch, A.H. and B.V. Marshall, Heat flow through the Arctic ocean floor: The Canada Basin-alpha rise boundary, J. Geophys. Res. 71, p. 1223-48, 1966.

Langseth, M.G., Techniques of measuring heat flow through the ocean floor, Terrestial Heat FLow, Geophysical Monograph 8, edited by W.H.K. Lee, ch. 4, p. 58-77, Amer. Geophys. Union, Wash. D.C., 1965.

Lister, C.R.B., Measurement of in situ conductivity by measurements of a Bullard-type probe, Geophys. J. 19, p. 521-33, 1970.

Lister, C.R.B., On the pulse probe method of conductivity measurement, Geophys. J. 7, p. 451-561, 1979.

Ratcliffe, E.H., Thermal conductivity of ocean sediments, J. Geophys. Res. 65, 1535-41, 1960.

Sclater, J.G., J. Crowe, and R.N. Anderson, On the reliability of oceanic heat flow measurement, J. Geophys. Res. 81, p. 2997-3006, 1976.

Sclater, J.G., C. Jaupart, and D. Galson, the heat flow through continents and oceans, Rev. of Geophys., p. 269-311, 1980.

See references from chapter I, p. 27.

APPENDICES

Appendix D

THERMCON data reduction program for needle probe measurements during AII108 leg 5 cruise. (see text)

```
THERMCON
8000 DEFINT I,N,Z:DEFSNG G,H,K,L,P,R,T,V,X:DEFDBL A-D:DEFSTR S
8010 ON ERROR GOTO 9940
8020 READ V9:IF ABS(V9)>0 THEN RESTORE:GOTO 8120
8030 HOME:INVERSE:PRINT"THERMAL CONDUCTIVITY":NORMAL:PRINT
8040 S="":INPUT"LOAD DATA FROM FILE (Y OR RETURN)";S:IF S="MENU" THEN LOAD"MENU",
R ELSE IF S<>"Y"THEN 8100
8050 PRINT:INPUT"WHICH DISK DRIVE (A OR B)";S:IF S="A" OR S="B"THEN 8060 ELSE PRI
NT"TYPE 'A' OR 'B' PLEASE":GOTO 8050
8060 HOME:PRINT:PRINT"FILES ON DISK":PRINT:SF=S+":*.DAT":FILES SF:PRINT:INPUT"DAT
A FILE TO LOAD";SF
8070 IF INSTR(SF,".")=0 THEN SF=SF+".DAT"
8080 HOME:VTAB 12:PRINT TAB(5),"WHEN DRIVE LIGHT GOES OUT TYPE RUN THEN PRESS RET
URN. YOUR DATA WILL BE READY"
8090 SF=S+":"+SF:MERGE SF
8100 HOME:PRINT"WHEN LINE NUMBER APPEARS TYPE 'DATA '","THEN YOUR DATA WITH A COM
MA BETWEEN"," ITEMS THEN TYPE RUN"
8110 AUTO 1,1
8120 REM THERMCON-CP/M G.PELLETIER
8130 HOME:INVERSE:PRINT"THERMCON":NORMAL:PRINT
8140 S="":INPUT"NUMBER OF NEEDLES (IF 5 THEN RETURN)";S:IF S="" THEN N1=5 ELSE N1
=VAL(S)
8150 S="":PRINT:INPUT"INITIAL VOLTAGE (IF 1.41V THEN RETURN)";S:IF S="" THEN V1=1
.41 ELSE V1=VAL(S)
8160 S="":PRINT:INPUT"REFRENCE VOLTAGE (IF 1.41V THEN RETURN)";S:IF S="" THEN V2=
1.41 ELSE V2=VAL(S)
8170 S="":PRINT:INPUT"BASE VOLTAGE (IF 5.0V THEN RETURN)";S:IF S="" THEN V3=5 ELS
E V3=VAL(S)
8180 S="":PRINT:INPUT"TOLERANCE (IF 0.03% THEN RETURN)";S:IF S="" THEN T9=.03 ELS
E T9=VAL(S)
8190 S="":PRINT:INPUT"TIME CONSTANT (IF 3 THEN RETURN)";S:1F S="" THEN T1=3 ELSE
T1=VAL(S)
8200 S="":PRINT:INPUT"DATA POINTS/NEEDLE";S:IF S="" THEN 8200 ELSE N2=VAL(S)
8210 S="":PRINT:INPUT"HEATER VOLTAGE";S:IF S="" THEN 8210 ELSE V4=VAL(S)
8220 S7="":PRINT:INPUT"MEASUREMENT DATE ";S7:IF S7="" THEN 8220
8230 S8="":PRINT:INPUT"PISTON CORE IDENTIFICATION ";S8:IF S8="" THEN 8230
8240 S="":PRINT:INPUT"K-BOX RUN NUMBER ";S:IF S="" THEN 8240 ELSE Z1$=S
8260 DIM N(5),R(10),P(15),S9(5)
8270 DIM V(200),T(20),H(20),U(20),RR(20)
8280 FOR I=1 TO N1
8290 S="":PRINT:PRINT"TYPE IN SERIAL # OF NEEDLE ";I;:INPUT" KWH-";S:IF S="" THEN
 8290 ELSE N(I)=VAL(S)
8295 S="":PRINT:INPUT"DISTANCE FROM TOP OF CORE (CM)";S:1F S="" THEN 8295 ELSE S9
(I)=S
8300 IF N(I)<>3 THEN 8370
8310 R(I)=26.681
8320 R(I+5)=1.261
8330 P(I)=1.09385E-03
8340 P(I+5)=2.8966E-04
8350 P(I+10)=1.98036E-07
8360 GOTO 8840
8370 IF N(I)<>4 THEN 8440
8380 R(I)=26.522
8390 R(I+5)=1.261
8400 P(I)=1.02739E-03
8410 P(I+5)=3.00873E-04
8420 P(I+10)=1.36127E-07
8430 GOTO 8840
8440 IF N(I)<>5 THEN 8510
8450 R(I)=26.687
8460 R(I+5)=1.261
8470 P(I)=9.97834E-04
8480 P(I+5)=3.16675E-04
8490 P(I+10)=6.96313E-08
```

```
8500 GOTO 8840
8510 IF N(I)<>6 THEN 8580
8520 R(I)=26.389
8530 R(I+5)=1.261
8540 P(I)=1.12201E-03
8550 P(I+5)=2.9768E-04
8560 P(I+10)=1.94361E-07
8570 GOTO 8840
8580 IF N(I)<>7 THEN 8650
8590 R(I)=26.675
8600 R(I+5)=1.261
8610 P(I)=9.6023E-04
8620 P(I+5)=3.28798E-04
8630 P(I+10)=2.89663E-08
8640 GOTO 8840
8650 IF N(I)<>9 THEN 8720
8660 R(I)=26.63
8670 R(I+5)=1.261
8680 P(I)=9.6023E-04
8690 P(I+5)=3.28798E-04
8700 P(I+10)=2.89664E-08
8710 GOTO 8840
8720 IF N(I)<>12 THEN 8790
8730 R(I)=26.424
8740 R(I+5)=1.261
8750 P(I)=1.17013E-03
8760 P(I+5)=2.79979E-04
8770 P(I+10)=2.86558E-07
8780 GOTO 8840
8790 INPUT"HEATER RES.";R(I)
8800 INPUT"SPECIFIC RES.(OHMS/CM)";R(I+5)
8810 INPUT"ALPHA #.######D-## ";P(I)
8820 INPUT"BETA  #.######D-## ";P(I+5)
8830 INPUT"GAMMA #.######D-## ";P(I+10)
8840 NEXT I
8850 I=N1+1
8860 N5=I-1
8870 N3=N2*(N1+1)
8880 LPRINT TAB(10) CHR$(29);"ATLANTIS II 108 LEG 5"'PUT CRUISE NAME HERE BETWEEN
 QUOTES
8890 LPRINT TAB(10) S7
8900 LPRINT TAB(10) "OUTPUT FOR DATA FROM PC-";S8
8910 LPRINT TAB(10) "K-BOX RUN # ";Z1$
8915 LPRINT:LPRINT TAB(10) USING"HEATER VOLTAGE = #.###";V4
8980 IFLG=0
8990 FOR K=1 TO (N1+1)*3
9000 READ V9
9010 IF ABS(V9-V1)<T9 THEN 9040
9020 NEXT K
9030 STOP
9040 K5=K
9050 FOR K=1 TO N1+1
9060 READ V9
9070 NEXT K
9080 IF ABS(V9-V2)<T9 THEN 9110
9090 K5=K5+N1+1
9100 GOTO 9050
9110 FOR K=1 TO N3
9120 READ V(K)
9130 IF V(K)>0 THEN 9170
9140 N3=K
9150 IFLG=1
9160 GOTO 9190
9170 NEXT K
9180 FOR I=1 TO N5
9181 IF I>1 AND I MOD 2=1 THEN LPRINT CHR$(12)
```

```
9182 LPRINT:LPRINT TAB(10) "K-BOX POSITION ";I
9184 LPRINT TAB(10) ".........NEEDLE KWH-";N(I)
9186 LPRINT TAB(10) "DISTANCE FROM TOP OF CORE (CM) =";S9(I)
9188 LPRINT:LPRINT TAB(10) " TIME (SEC)   TEMP (DEG C)   DEVIATION (DEG C)"
9190 B1=0
9200 B2=0
9210 C1=0
9220 C2=0
9230 C3=0
9240 D1=0
9250 D2=0
9260 D3=0
9270 G5=0
9280 V3=7*V9/2
9290 P1=P(I)
9300 P2=P(I+N1)
9310 P3=P(I+2*N1)
9320 I1=N1-I+1
9330 K8=0
9340 I9=0
9350 FOR K=I TO N3 STEP N1+1
9360 V8=ABS(V(K+I1)-V2)
9370 IF V8>T9 THEN 9580
9380 IF I9>0 THEN 9600
9390 T5=(K5+N1+K)*T1
9400 R4=(10000*V(K))/(V3-V(K))
9410 L4=LOG(R4)
9420 X4=P1+P2*L4+P3*L4*L4*L4
9430 H5=1/X4-273.16
9440 U5=LOG(T5)
9450 B1=B1+T5
9460 B2=B2+T5*T5
9470 C1=C1+U5
9480 C2=C2+T5*U5
9490 C3=C3+U5*U5
9500 D1=D1+H5
9510 D2=D2+H5*T5
9520 D3=D3+U5*H5
9530 K8=K8+1
9540 T(K8)=T5
9550 H(K8)=H5
9560 U(K8)=U5
9565 RR(K8)=R4
9570 GOTO 9610
9580 I9=1
9590 GOTO 9620
9600 I9=0
9610 V3=7*V(K+I1)/2
9620 NEXT K
9630 A1=K8
9640 A2=B1
9650 A3=C1
9660 B3=C2
9670 D4=A1*B2*C3+B1*C2*A3+C1*A2*B3-A3*B2*C1-B3*C2*A1-C3*A2*B1
9680 A4=D1*B2*C3+B1*C2*D3+C1*D2*B3-D3*B2*C1-B3*C2*D1-C3*D2*B1
9690 B4=A1*D2*C3+D1*C2*A3+C1*A2*D3-A3*D2*C1-D3*C2*A1-C3*A2*D1
9700 C4=A1*B2*D3+B1*D2*A3+D1*A2*B3-A3*B2*D1-B3*D2*A1-D3*A2*B1
9710 A=A4/D4
9720 B=B4/D4
9730 C=C4/D4
9740 K9=V4*V4*R(I+N1)*.03802/(C*R(I)*R(I))
9750 FOR K=1 TO K8
9760 G9=H(K)-(A+B*T(K)+C*U(K))
9770 G5=G5+G9*G9
9780 LPRINT TAB(10) USING" ###          ##.###          #.########          ";T(K),
H(K),G9
```

```
9790 NEXT K
9800 G4=SQR(G5/K8)
9810 LPRINT TAB(10) USING"CURVE FIT PARAMETER--------- #.######";G4
9820 D9=B*60
9830 LPRINT TAB(10) USING"TEMP DRIFT RATE ------------ #.###### (DEG C)/MIN";D9
9840 LPRINT TAB(10) USING"CONDUCTIVITY --------------- #.########";K9
9850 LPRINT:NEXT I
9860 IF IFLG>0 THEN 9920
9870 FOR K=1 TO 200
9880 READ V9
9890 IF V9<0 THEN 9920
9900 NEXT K
9910 STOP
9920 LPRINT CHR$(12):LOAD"MENU",R
9930 END
9940 IF ERR=4 AND ERL=8020 THEN RESUME 8030
9950 PRINT"ERROR ";ERR;"ON LINE ";ERL:IF ERR=4 THEN RESUME 9920 ELSE STOP
```

APPENDIX E

Sample needle probe data output from THERMCON. Temperature versus time profile, conductivity, temperature drift rate, and curve fit parameter are shown at five needle positions in GC 3, section 3, bottom. (see text)

ATLANTIS II 108 LEG 5
27 MAY 81
OUTPUT FOR DATA FROM PC-GC3
K-BOX RUN # S31

HEATER VOLTAGE = 4.784

K-BOX POSITION 1
.....NEEDLE KWH- 12
DISTANCE FROM TOP OF CORE (CM) =1

TIME (SEC)	TEMP (DEG C)	DEVIATION (DEG C)
36	30.744	0.358E-02
54	31.028	-.486E-02
72	31.237	-.333E-02
90	31.398	-.238E-02
108	31.535	0.388E-02
126	31.645	0.474E-02
144	31.738	0.293E-02
162	31.819	0.759E-03
180	31.892	-.583E-03
198	31.961	0.188E-02
216	32.016	-.404E-02
234	32.070	-.477E-02
252	32.125	-.105E-02
270	32.174	0.371E-03
288	32.217	%-1.000E-03
306	32.262	0.293E-02
324	32.299	0.936E-03

CURVE FIT PARAMETER--------- 0.301E-02
TEMP DRIFT RATE ------------ -.974D-02 (DEG C)/MIN
CONDUCTIVITY --------------- 0.2152E-02

K-BOX POSITION 2
.....NEEDLE KWH- 9
DISTANCE FROM TOP OF CORE (CM) =1

TIME (SEC)	TEMP (DEG C)	DEVIATION (DEG C)
39	30.310	0.585E-02
57	30.571	-.431E-02
75	30.765	-.620E-02
93	30.924	-.166E-03
111	31.050	-.509E-03
129	31.161	0.261E-02
147	31.252	-.208E-03
165	31.336	0.118E-02
183	31.411	0.207E-02
201	31.475	-.122E-02
219	31.536	-.105E-02
237	31.598	0.403E-02
255	31.646	-.333E-03
273	31.701	0.579E-02
291	31.735	-.559E-02
309	31.786	0.207E-02
327	31.821	-.402E-02

CURVE FIT PARAMETER--------- 0.350E-02
TEMP DRIFT RATE ------------ 0.103D-02 (DEG C)/MIN
CONDUCTIVITY --------------- 0.2170E-02

K-BOX POSITION 3
.....NEEDLE KWH- 6
DISTANCE FROM TOP OF CORE (CM) =1

TIME (SEC)	TEMP (DEG C)	DEVIATION (DEG C)
42	30.785	0.242E-02
60	31.031	-.801E-03
78	31.211	-.504E-02
96	31.363	0.107E-02
114	31.482	-.133E-02
132	31.592	0.514E-02
150	31.676	-.200E-02
168	31.759	0.117E-02
186	31.827	-.341E-02
204	31.897	0.116E-02
222	31.958	0.208E-02
240	32.013	0.899E-03
258	32.068	0.371E-02
276	32.109	-.367E-02
294	32.157	-.118E-02
312	32.200	-.446E-03
330	32.242	0.230E-03

CURVE FIT PARAMETER--------- 0.258E-02
TEMP DRIFT RATE ------------ 0.506D-02 (DEG C)/MIN
CONDUCTIVITY --------------- 0.2264E-02

K-BOX POSITION 4
.....NEEDLE KWH- 4
DISTANCE FROM TOP OF CORE (CM) =1

TIME (SEC)	TEMP (DEG C)	DEVIATION (DEG C)
45	31.362	0.175E-02
63	31.599	-.162E-02
81	31.778	-.274E-02
99	31.925	0.415E-04
117	32.049	0.352E-02
135	32.149	0.313E-03
153	32.238	-.848E-03
171	32.317	-.282E-02
189	32.394	0.835E-03
207	32.462	0.261E-02
225	32.522	0.192E-02
243	32.577	0.402E-03
261	32.627	-.265E-02
279	32.676	-.224E-02
297	32.726	0.119E-02
315	32.767	-.132E-02
333	32.812	0.165E-02

CURVE FIT PARAMETER--------- 0.194E-02
TEMP DRIFT RATE ------------ 0.673D-02 (DEG C)/MIN
CONDUCTIVITY --------------- 0.2203E-02

K-BOX POSITION 5
.....NEEDLE KWH- 3
DISTANCE FROM TOP OF CORE (CM) =1

TIME (SEC)	TEMP (DEG C)	DEVIATION (DEG C)
48	30.698	0.360E-02
66	30.918	-.135E-02
84	31.085	-.442E-02
102	31.226	-.922E-03
120	31.344	0.195E-02
138	31.438	-.275E-02
156	31.526	-.558E-03
174	31.605	0.523E-03
192	31.675	0.153E-02
210	31.738	0.358E-03
228	31.798	0.210E-02
246	31.852	0.287E-02
264	31.902	0.209E-02
282	31.945	-.878E-03
300	31.989	-.873E-03
318	32.030	-.135E-02
336	32.069	-.191E-02

CURVE FIT PARAMETER---------- 0.208E-02
TEMP DRIFT RATE ------------ 0.926D-03 (DEG C)/MIN
CONDUCTIVITY --------------- 0.2187E-02

APPENDIX F

Conductivity versus depth for *in situ* measurements from five representative penetrations during the Knorr 77 cruise. Scale shown on plot. (see text)

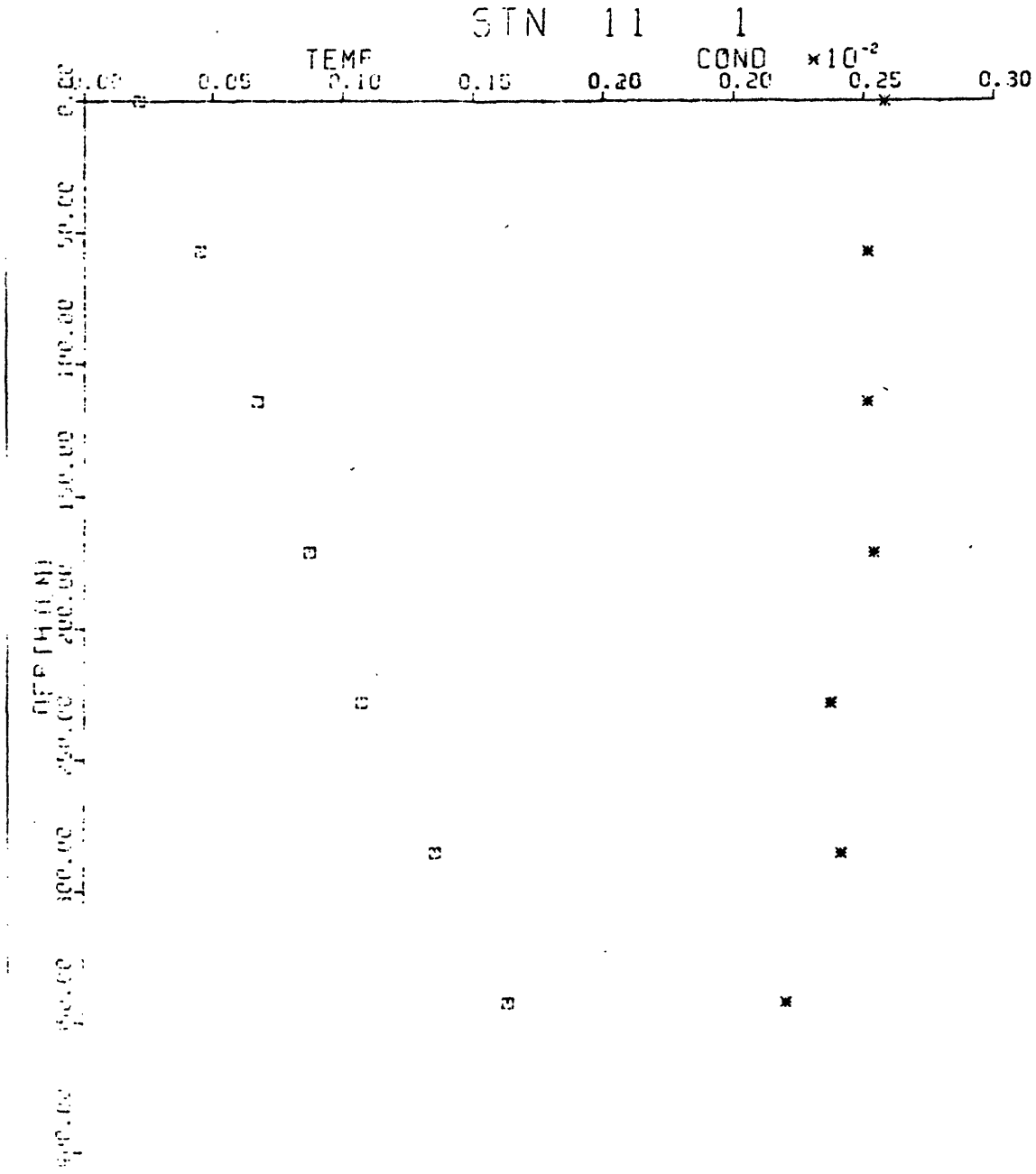
STN 11 1
TEMP
COND ×10⁻²
0.05
0.10
0.15
0.20
0.20
0.25
0.30
DEPTH (M)
100.00
200.00
300.00

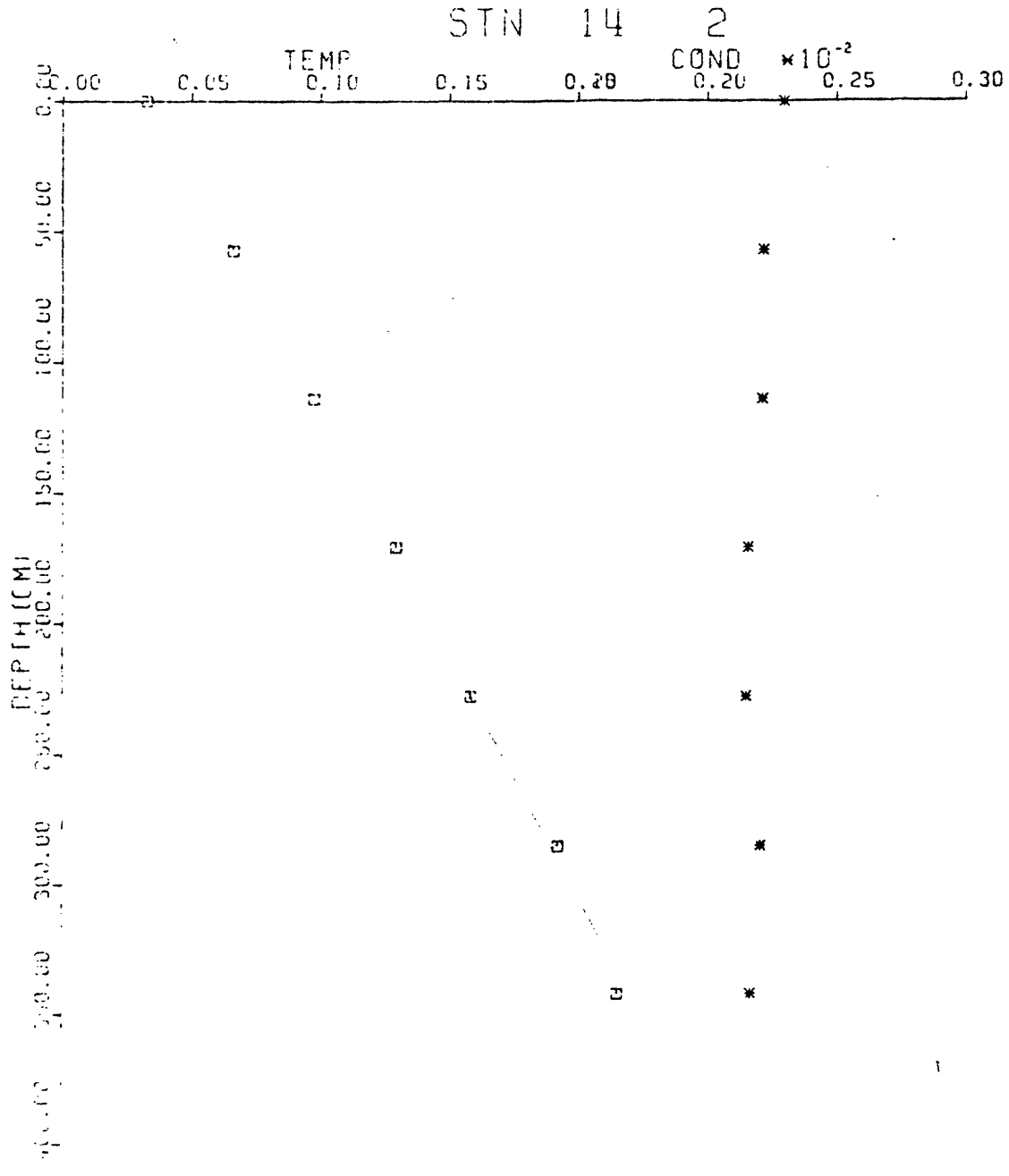
STN 14 2
TEMP
COND ×10⁻²
0.00
0.05
0.10
0.15
0.20
0.25
0.30
100.00
150.00
200.00
300.00

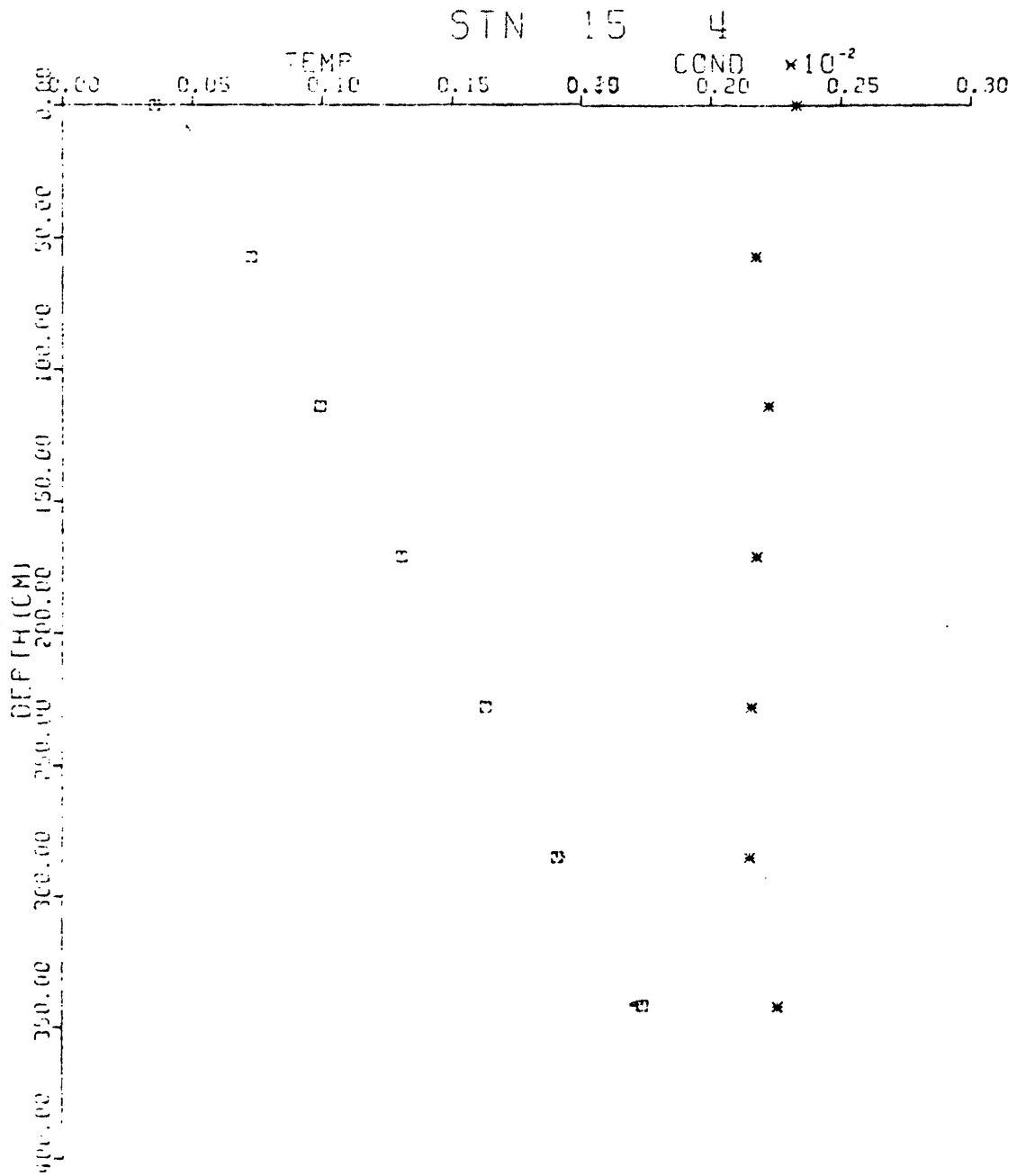
STN 15 4
TEMP
COND ×10⁻²
0.00
0.05
0.10
0.15
0.20
0.25
0.30
DEPTH (CM)
50.00
100.00
150.00
200.00
250.00
300.00
350.00

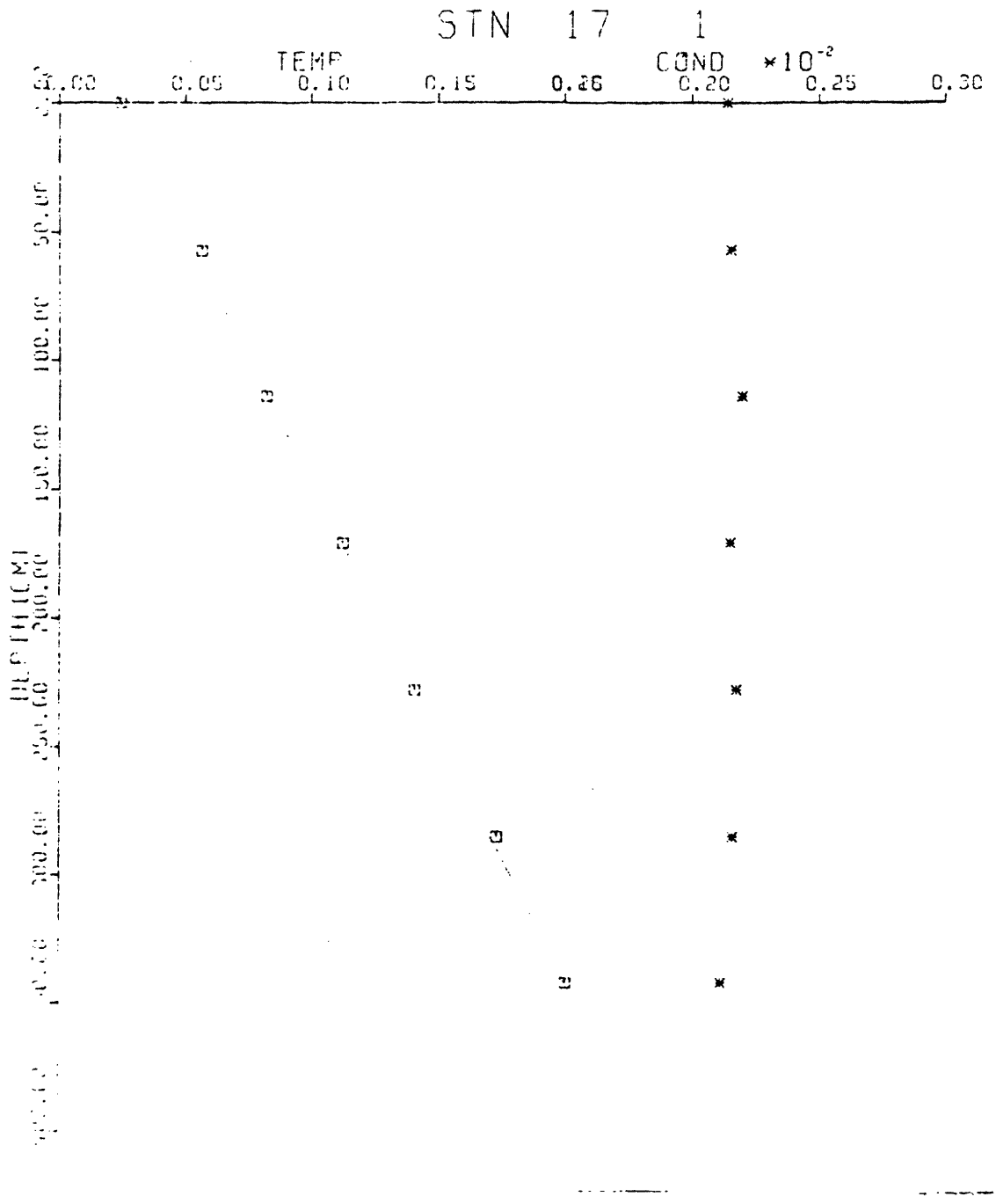
STN 17 1
TEMP
COND ×10⁻²
0.00
0.05
0.10
0.15
0.20
0.25
0.30
50.00
100.00
150.00
200.00
250.00
300.00

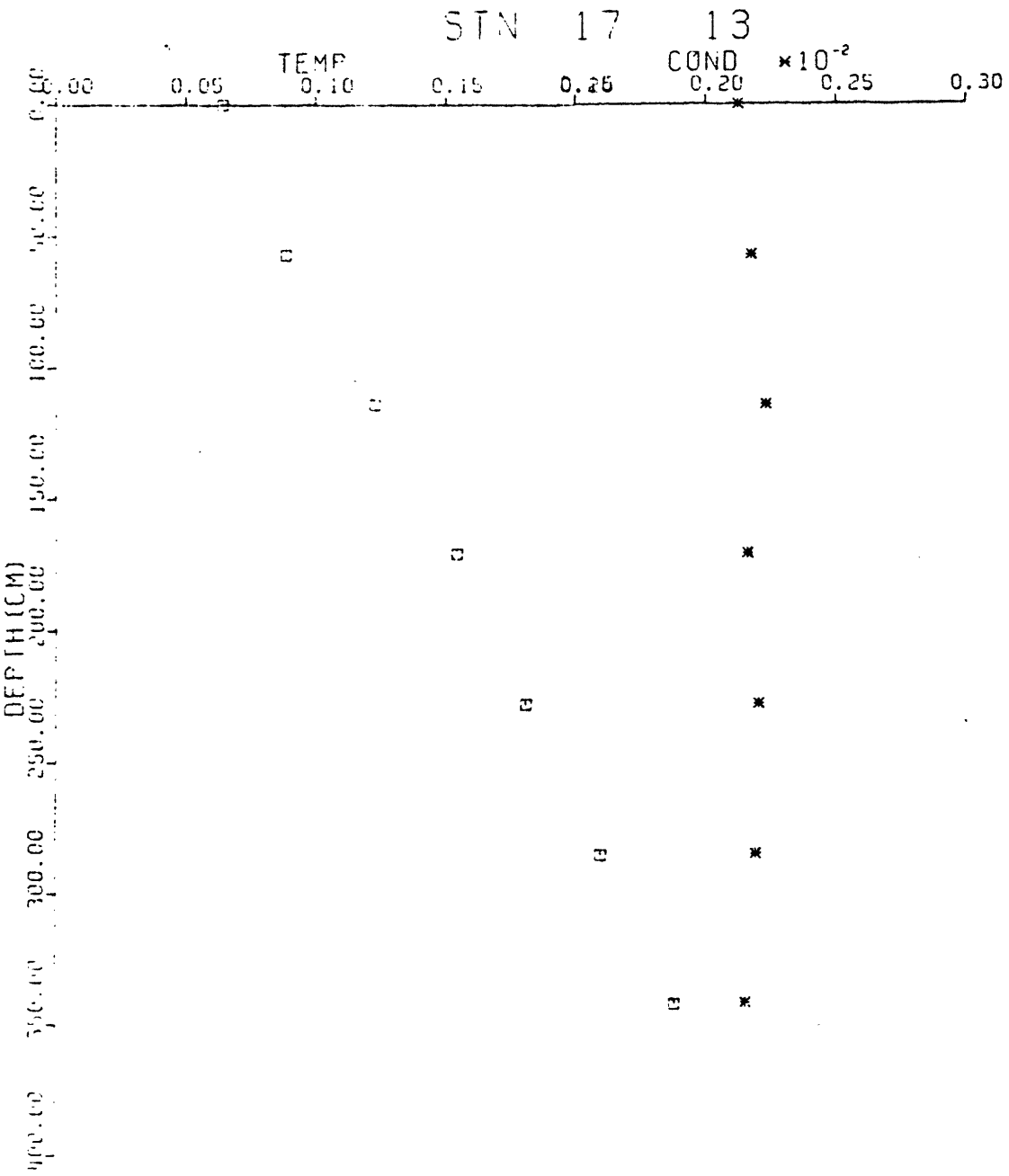
STN 17 13
TEMP
COND ×10⁻²
0.00
0.05
0.10
0.15
0.20
0.25
0.30
DEPTH (CM)
100.00
150.00
200.00
250.00
300.00

APPENDIX G

Sample *in situ* reduced conductivity data output of five representative penetrations during the KR77 cruise, 11-1, 14-2, 15-4, 17-1, 17-13. Conductivities are in cal/(cm s °C) x 10^{-2}. Mean values at each sensor are listed on the third sheet of each penetration printout. (see text)

```
FILE: OUTPUT   DATA     A                    CONVERSATIONAL MONITOR SYSTEM

 ************************************************
 *                                              *
 *     STATION:    11        PENETRATION:     1 *
 *     INSTRUMENT:     3     SENSOR:      3     *
 *     LATITUDE:    0.0     LONGITUDE:     0.0  *
 *     DEPTH(M):    0.                         *
 *                                              *
 ************************************************
  DELAY TIMES  0.17000D+02  0.17000D+02  0.17000D+02
   0.17000D+02   0.22000D+02   0.24000D+02   0.34000D+02

 T0= 0.10000D+01   T01= 0.10000D+01
  HCN FROM T(0)= 0.57810D+03


 SENSOR  1

  0.22112D-02
  0.22083D-02
  0.22061D-02
  0.22117D-02
  0.22084D-02
  0.22109D-02
  0.22000D-02 ****
  0.22101D-02
  0.22050D-02
  0.22153D-02
  0.22155D-02

 SENSOR  2

  0.24271D-02
  0.24170D-02
  0.24161D-02
  0.24129D-02
  0.24158D-02
  0.24111D-02
  0.24220D-02
  0.24253D-02
  0.24092D-02
  0.24256D-02
  0.24403D-02 ****

 SENSOR  3

  0.23526D-02 ****
  0.23879D-02
  0.23837D-02
  0.23951D-02 ****
  0.23778D-02
  0.23810D-02
  0.23817D-02
  0.23727D-02
  0.23647D-02
  0.23623D-02
```

```
 0.23532D-02 ****

SENSOR  4

 0.25465D-02
 0.25492D-02
 0.25501D-02
 0.25397D-02
 0.25410D-02
 0.25364D-02
 0.25444D-02
 0.25392D-02
 0.25485D-02
 0.25602D-02 ****
 0.25599D-02 ****

SENSOR  5

 0.25372D-02
 0.25278D-02
 0.25069D-02
 0.25012D-02
 0.25023D-02
 0.25042D-02
 0.24922D-02
 0.25253D-02
 0.25270D-02
 0.25498D-02
 0.25873D-02 ****

SENSOR  6

 0.25296D-02
 0.25222D-02
 0.25155D-02
 0.25086D-02
 0.25011D-02
 0.24929D-02
 0.25112D-02
 0.25231D-02
 0.25259D-02
 0.25336D-02
 0.25709D-02 ****

SENSOR  7

 0.25653D-02
 0.25868D-02
 0.25933D-02
 0.25850D-02
 0.25962D-02
 0.25948D-02
 0.25853D-02
 0.25786D-02
 0.25560D-02 ****
```

```
 0.25716D-02
 0.25656D-02


ITERATION  2


                    L                   M                   U
          1         2         3         4         5         6         7
          *- - - - - - - - - *- - - - - - - - - *- - - - - - - - - -*

 TW   0.22507D+01        0.22487D+01        0.22433D+01        0.22576D+01
               0.22521D+01        0.22462D+01        0.22460D+01

 TS   0.16389D+00        0.10756D+00        0.66898D-01        0.21243D-01
               0.13542D+00        0.87468D-01        0.44957D-01

 TE   0.37376D-02       -0.13734D-02        0.70957D-02       -0.41591D-02
               0.54342D-02        0.15041D-02        0.60582D-02

  K   0.22103D-02        0.23765D-02        0.25174D-02        0.25823D-02
               0.24182D-02        0.25439D-02        0.25164D-02

GRADT          0.49452D-03        0.35700D-03        0.40083D-03

  Q            0.11959D-05        0.90817D-06        0.10086D-05

**************************************************
*                                                *
*     STATION:    11         PENETRATION:     3  *
*     INSTRUMENT:     3      SENSOR:      3     *
*     LATITUDE:    0.0      LONGITUDE:     0.0   *
*     DEPTH(M):    0.                           *
*                                                *
**************************************************
 DELAY TIMES  0.17000D+02  0.17000D+02  0.17000D+02
  0.17000D+02   0.22000D+02   0.24000D+02   0.34000D+02

T0= 0.40000D+01  T01= 0.40000D+01
 HON FROM T(0)= 0.58529D+03


SENSOR  1

 0.19444D-02
 0.20214D-02
 0.20275D-02
 0.20040D-02
 0.19520D-02
 0.19707D-02

SENSOR  2
```

```
FILE: OUTPUT   DATA     A                    CONVERSATIONAL MONITOR SYSTEM

 ********************************************
 *                                          *
 *     STATION:    14        PENETRATION:    2     *
 *     INSTRUMENT:    3      SENSOR:    3          *
 *     LATITUDE:    0.0     LONGITUDE:    0.0      *
 *     DEPTH(M):    0.                            *
 *                                          *
 ********************************************
  DELAY TIMES  0.17000D+02  0.17000D+02  0.17000D+02
   0.17000D+02   0.22000D+02   0.24000D+02   0.34000D+02

 T0= 0.10000D+01   T01= 0.10000D+01
  HON FROM T(0)= 0.58940D+03


 SENSOR  1

  0.21648D-02
  0.21633D-02
  0.21719D-02
  0.21717D-02
  0.21792D-02
  0.21646D-02
  0.21644D-02
  0.21658D-02
  0.21539D-02
  0.21653D-02
  0.21571D-02
  0.21505D-02 ****
  0.21532D-02 ****
  0.21775D-02

 SENSOR  2

  0.22098D-02
  0.22087D-02
  0.22156D-02
  0.22007D-02
  0.21998D-02
  0.21932D-02
  0.21884D-02
  0.21975D-02
  0.21931D-02
  0.22019D-02
  0.22064D-02
  0.22144D-02
  0.22441D-02
  0.23110D-02 ****

 SENSOR  3

  0.21640D-02
  0.21081D-02 ****
  0.21585D-02
  0.21539D-02
```

```
 0.21493D-02
 0.21387D-02
 0.21424D-02
 0.21480D-02
 0.21572D-02
 0.21420D-02
 0.21161D-02 ****
 0.21398D-02
 0.21531D-02
 0.21995D-02 ****

SENSOR  4

 0.21661D-02
 0.21645D-02
 0.21600D-02
 0.21574D-02
 0.21444D-02
 0.21441D-02
 0.21482D-02
 0.21392D-02
 0.21633D-02
 0.21479D-02
 0.21685D-02
 0.21717D-02
 0.22267D-02 ****
 0.22435D-02 ****

SENSOR  5

 0.22443D-02
 0.22201D-02
 0.22098D-02
 0.21928D-02
 0.21849D-02
 0.21957D-02
 0.21755D-02
 0.21810D-02
 0.22079D-02
 0.22183D-02
 0.22505D-02
 0.22650D-02
 0.23498D-02 ****
 0.24479D-02 ****

SENSOR  6

 0.22305D-02
 0.22325D-02
 0.22218D-02
 0.22054D-02
 0.21993D-02
 0.21892D-02
 0.21953D-02
 0.22043D-02
```

```
 0.22003D-02
 0.22109D-02
 0.22438D-02
 0.22595D-02
 0.23475D-02 ****
 0.23475D-02 ****

SENSOR  7

 0.22997D-02
 0.23054D-02
 0.23086D-02
 0.22968D-02
 0.22923D-02
 0.22774D-02
 0.22678D-02
 0.22915D-02
 0.22895D-02
 0.23046D-02
 0.22927D-02
 0.23089D-02
 0.23606D-02 ****
 0.24066D-02 ****


ITERATION  2


                 L                    M                   U
         1       2        3           4         5         6         7
         *- - - - - - - - -*- - - - - - - - - -*- - - - - - - - - - -*

 TW   0.22816D+01     0.22786D+01       0.22742D+01        0.22873D+01
              0.22831D+01       0.22760D+01        0.22779D+01

 TS   0.21535D+00     0.15855D+00       0.97815D-01        0.32946D-01
              0.19236D+00       0.12968D+00        0.66512D-01

 TE  -0.61301D-03    -0.20894D-02       0.36973D-02        0.89953D-04
             -0.50169D-02       0.20401D-03        0.39142D-02

  K   0.21667D-02     0.21497D-02       0.22121D-02        0.22947D-02
              0.22056D-02       0.21563D-02        0.22161D-02

GRADT         0.49875D-03       0.53320D-03        0.56952D-03

  Q           0.11000D-05       0.11497D-05        0.12621D-05

****************************************************
*                                                  *
*     STATION:   14        PENETRATION:    3       *
*     INSTRUMENT:    3     SENSOR:    3            *
*     LATITUDE:   0.0     LONGITUDE:    0.0        *
```

```
                    L                   M                 C
      1             2         3         4         5         6         7
      . - - - - - - - - - - - + - - - - - - - - - + - - - - - - - - - .

TS  [illegible]D+01        0.22765D+01        0.22561D+01        [illegible]D+01
            0.22645D+01        0.22595D+01        0.22[illegible]

TS  [illegible]340D+00     0.157[illegible]D+00   0.10758D+00       [illegible]1945D-01
            0.20020D+00        0.14000D+00        0.80[illegible]

TE  -0.42[illegible]D-01   0.16775D-01        0.21732D-01        [illegible]D-01
            0.25232D-01        0.19230D-01        0.2155[illegible]

    [illegible]D-02        0.23454D-02        0.23159D-02        0.20329D-02
            0.24067D-02        0.22936D-02        0.230[illegible]

[illegible]         0.39961D-03        0.40[illegible]D-03     0.57[illegible]

[illegible]         0.14431D-05        0.99236D-06        0.13094[illegible]

********************************************************
*                                                      *
*     STATION:    15        PENETRATION:     4         *
*     INSTRUMENT:    3      SENSOR:    3               *
*     LATITUDE:    0.0      LONGITUDE:    0.0          *
*     [illegible]:    0.                               *
*                                                      *
********************************************************
DELAY TIMES  0.17000D+02  0.17000D+02  0.17000D+02
 0.[illegible]D+02  0.22000D+02  0.24000D+02  0.34000D+02

T0= 0.[illegible]  T01= 0.50000D+01
 [illegible] = 0.51816D+03

SENSOR 1

 0.22[illegible]D-02
 0.22[illegible]D-02
 0.2[illegible]D-02
 0.22[illegible]D-02
 0.22[illegible]D-02
 0.22[illegible]D-02
 0.22733D-02
 0.22754D-02 ****
 0.22270D-02

SENSOR 2

 0.21886D-02
 0.21864D-02
```

0.216930-02
0.214630-02
0.217090-02
0.213490-02
0.213630-02
0.214130-02
0.203720-02 ****

SENSOR 3

0.216410-02
0.216160-02
0.213840-02
0.214020-02
0.213930-02
0.216010-02
0.217030-02
0.216130-02
0.214750-02 ****

SENSOR 4

0.216750-02
0.216450-02
0.217060-02
0.216510-02
0.216920-02
0.220280-02
0.217120-02
0.220840-02
0.207090-02 ****

SENSOR 5

0.220760-02
0.220790-02
0.221220-02
0.220770-02
0.222420-02
0.220480-02
0.221490-02
0.221400-02
0.220930-02 ****

SENSOR 6

0.211360-02
0.216660-02
0.216430-02
0.216290-02
0.216270-02
0.217620-02
0.217620-02
0.219230-02
0.219350-02 ****

FILE: OUTPUT DATA A CONVERSATIONAL MONITOR SYSTEM

SENSOR 7

0.233700D-02
0.231400D-02
0.230000D-02
0.232400D-02
0.234600D-02
0.233940D-02
0.232350D-02
0.233570D-02
0.234150D-02

ITERATION 2

	1	L 2	M 4	5	U 6	7
TK	0.226410D+01	0.226310D+01	0.225770D+01	0.226990D+01		
	0.226560D+01	0.226060D+01	0.225940D+01			
TS	0.223730D+00	0.153100D+00	0.596140D-01	0.364490D-01		
	0.190820D+00	0.130680D+00	0.729350D-01			
TE	0.877010D-02	0.499630D-02	0.134470D-01	0.116860D-01		
	0.229030D-02	0.107360D-01	0.881860D-02			
K	0.220090D-02	0.215780D-02	0.220170D-02	0.232850D-02		
	0.215250D-02	0.217820D-02	0.217300D-02			
GRAD		0.532340D-03	0.557350D-03	0.583350D-03		
Q		0.114560D-05	0.121400D-05	0.122420D-05		

```
*****************************************
*                                       *
*     STATION:    15      PENETRATION:    5     *
*     INSTRUMENT:    3    SENSOR:    3          *
*     LATITUDE:    0.0    LONGITUDE:    0.0     *
*     DEPTH(M):    0.                          *
*                                       *
*****************************************
```

DELAY TIMES 0.170000D+02 0.170000D+02 0.170000D+02
0.170000D+02 0.220000D+02 0.240000D+02 0.340000D+02

T0= 0.200000D+01 T01= 0.200000D+01
HCN FROM T(0)= 0.624320D+03

SENSOR 1

```
FILE: OUTPUT1  DATA      A                        CONVERSATIONAL MONITOR SYSTEM


 ************************************************
 *                                              *
 *      STATION:    17         PENETRATION:     1      *
 *      INSTRUMENT:     3      SENSOR:     3           *
 *      LATITUDE:    0.0      LONGITUDE:     0.0       *
 *      DEPTH(M):    0.                               *
 *                                              *
 ************************************************
  DELAY TIMES  0.17000D+02  0.17000D+02  0.17000D+02
   0.17000D+02    0.22000D+02    0.24000D+02    0.34000D+02

 T0= 0.50000D+01   T01= 0.50000D+01
  HON FROM T(0)= 0.56782D+03


 SENSOR  1

  0.21131D-02
  0.21168D-02
  0.21075D-02 ****
  0.21158D-02
  0.21161D-02
  0.21168D-02
  0.21054D-02 ****
  0.21155D-02
  0.21155D-02

 SENSOR  2

  0.21587D-02
  0.21562D-02
  0.21362D-02 ****
  0.21635D-02
  0.21585D-02
  0.21359D-02 ****
  0.21582D-02
  0.21728D-02 ****
  0.21516D-02

 SENSOR  3

  0.21771D-02
  0.21689D-02
  0.21740D-02
  0.21862D-02
  0.21599D-02 ****
  0.21816D-02
  0.21614D-02
  0.21768D-02
  0.21887D-02

 SENSOR  4

  0.21553D-02
  0.21541D-02
```

```
 0.21505D-02
 0.21499D-02
 0.21460D-02
 0.21675D-02 ****
 0.21476D-02
 0.21628D-02
 0.21531D-02

SENSOR  5

 0.22147D-02
 0.22009D-02
 0.22042D-02
 0.21941D-02
 0.21915D-02
 0.22009D-02
 0.21985D-02
 0.22366D-02 ****
 0.22379D-02 ****

SENSOR  6

 0.21618D-02
 0.21511D-02
 0.21559D-02
 0.21415D-02
 0.21473D-02
 0.21545D-02
 0.21506D-02
 0.21677D-02
 0.21658D-02 ****

SENSOR  7

 0.21483D-02
 0.21302D-02
 0.21386D-02
 0.21468D-02
 0.21546D-02
 0.21276D-02
 0.21400D-02
 0.21248D-02
 0.21701D-02 ****


ITERATION  2
```

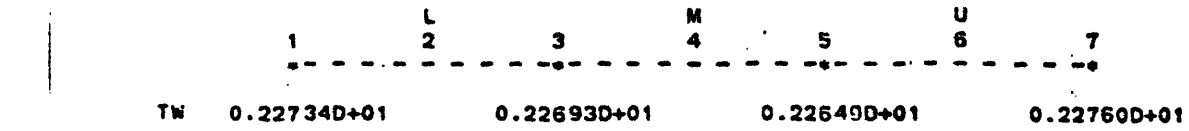


```
TW   0.22734D+01      0.22693D+01      0.22649D+01      0.22760D+01
```

```
FILE: OUTPUT1  DATA     A                    CONVERSATIONAL MONITOR SYSTEM

                0.22728D+01        0.22688D+01        0.22656D+01

 TS  0.20015D+00        0.14084D+00        0.82221D-01        0.24326D-01
                0.17284D+00        0.11218D+00        0.56585D-01

 TE  -0.22868D-03       0.33670D-03        0.29612D-03        0.17975D-02
                0.10035D-02       -0.29420D-02       -0.89830D-03

  K   0.21157D-02       0.21768D-02        0.22007D-02        0.21396D-02
                0.21594D-02        0.21524D-02        0.21538D-02

GRADT                  0.52077D-03        0.51462D-03        0.50830D-03

  Q                    0.11246D-05        0.11077D-05        0.10948D-05

**************************************************
*                                                *
*     STATION:    17         PENETRATION:     2  *
*     INSTRUMENT:     3      SENSOR:     3       *
*     LATITUDE:    0.0      LONGITUDE:     0.0   *
*     DEPTH(M):    0.                            *
*                                                *
**************************************************
 DELAY TIMES  0.17000D+02  0.17000D+02  0.17000D+02
  0.17000D+02   0.22000D+02   0.24000D+02   0.34000D+02

T0= 0.60000D+01   T01= 0.78000D+02
 HON FROM T(0)= 0.57707D+03


SENSOR  1

 0.22010D-02
 0.21945D-02
 0.21958D-02
 0.21991D-02
 0.21844D-02 ****
 0.22124D-02 ****
 0.21953D-02
 0.21989D-02
 0.22060D-02

SENSOR  2

 0.21780D-02
 0.21735D-02
 0.21662D-02
 0.21564D-02
 0.21626D-02
 0.21744D-02
 0.21706D-02
 0.21907D-02
 0.21977D-02 ****

SENSOR  3
```

```
FILE: OUTPUT1  DATA     A                    CONVERSATIONAL MONITOR SYSTEM

                0.23728D+00        0.17201D+00        0.10232D+00

 TE  -0.12242D-03        0.79255D-03       -0.30313D-02        0.20163D-02
                0.13799D-02       -0.36805D-02       -0.14509D-02

  K   0.22194D-02        0.21384D-02        0.22867D-02        0.21529D-02
                0.22301D-02        0.22049D-02        0.22313D-02

GRADT           0.58723D-03        0.53837D-03        0.99983D-03

  Q             0.13096D-05        0.11870D-05        0.22310D-05

**************************************************
*                                                *
*     STATION:    17         PENETRATION:    13  *
*     INSTRUMENT:     3      SENSOR:     3       *
*     LATITUDE:    0.0      LONGITUDE:     0.0   *
*     DEPTH(M):    0.                            *
*                                                *
**************************************************
 DELAY TIMES  0.17000D+02  0.17000D+02  0.17000D+02
  0.17000D+02   0.22000D+02   0.24000D+02   0.34000D+02

T0= 0.0           T01= 0.56000D+02
 HON FROM T(0)= 0.60070D+03


SENSOR  1

 0.21677D-02
 0.21597D-02
 0.21725D-02
 0.21584D-02
 0.21554D-02
 0.21629D-02
 0.21585D-02
 0.21570D-02
 0.21644D-02 ****
 0.21714D-02

SENSOR  2

 0.22029D-02
 0.22015D-02
 0.21952D-02
 0.21832D-02
 0.21845D-02
 0.21714D-02 ****
 0.21952D-02
 0.22132D-02
 0.22100D-02
 0.22179D-02

SENSOR  3
```

```
 0.22157D-02
 0.22119D-02
 0.22160D-02
 0.22167D-02
 0.22057D-02
 0.21978D-02
 0.22130D-02
 0.22018D-02
 0.22160D-02
 0.22469D-02 ****

SENSOR  4

 0.21701D-02
 0.21709D-02
 0.21657D-02
 0.21550D-02
 0.21680D-02
 0.21577D-02
 0.21697D-02
 0.21562D-02
 0.21677D-02
 0.21938D-02 ****

SENSOR  5

 0.22381D-02
 0.22657D-02 ****
 0.22296D-02
 0.22363D-02
 0.22228D-02
 0.22265D-02
 0.22291D-02
 0.22519D-02
 0.22530D-02
 0.22670D-02 ****

SENSOR  6

 0.21908D-02
 0.21596D-02
 0.21845D-02
 0.21684D-02
 0.21828D-02
 0.21911D-02
 0.21595D-02
 0.21711D-02
 0.21802D-02
 0.22041D-02 ****

SENSOR  7

 0.21400D-02
 0.20816D-02 ****
 0.21211D-02
```

```
 0.21291D-02
 0.21206D-02
 0.21216D-02
 0.21042D-02
 0.21206D-02
 0.21228D-02
 0.21395D-02

ITERATION  2

                      L                    M                    U
          1           2          3         4          5         6          7
          *- - - - - - - - - -*- - - - - - - - - -*- - - - - - - - - -*

 TW   0.22240D+01        0.22218D+01        0.22155D+01        0.22290D+01
                0.22253D+01        0.22184D+01        0.22181D+01

 TS   0.23888D+00        0.18122D+00        0.12288D+00        0.64558D-01
                0.21021D+00        0.15451D+00        0.88469D-01

 TE  -0.96945D-04       -0.19885D-02       -0.49152D-03       -0.21078D-02
                0.10267D-02       -0.47440D-02        0.38912D-02

  K   0.21626D-02        0.22105D-02        0.22359D-02        0.21244D-02
                0.22004D-02        0.21646D-02        0.21765D-02

GRADT           0.50628D-03        0.51221D-03        0.51204D-03

  Q             0.11140D-05        0.11087D-05        0.11144D-05

**************************************************
*                                                *
*     STATION:    17         PENETRATION:    14  *
*     INSTRUMENT:     3     SENSOR:     3        *
*     LATITUDE:    0.0      LONGITUDE:     0.0   *
*     DEPTH(M):    0.                            *
*                                                *
**************************************************
 DELAY TIMES  0.17000D+02  0.17000D+02  0.17000D+02
  0.17000D+02   0.22000D+02   0.24000D+02   0.34000D+02

T0= 0.30000D+01  T01= 0.43000D+02
 MON FROM T(0)= 0.59967D+03

SENSOR  1

 0.21973D-02
 0.21889D-02
 0.21845D-02
 0.21792D-02
```

APPENDIX H

$F(\alpha, \tau)$ versus in situ temperature at each sensor from five representative penetrations. Second plot has expanded temperature scale (+5°C/sensor) to clearly show linearity of $F(\alpha, \tau)$. (see text)

TEMP
0.20
0.24
STN 11

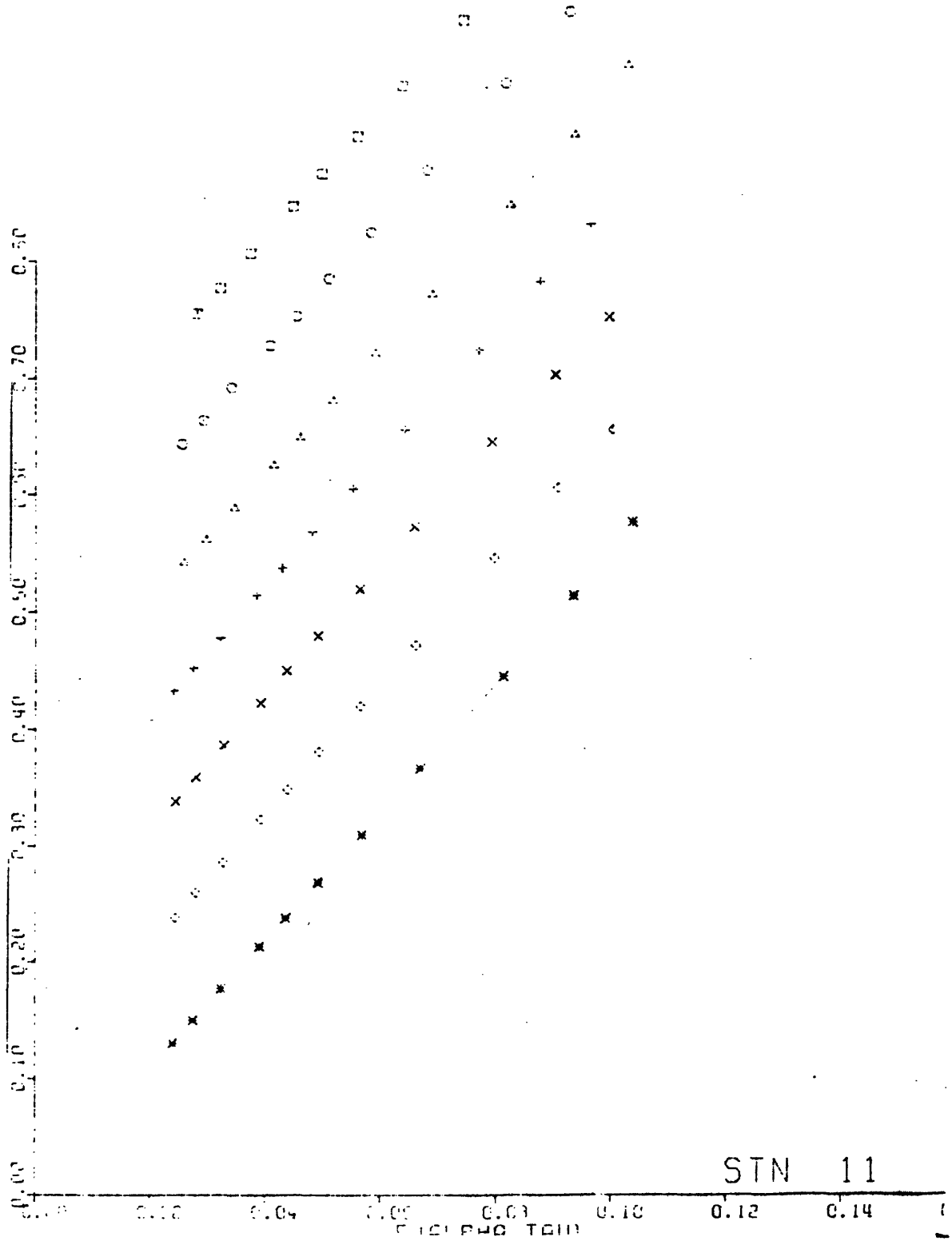
STN 11
0.10
0.12
0.14

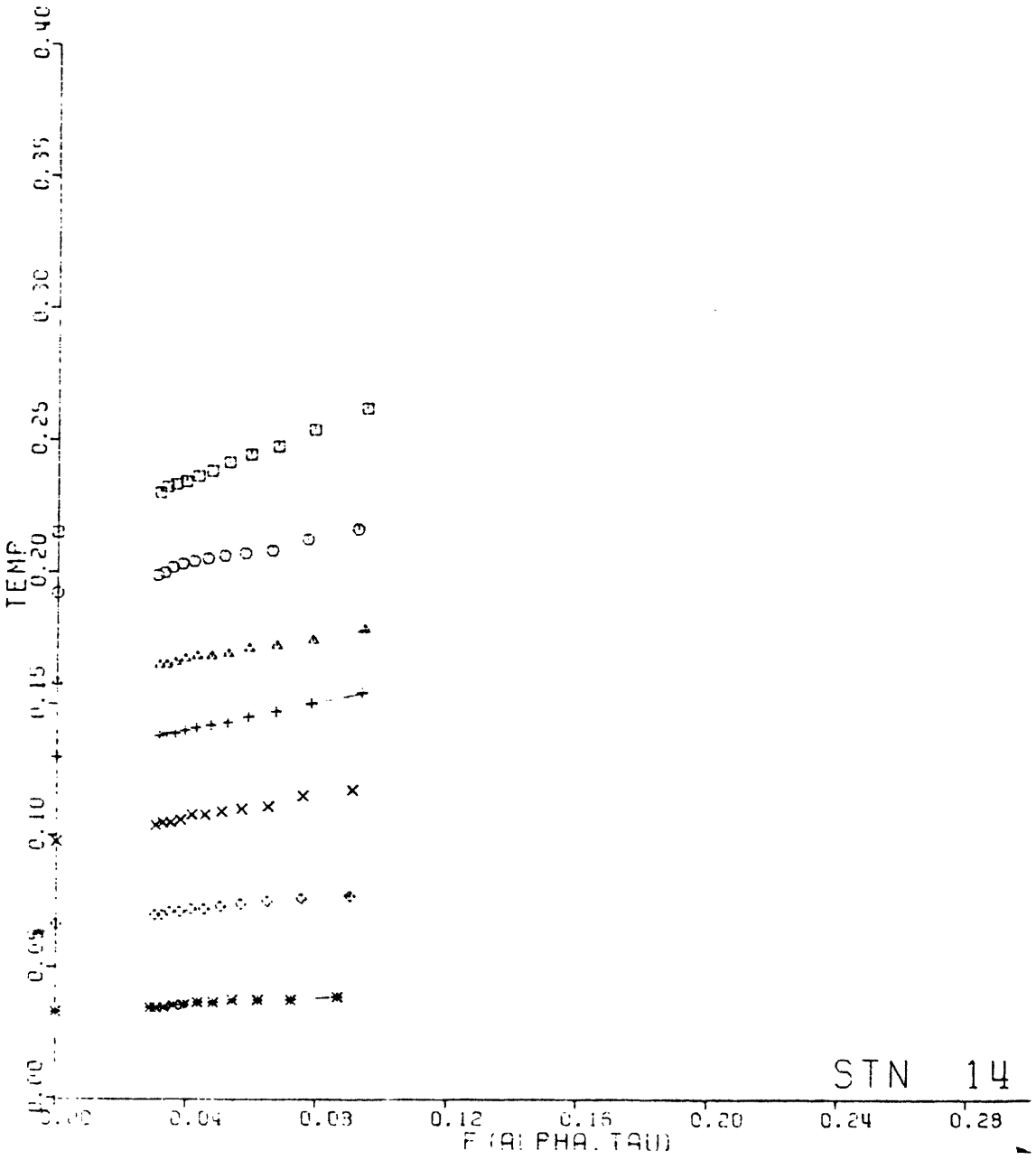
TEMP
0.40
0.35
0.30
0.25
0.20
0.15
0.10
0.05
0.00
0.04
0.08
0.12
0.16
0.20
0.24
0.28
F(ALPHA,TAU)
STN 14

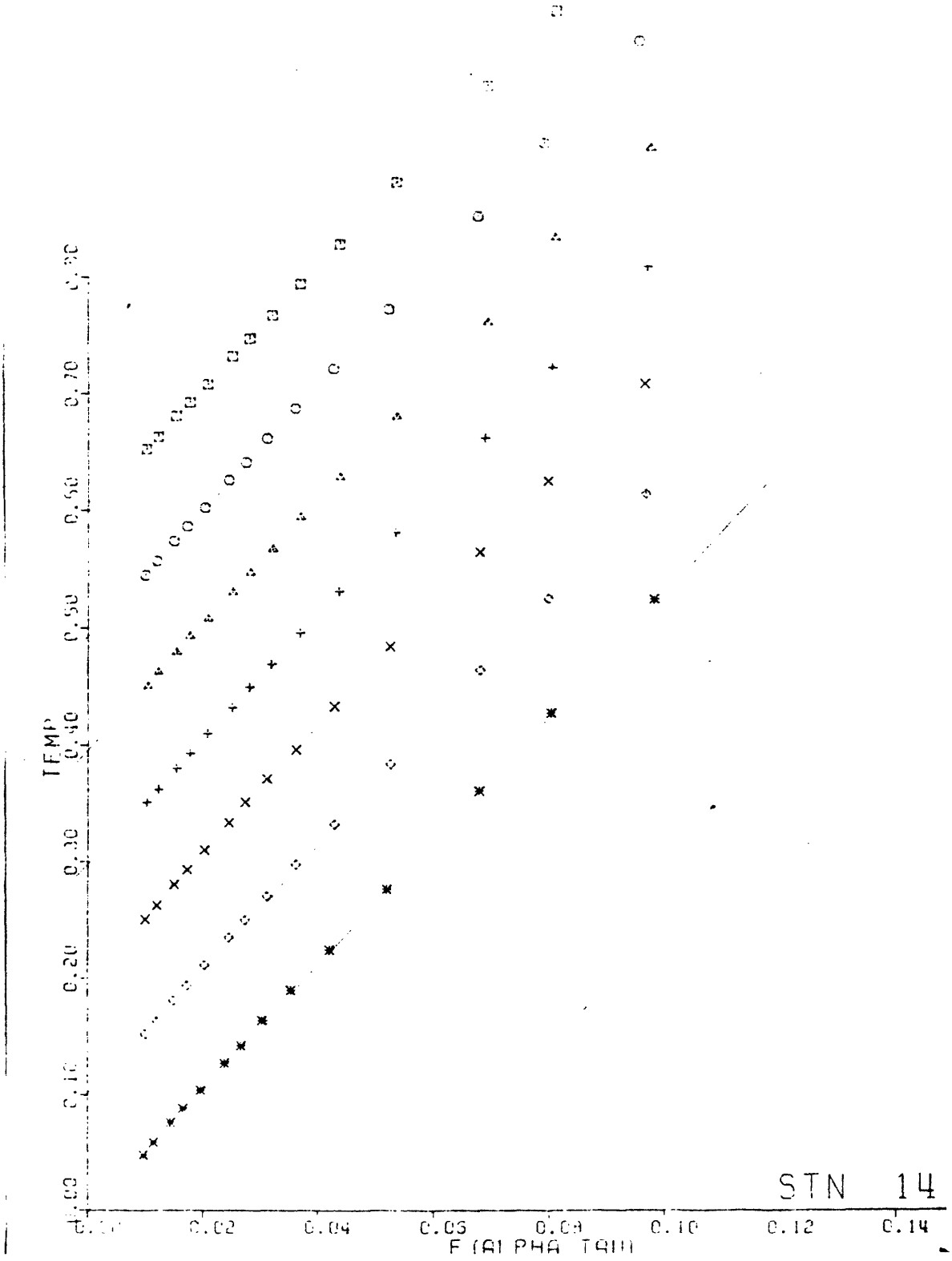
TEMP
0.40
0.50
0.60
0.70
0.80
0.20
0.30
0.02
0.04
0.06
0.08
0.10
0.12
0.14
STN 14

STN 15
0.20
0.24
0.28

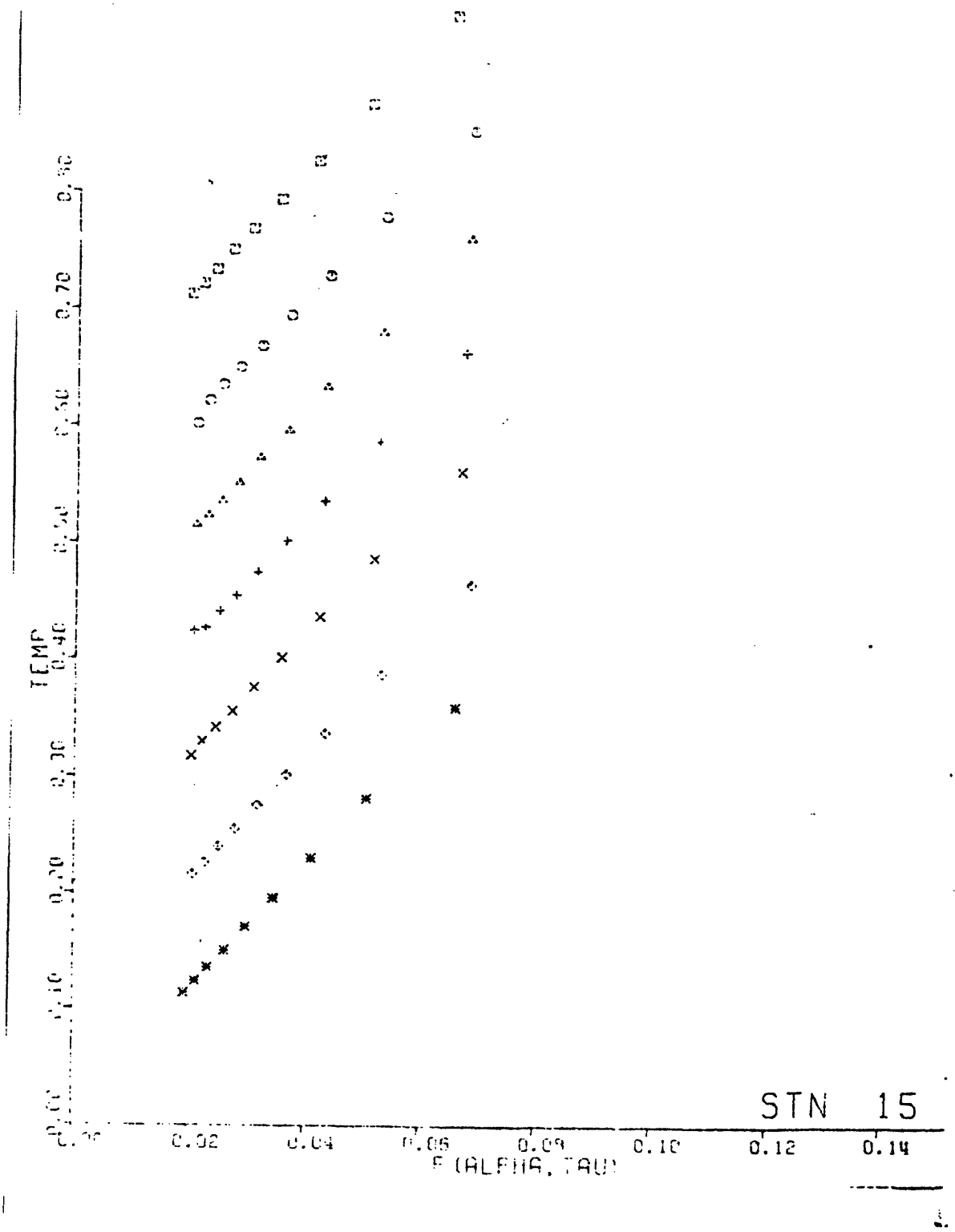
TEMP
0.70
0.40
0.10
0.02
0.04
0.06
0.08
0.10
0.12
0.14
F (ALPHA, TAU)
STN 15

TEMP
0.40
0.30
0.25
0.20
0.15
0.10
STN 1
0.24
0.28
P(ALPHA, TAU)

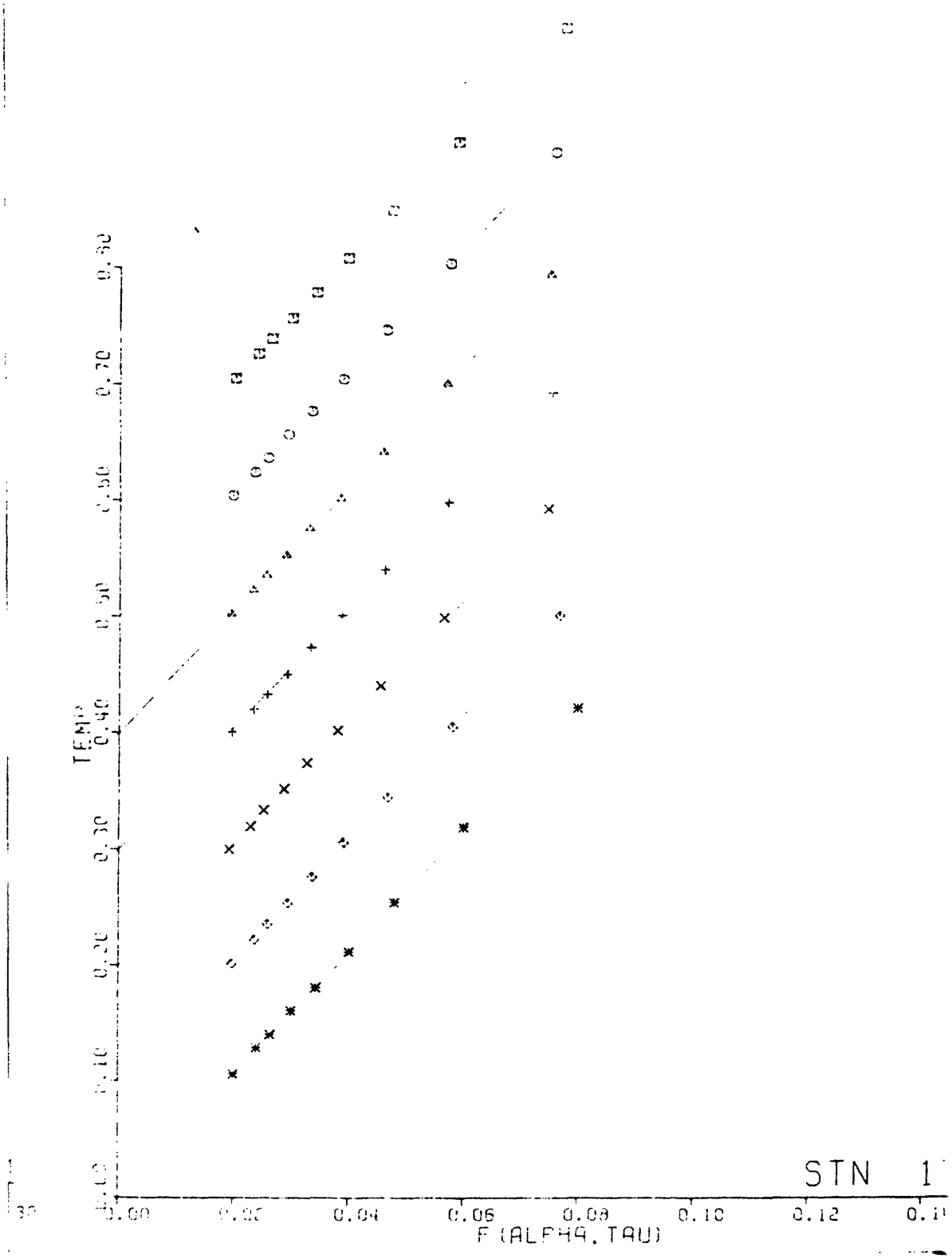
TEMP
0.70
0.50
0.40
0.30
0.00
0.04
0.06
0.08
0.10
0.12
F (ALPHA, TAU)
STN 1

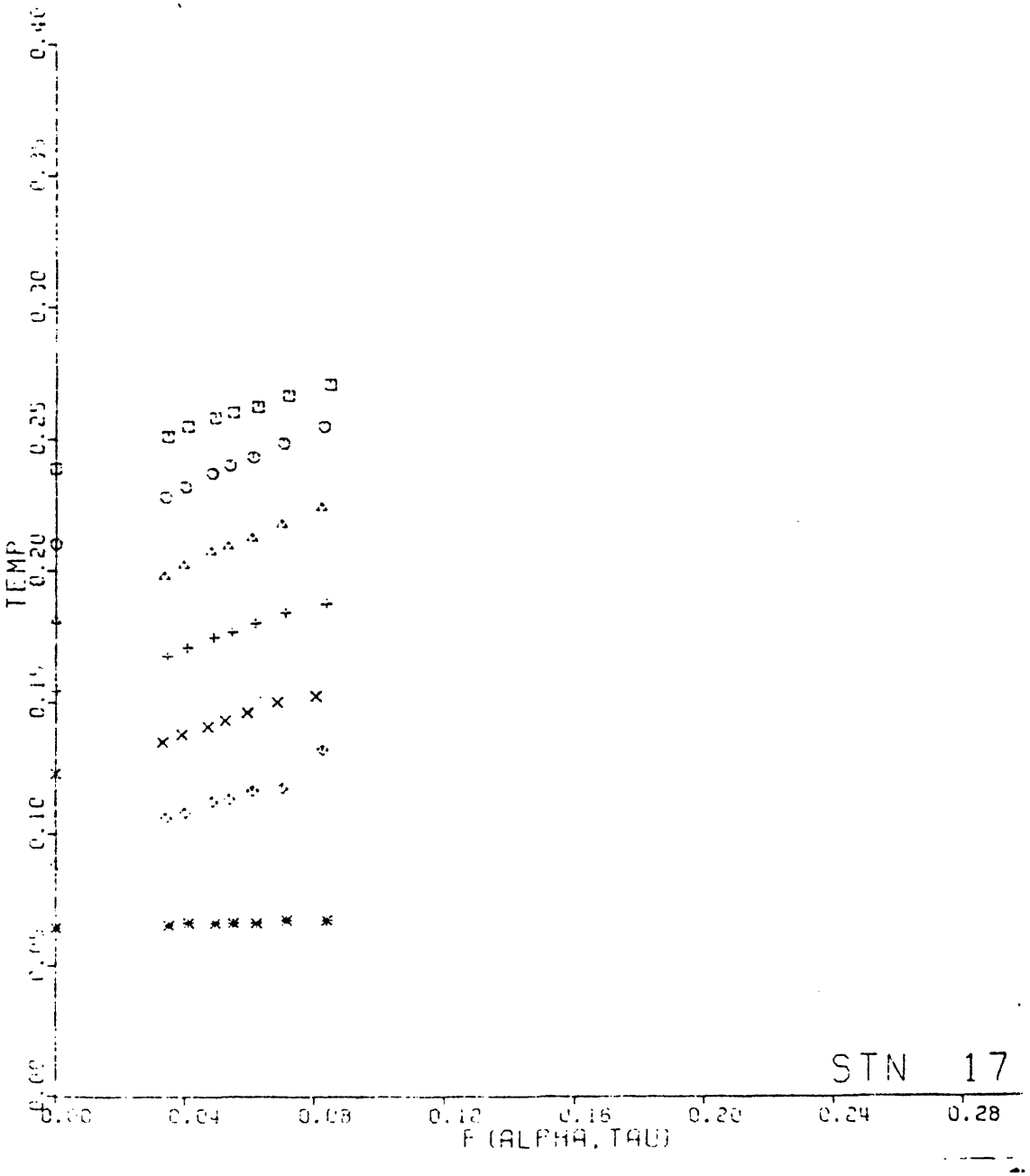
TEMP
0.10
0.20
0.25
0.30
0.00
0.04
0.08
0.12
0.16
0.20
0.24
0.28
F (ALPHA, TAU)
STN 17

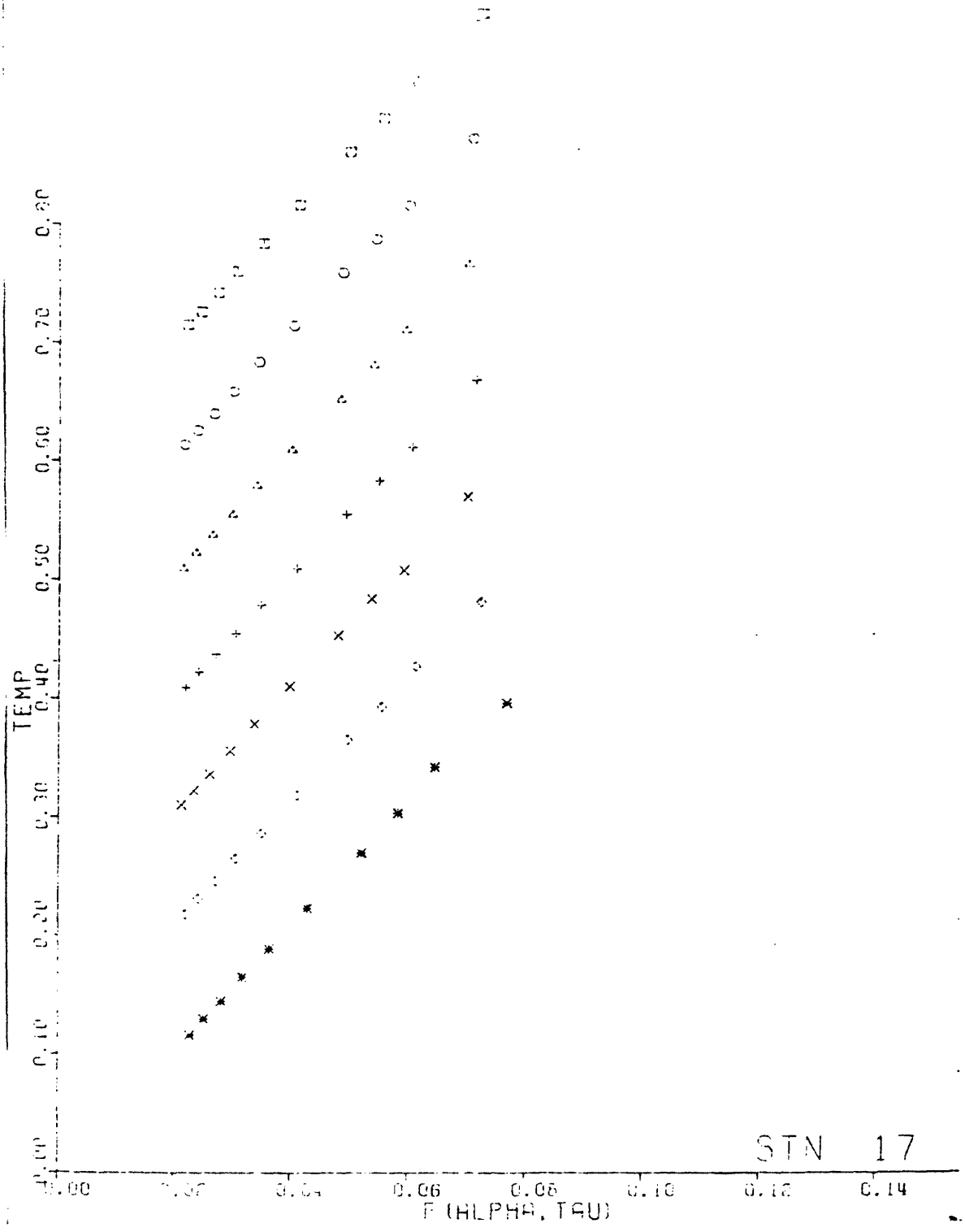
TEMP
0.40
0.50
0.60
0.70
0.80
0.30
0.20
0.10
0.00
0.00
0.04
0.06
0.08
0.10
0.12
0.14
F (ALPHA, TAU)
STN 17

MIT Libraries
Document Services

Room 14-0551
77 Massachusetts Avenue
Cambridge, MA 02139
Ph: 617.253.5668 Fax: 617.253.1690
Email: docs@mit.edu
http://libraries.mit.edu/docs

DISCLAIMER OF QUALITY

Due to the condition of the original material, there are unavoidable flaws in this reproduction. We have made every effort possible to provide you with the best copy available. If you are dissatisfied with this product and find it unusable, please contact Document Services as soon as possible.

Thank you.

Some pages in the original document contain color pictures or graphics that will not scan or reproduce well.